MAX-PLANCK-INSTITUT
FÜR PLASMAPHYSIK

Low temperature plasmas Properties, diagnostics & their relevance in fusion

Ursel Fantz, Dirk Wünderlich, Richard Bergmayr

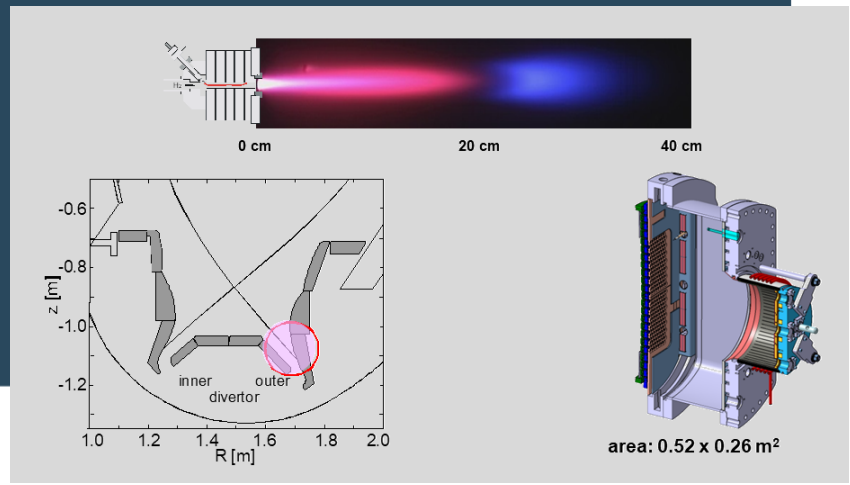

EUROfusion

This work has been carried out within the framework of the EUROfusion Consortium, funded by the European Union via the Euratom Research and Training Programme (Grant Agreement No 101052200 — EUROfusion). Views and opinions expressed are however those of the author(s) only and do not necessarily reflect those of the European Union or the European Commission. Neither the European Union nor the European Commission can be held responsible for them.

Low temperature plasmas

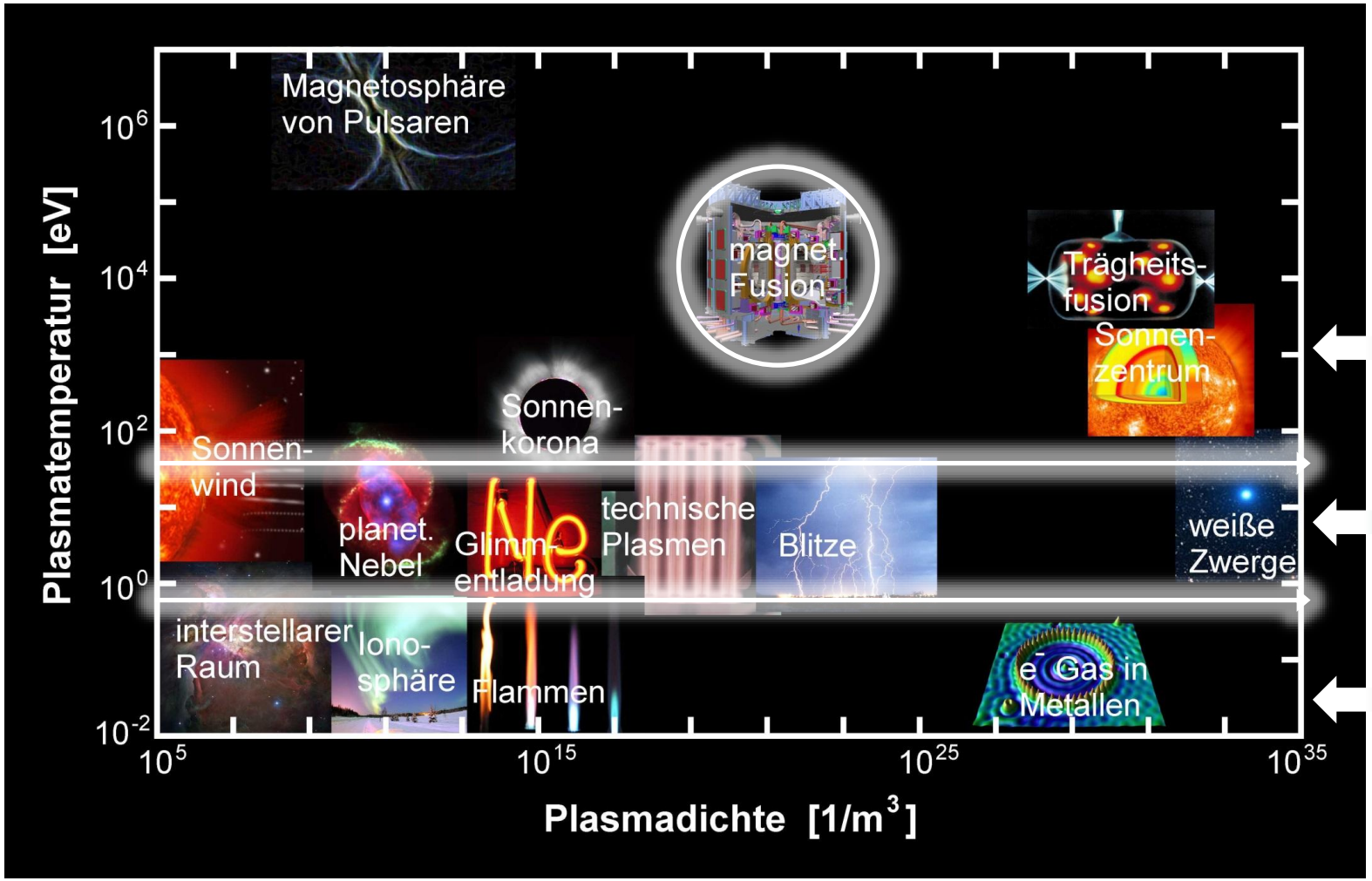

https://scilogs.spektrum.de/formbar/plasmazoo/ zuletzt besucht: Nov. 2022

Sun‘s core temperature

≈ 1 keV

Low temperature plasmas

≈ 1 - 50 eV

Room temperature

≈ 1/40 eV

Low temperature plasmas

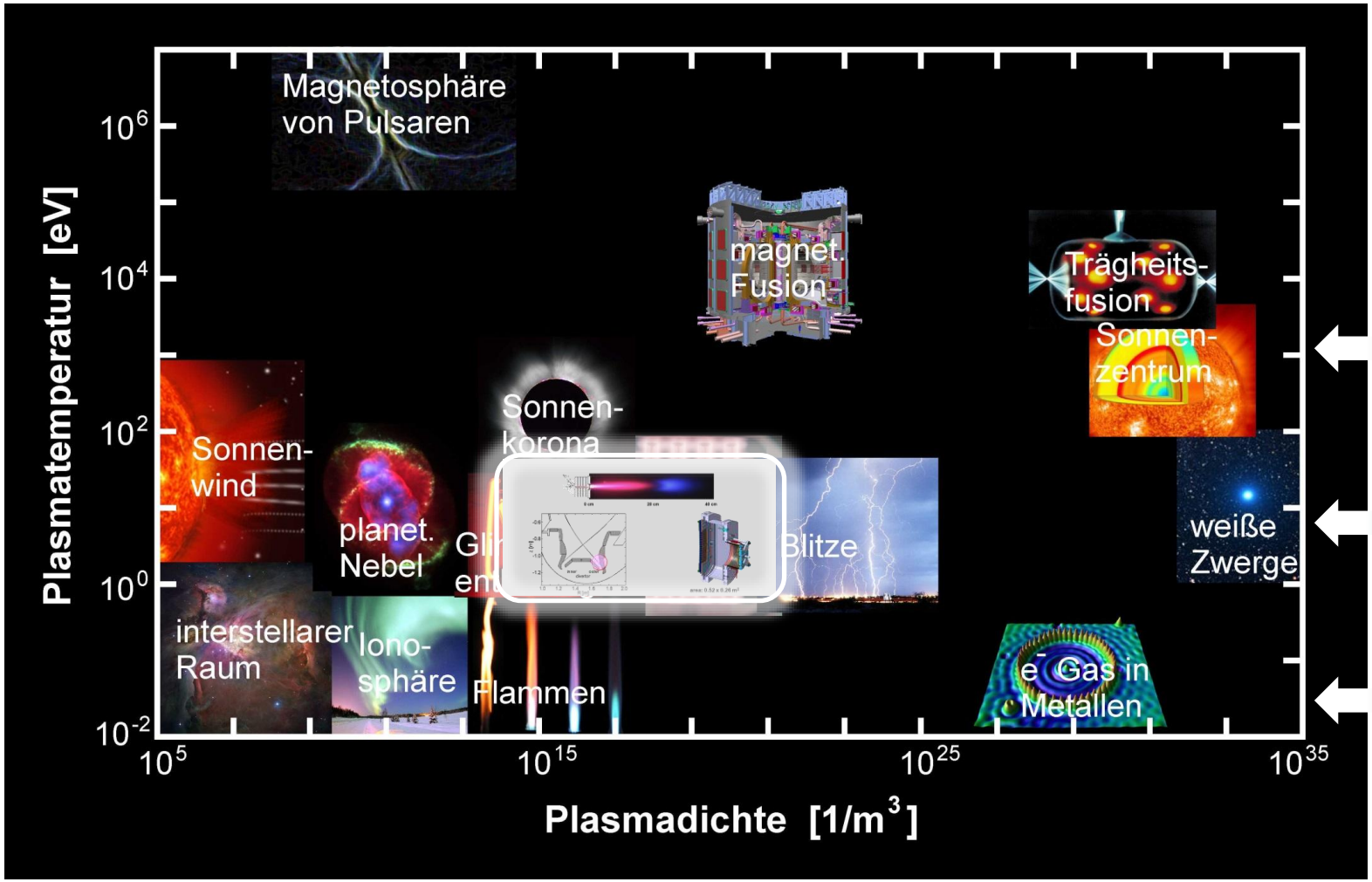

https://scilogs.spektrum.de/formbar/plasmazoo/ zuletzt besucht: Nov. 2022

Sun‘s core temperature

≈ 1 keV

Low temperature plasmas

≈ 1-50 eV

Room temperature

≈ 1/40 eV

Properties of low temperature plasmas & plasma reactors

Low temperature plasmas
A multi-component system

$T_e = 1 – 10$ eV, $n_e = 10^{15} – 10^{21}$ m^{-3}

Volume processes: complex plasma chemistry

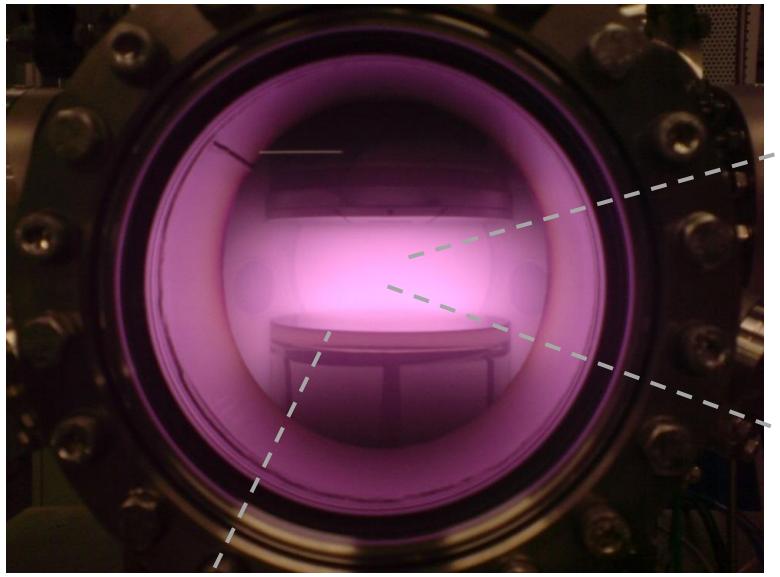

Plasma surface interaction

on **macroscopic** and **microscopic** scale

coating, cleaning, etching, …

plasma sheath, ambipolar diffusion, potentials, …

Example Helium

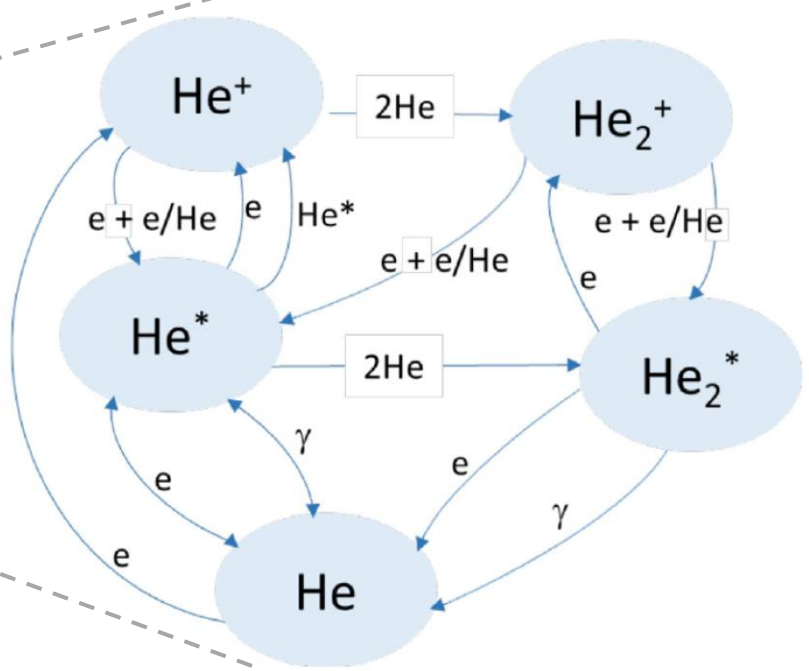

S. Samukawa, The 2012 Plasma Roadmap J.Phys.D: Applied Physics 45 (2012)

Electrons, ions, radicals and photons

which interact via collisions

Plasma sheath – the plasma meets a surface

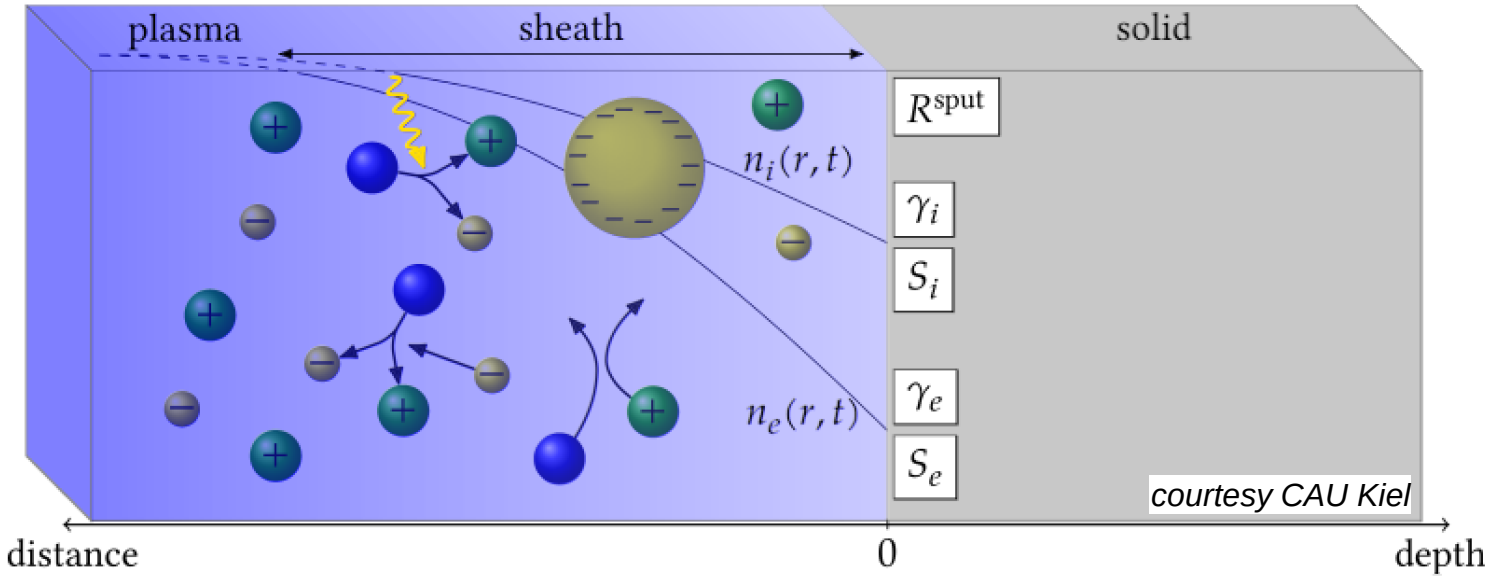

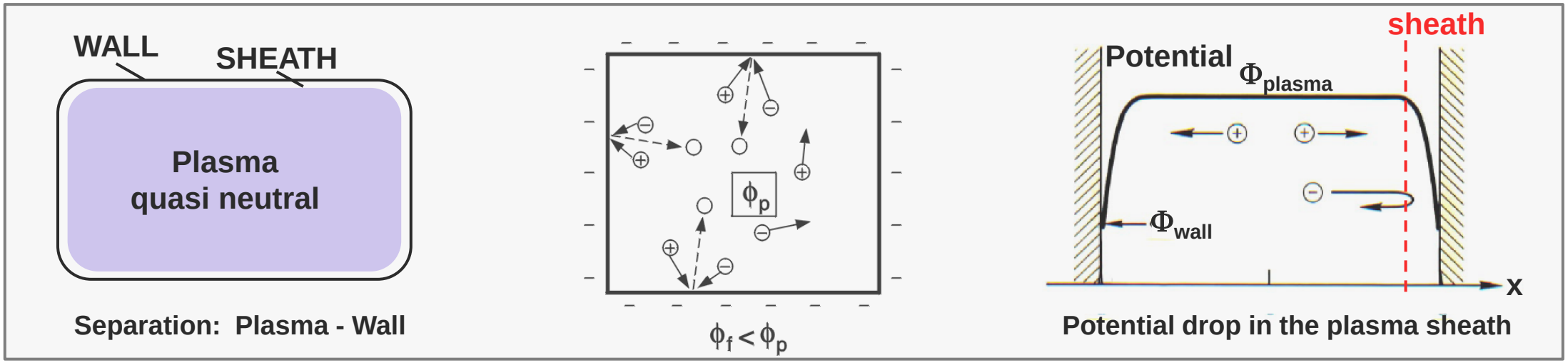

Low temperature plasmas
Dedicated plasma surface interaction studies

Plasma chemistry and discharge affected by

Plasma	**Catalyst**
heat, electrons, photons, radicals, excited species	material, dielectric properties, porosity, catalyst size

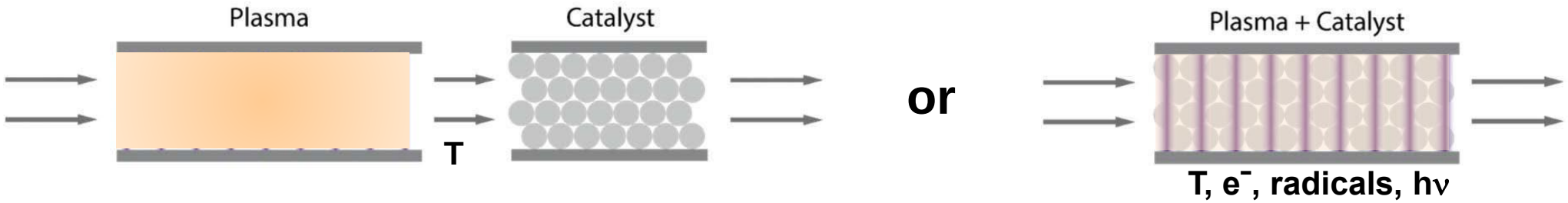

Plasma supplies

- Heat (gas heating)
- Stable radicals
- UV radiation

Plasma supplies

- Heat
- Radicals (also unstable ones)
- (V)UV radiation
- Ions & electrons

Plasma – surface interaction & interaction plasma – surface

Ammonia example: nitrogen-hydrogen plasma on a catalytic surface

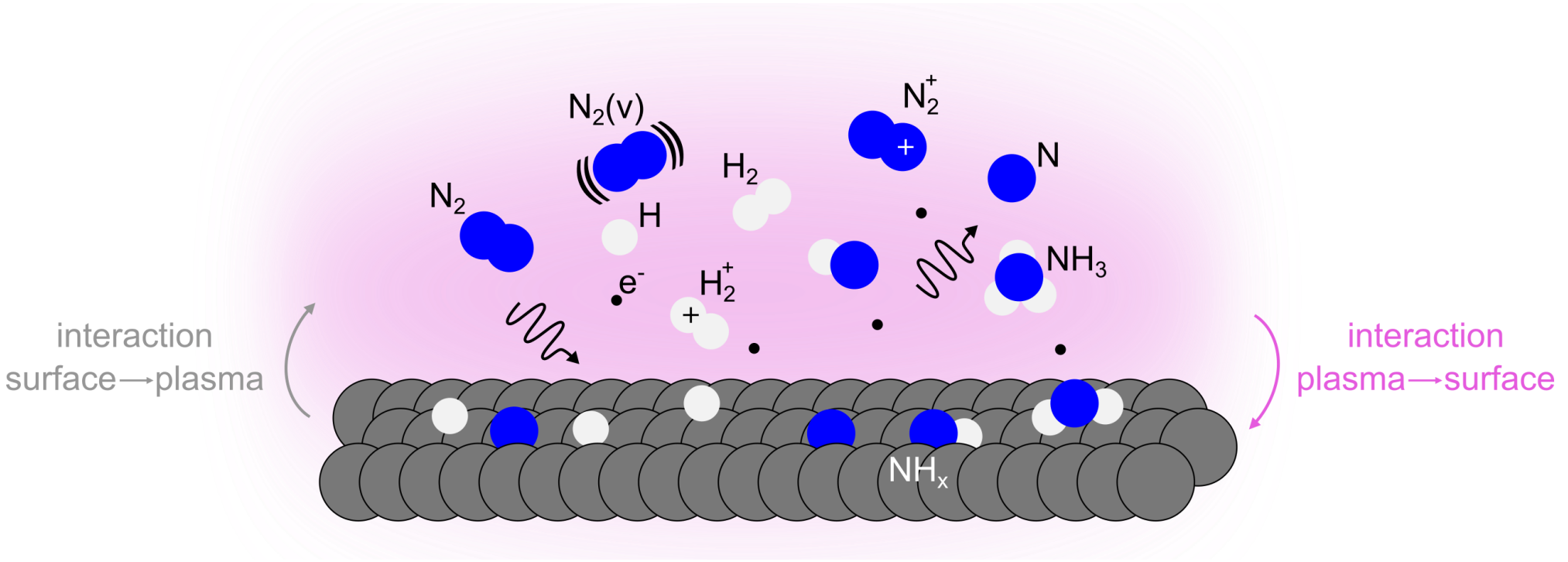

Low temperature plasmas

Surface treatment combined with surface analysis techniques

DBD @ 1 atm.

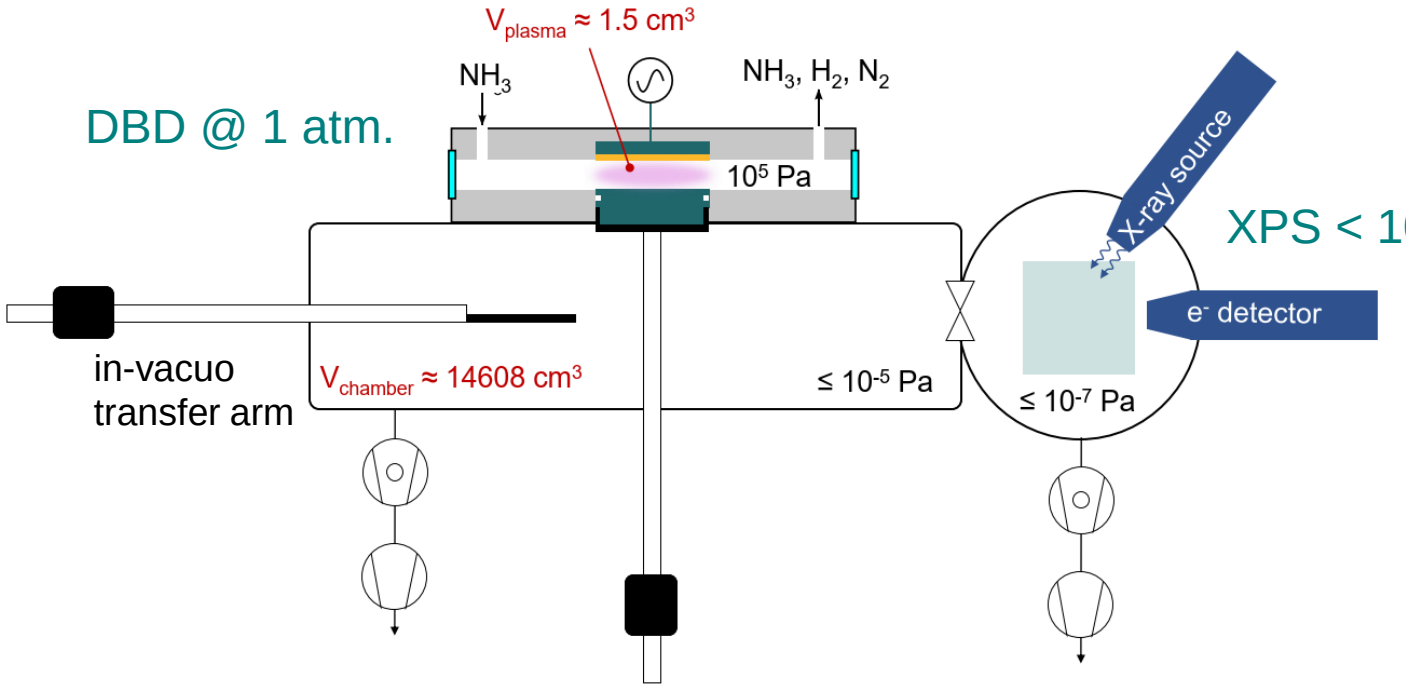

Combined with in-operando analysis of DBD plasma

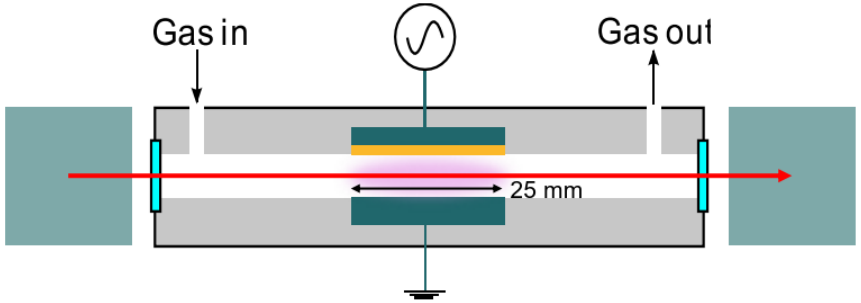

Goal: in-vacuo studies of plasma exposed surfaces

- Role of plasma? Role of surface in ammonia formation?
- What species do preferentially adsorb and/or are formed on the surface?
- How does the nitration affect the reaction rates?

Temperature and pressure map of plasmas
Working regimes

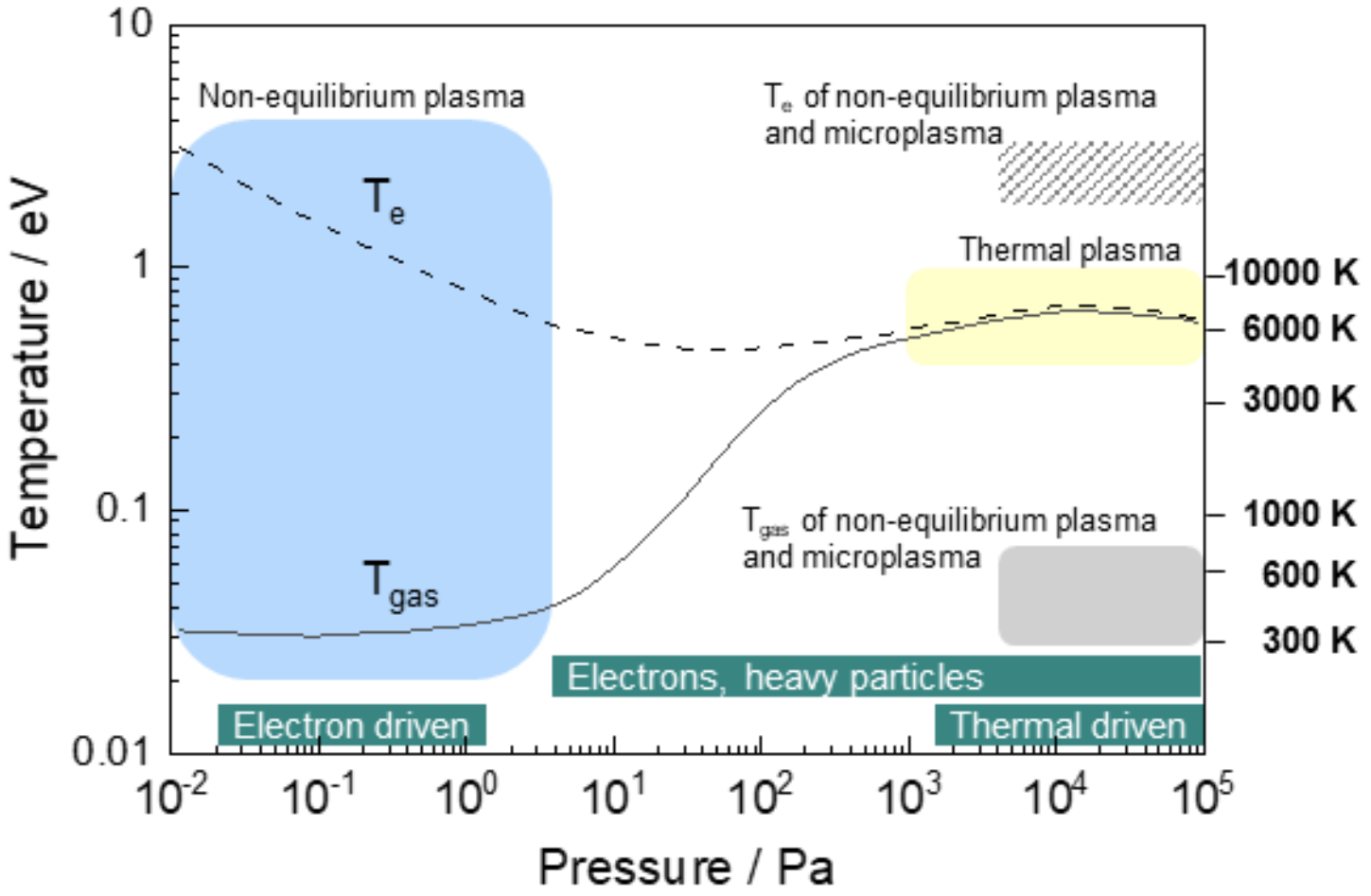

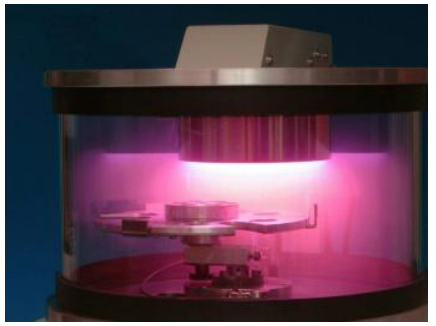

Low pressure

High pressure

Atmospheric pressure

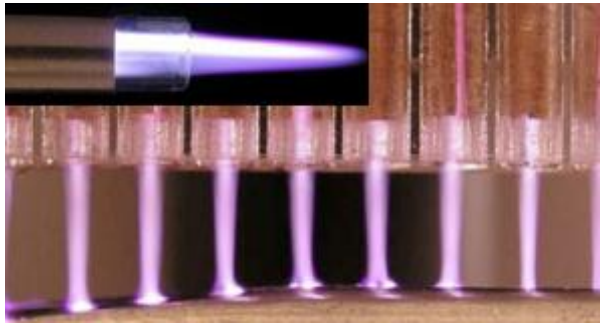

Typical plasma reactors for atmospheric plasmas

Dielectric Barrier Discharge

planar DBD

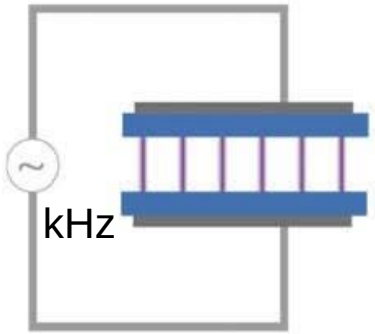

cylindrical DBD

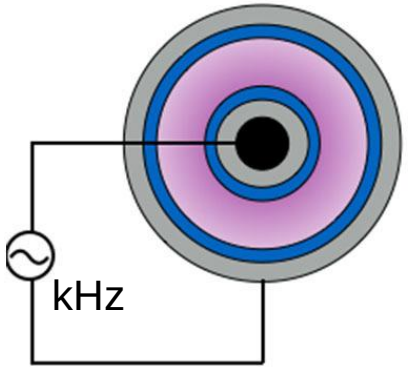

Microwave plasma

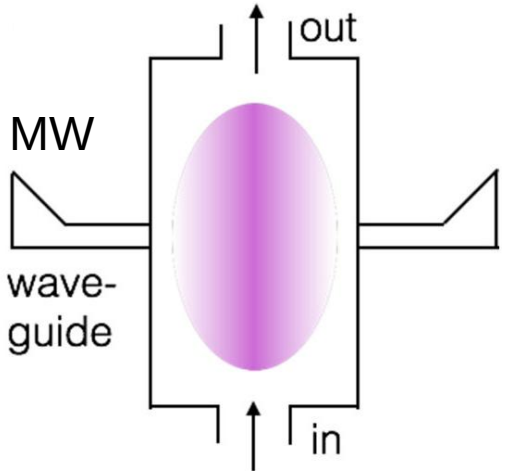

Gliding arc

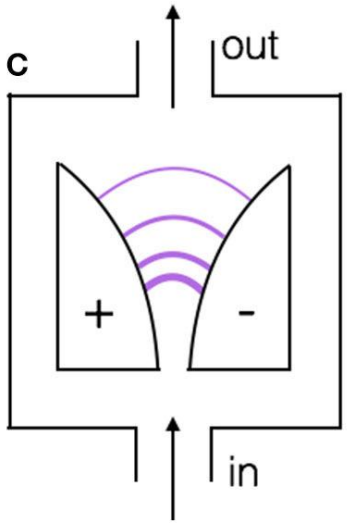

Gliding arc plasmatron

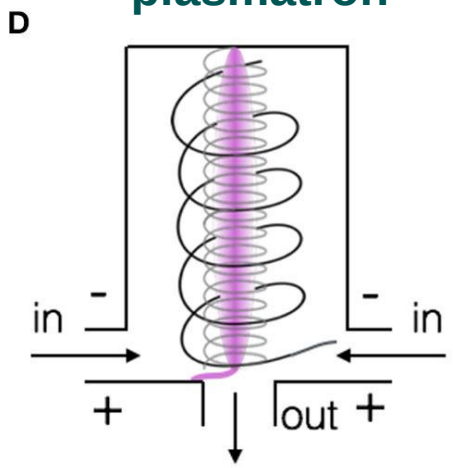

Bogaerts and Centi 2020 *Front. Energy Res.* **8** 111
Snoecks and Bogaerts 2017 *Chem. Soc. Rev.* ***46*** *5805*

Covering a wide pressure range

Surfaguide	Plasma Torch	Dielectric Barrier Discharge (DBD)
Pressure: 0.1 – 100 mbar	Pressure: 20 – 1000 mbar	Pressure: 10 – 1000 mbar
Gas temperature: 1000 – 2000 K	Gas temperature: ≈ 6000 K	Gas temperature: ≈ 600 K
Electron driven	Thermal plasma	Electrons & Heavy particles

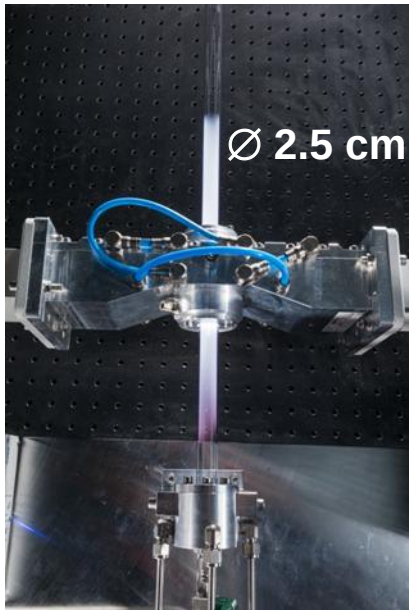

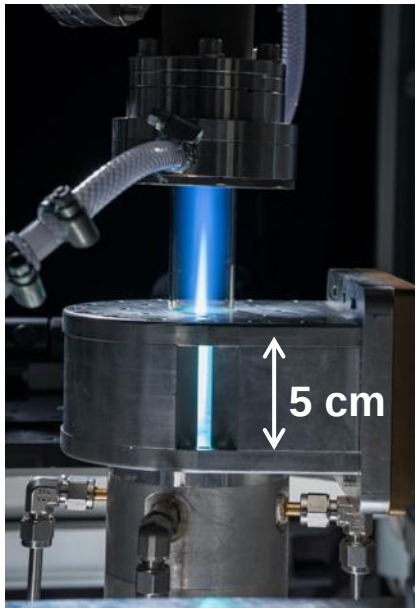

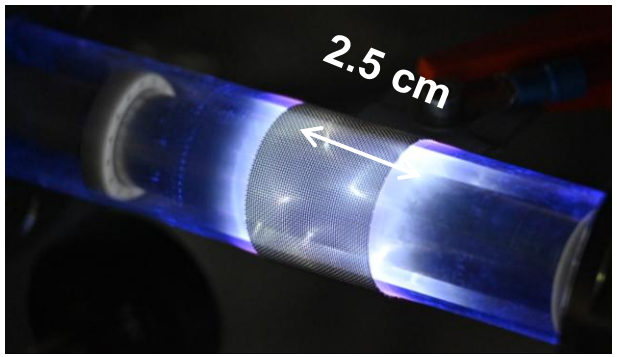

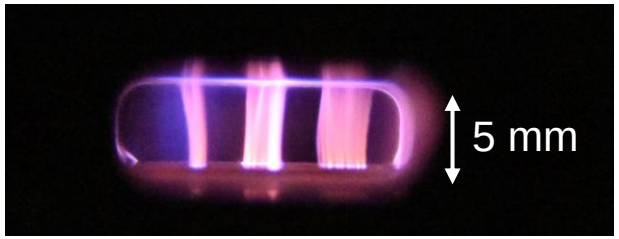

Power: 0.2 – 1.2 kW	Power: 0.3 – 6 kW	Power: < 500 W

Covering a wide pressure range
Example: DBD

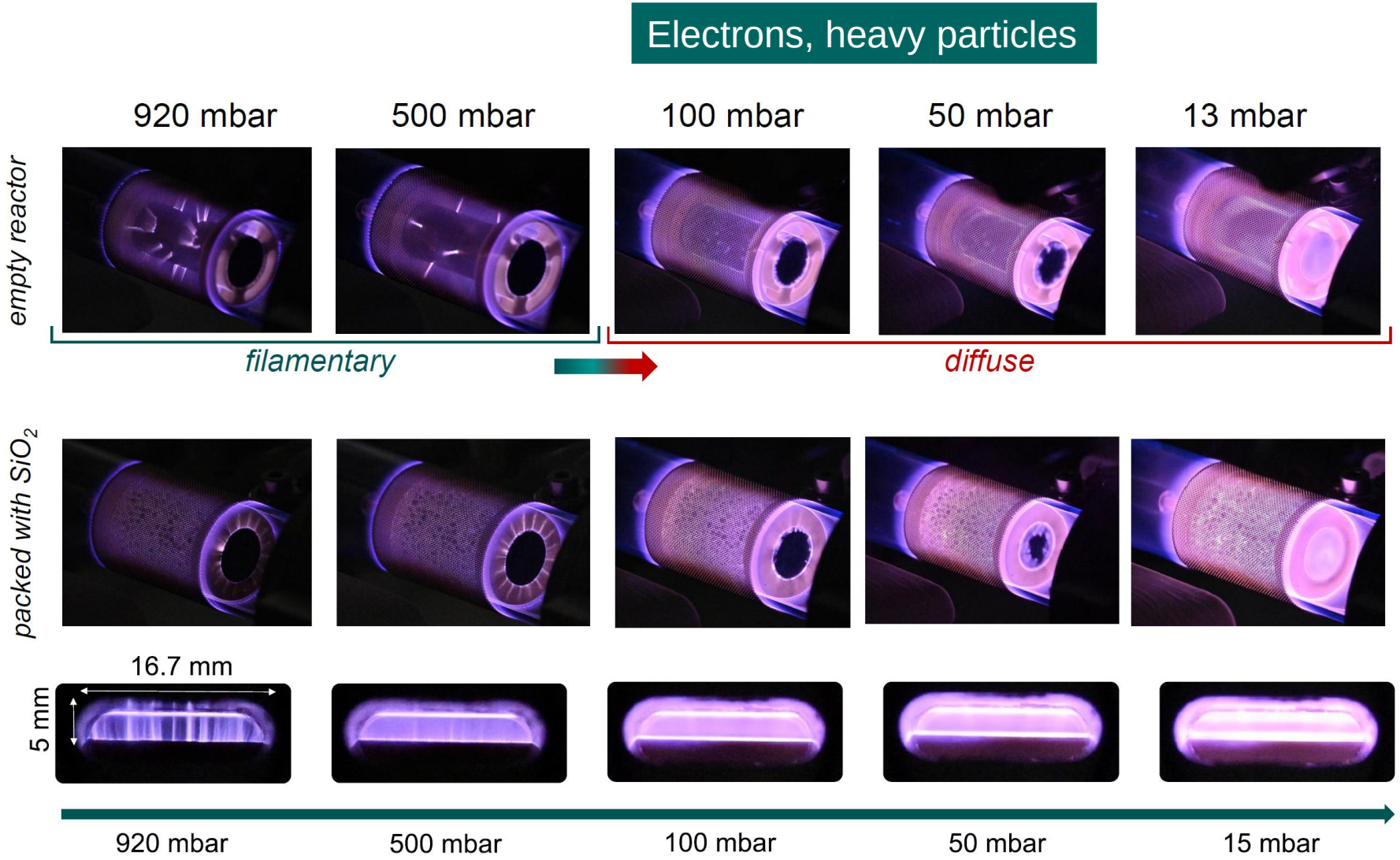

R. Antunes et al, in preparation

A. Ben Yaala, under investigation

Rationale

- Enhancing the impact of electron collisions
- Performance analysis in a wide pressure range
- Improved diagnostic capabilities

Covering a wide pressure range
Temperatures measured from molecular emission

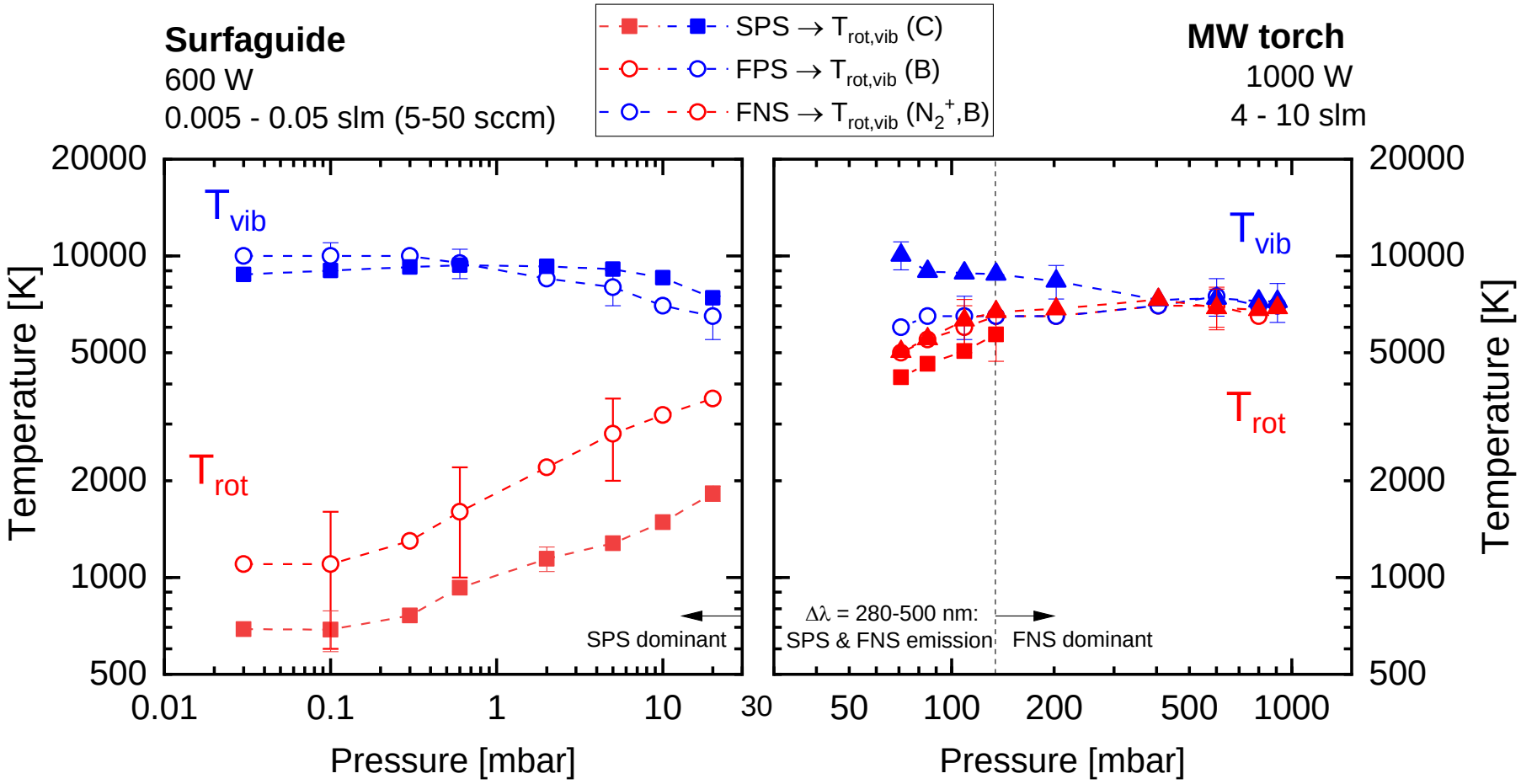

Electron driven

Electrons, heavy particles

Thermal driven

An example of an application
CO_2 conversion in a MW torch

Power

Gas

The building block

Plasma reactor

$CO_2 \rightarrow CO + ½\ O_2$

O_2

Separation step

CO_2, CO

Next process step(s)

Syngas / Synthetic fuels

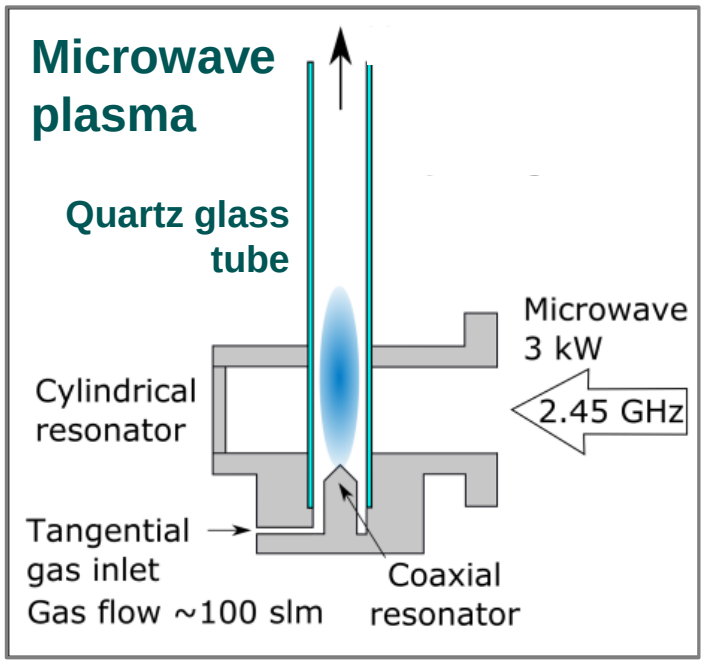

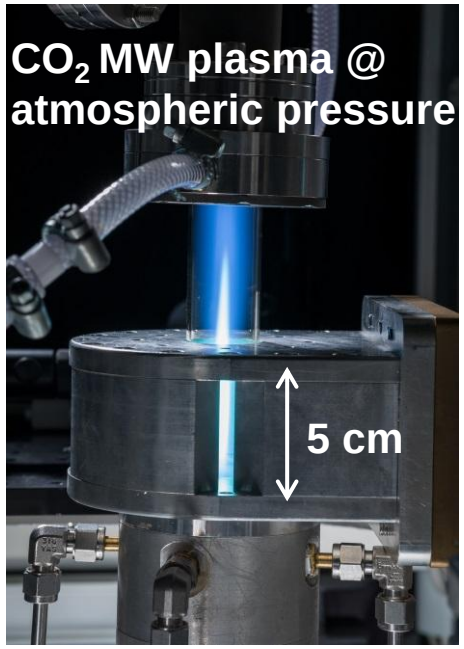

Emission spectroscopy as diagnostic tool

Example: dry reforming of methane in MW torch $CH_4 + CO_2 \rightarrow 2CO + 2H_2$

High resolution Echelle spectrometer

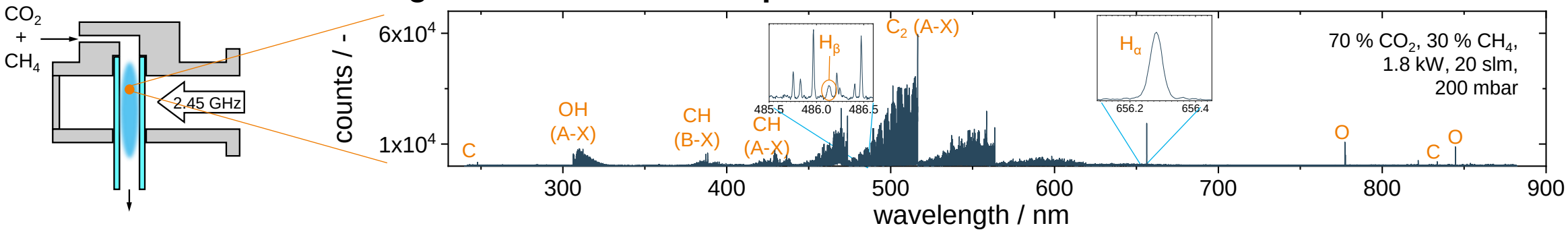

Rotational and vibrational temperatures

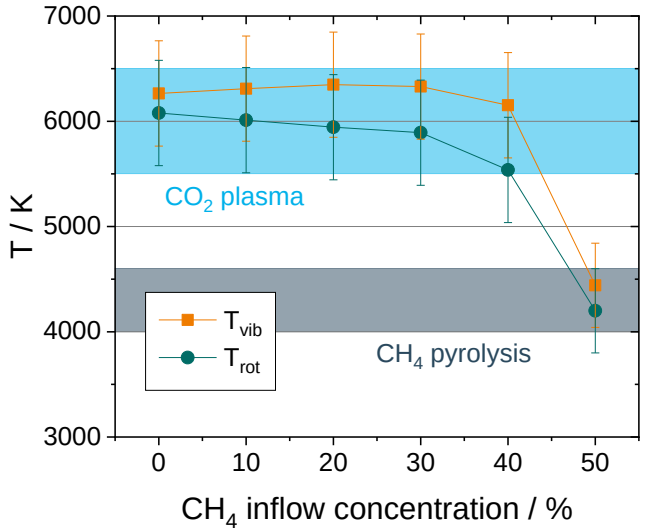

H lineshape analysis

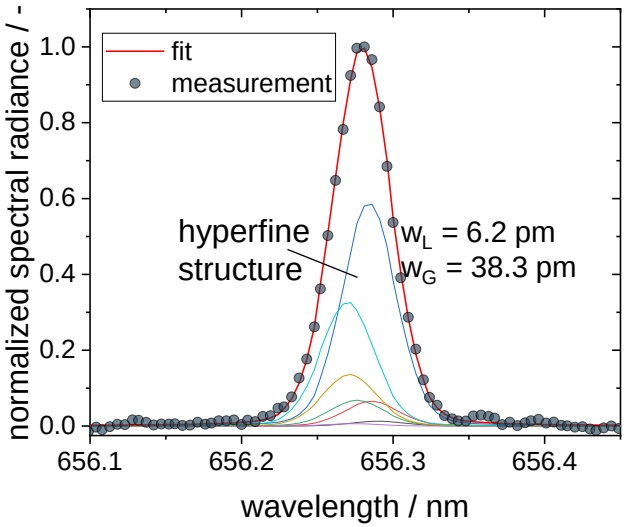

n_e from Stark broadening

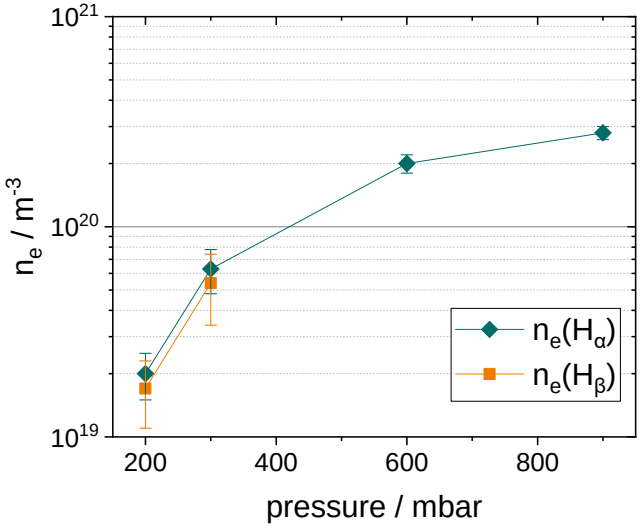

RF discharges
Low pressure plasmas

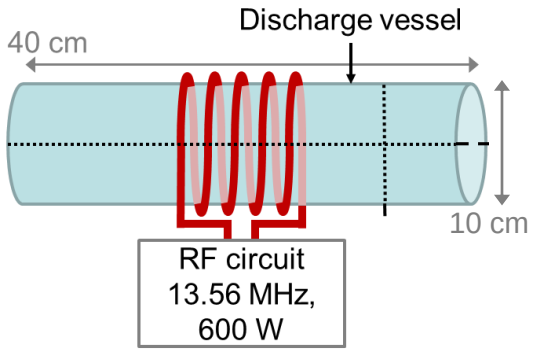

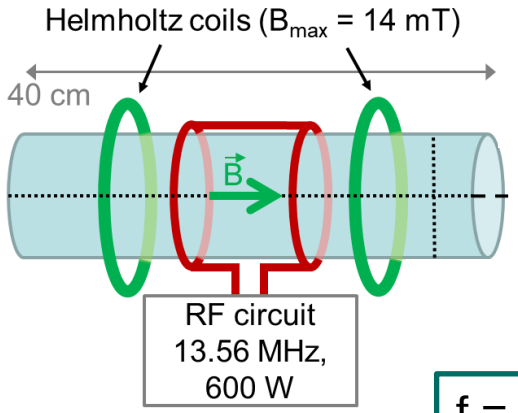

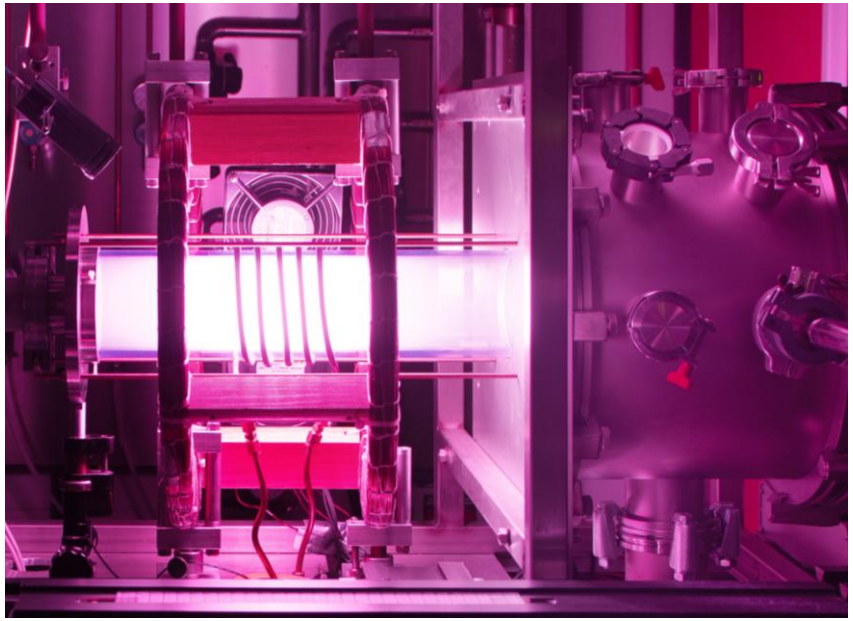

f = 1 -27.12 MHz
$P_{RF} \leq 2$ kW
p = 1 – 100 Pa

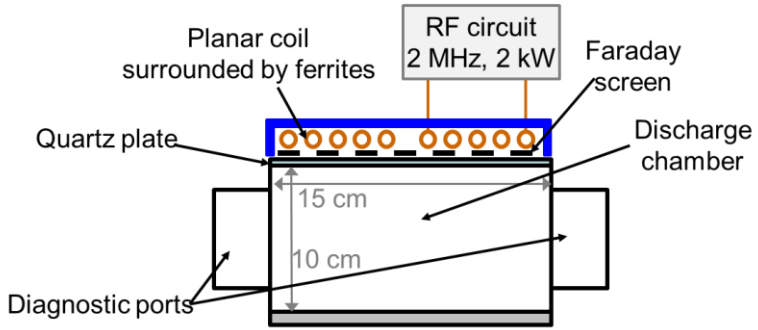

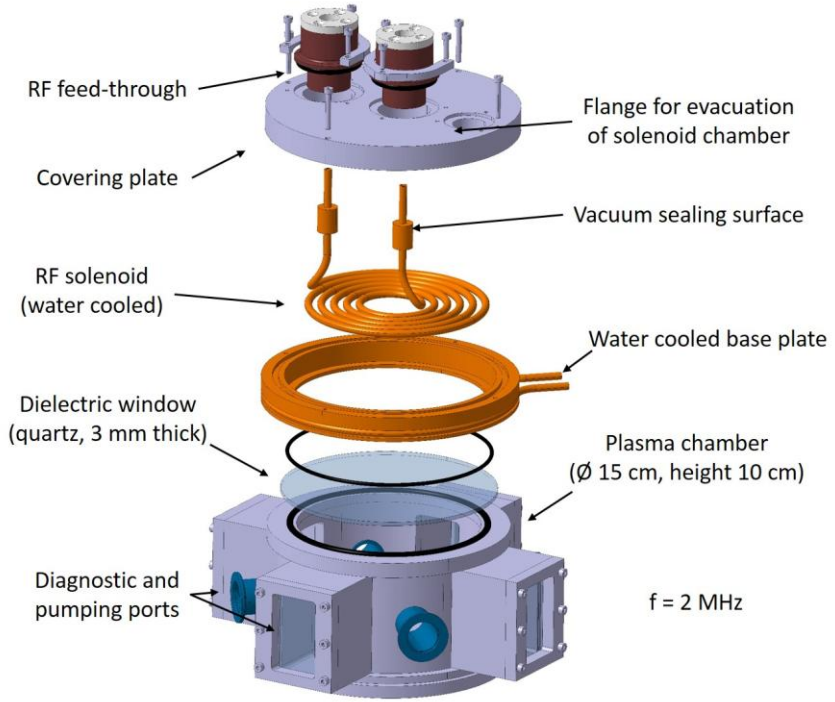

Powerful ICPs
H^- ion source at 0.3 Pa

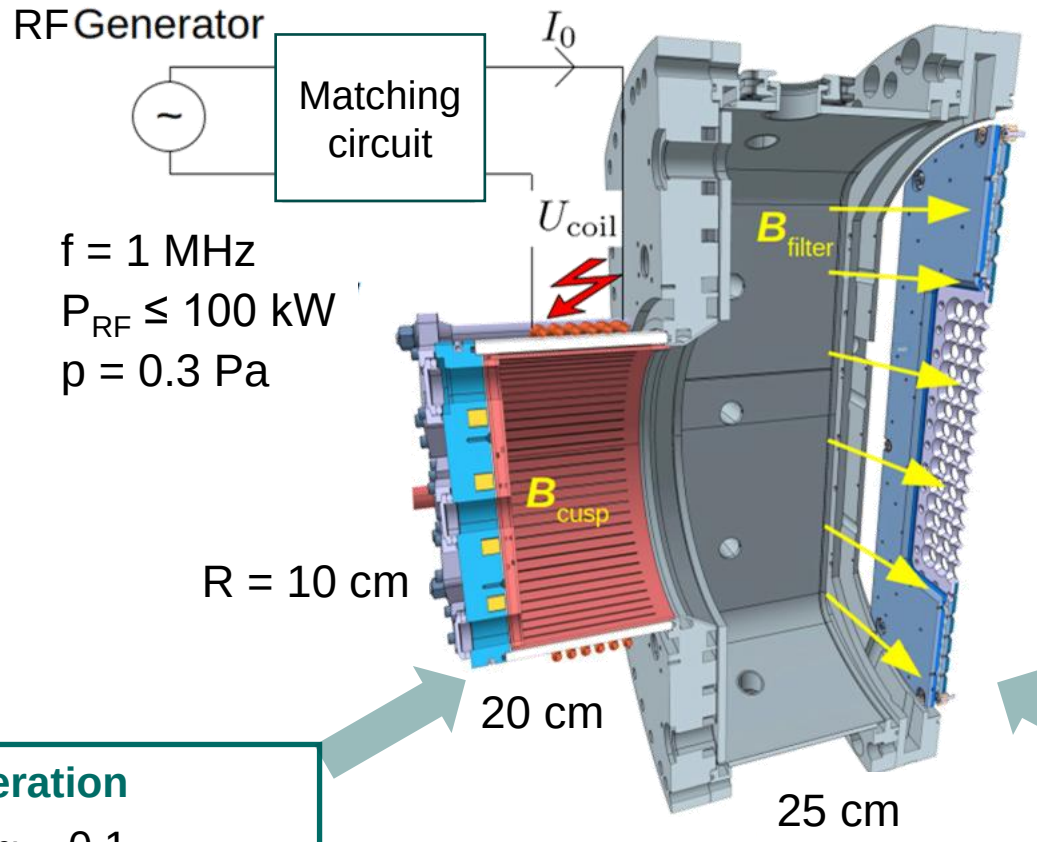

Plasma generation
- Ionisation: $\alpha \approx 0.1$
- Dissociation: $H/H_2 \approx 0.2$
- **$T_e \approx 10$ eV, $n_e \approx 5\times10^{18}$ m^{-3}**

Magnetic filter field
grad-B drifts

H^- generation
- **$H^-/n_e \approx$ 0.1 – 5**
- Dissociation: $H/H_2 \approx 0.2$
- **$T_e \approx 2$ eV, $n_e \approx 6\times10^{16}$ m^{-3}**

Hydrogen plasmas

Low temperature hydrogen plasmas

H_2, H, H^+, H_2^+,H_3^+, e

$T_e \approx 10$ eV ⟶ below 1 eV

$n_e \approx 10^{15}$ m^{-3} ⟶ 10^{22} m^{-3}

Ionising ⟶ recombining plasma

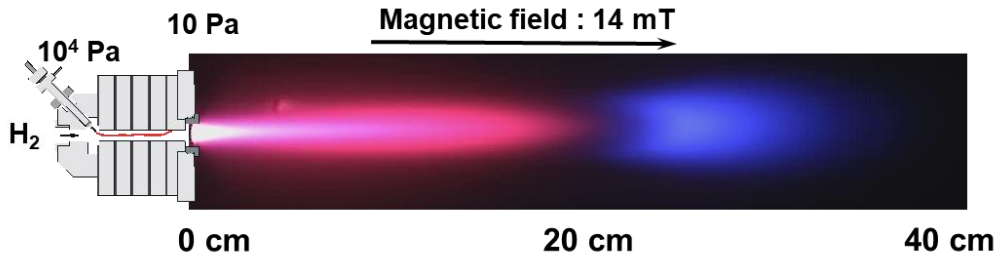

Linear plasma device: cascaded arc

TU/e EINDHOVEN UNIVERSITY OF TECHNOLOGY

Divertor plasmas

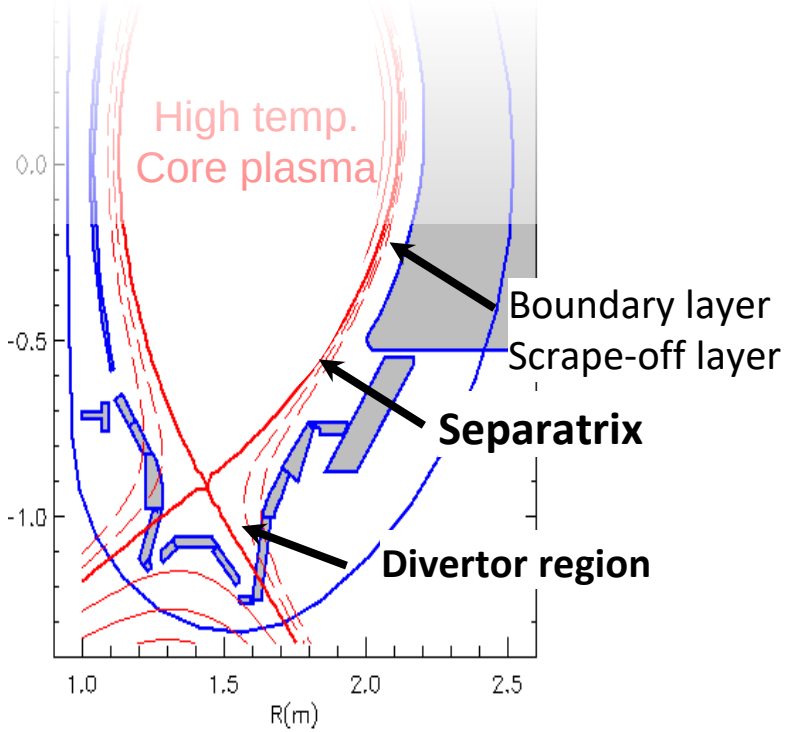

H^- source

0.3 Pa

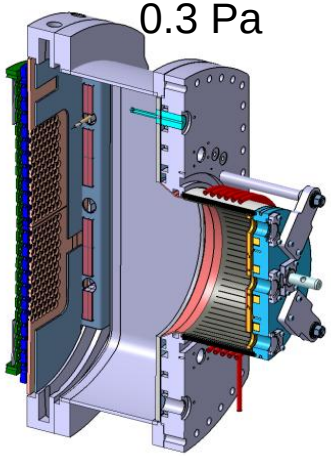

area: 0.52 x 0.26 m²

& Plasmas for plasma technology

ICP, ECR, DBD, MW torch, Surfaguide, …

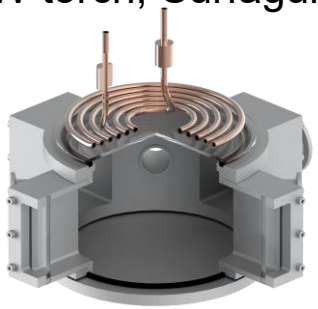

∅ = 15 cm
h = 10 cm

Hydrogen spectra
Emission of H_2 and H particles (OES)

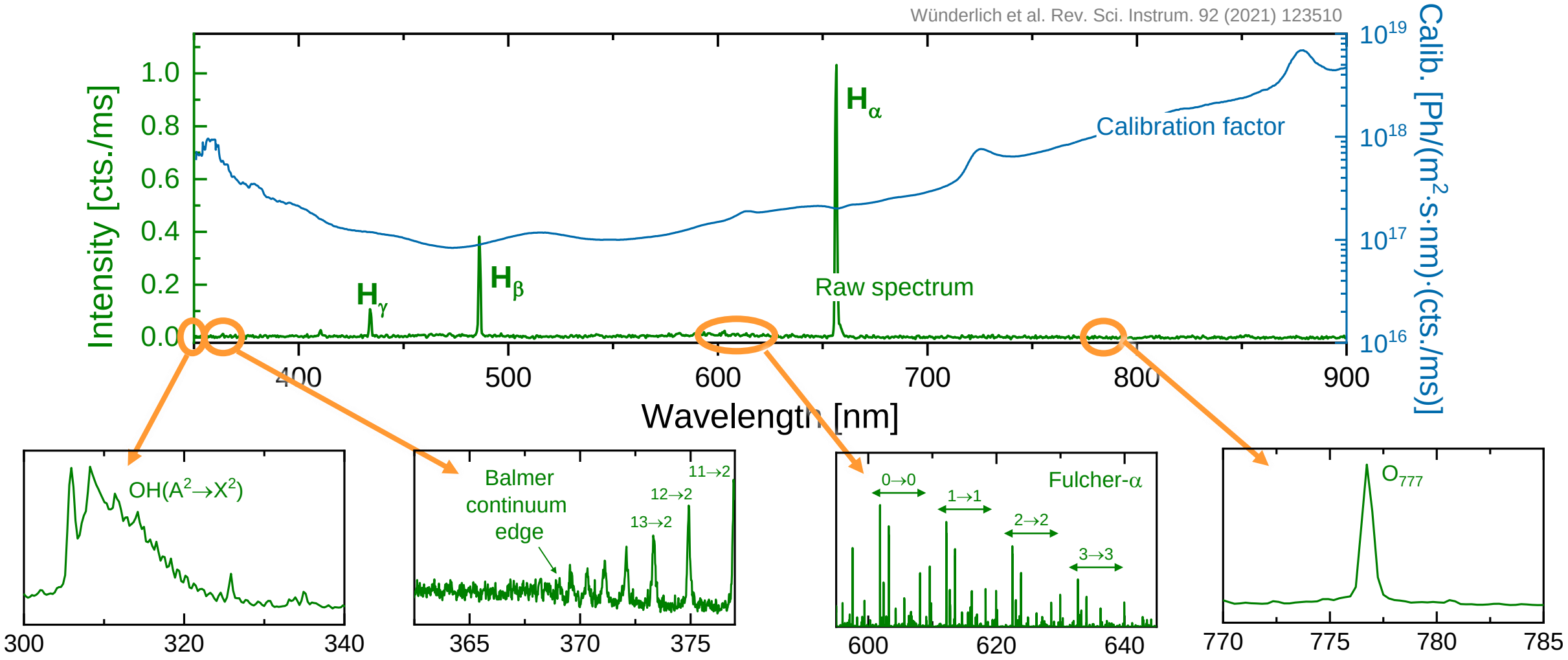

Hydrogen spectra

Emission of H_2 and H particles (OES extended by VUV)

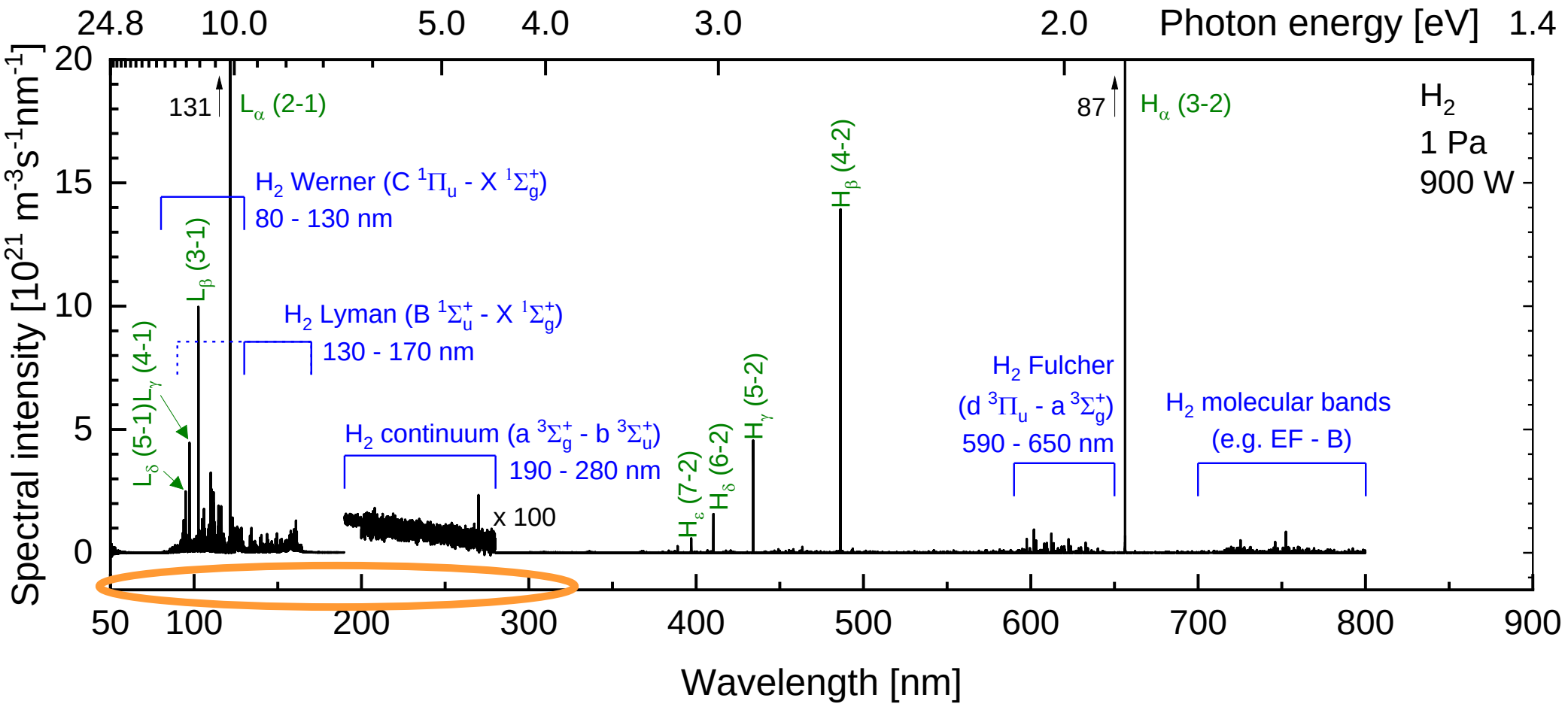

Wünderlich et al. Rev. Sci. Instrum. 92 (2021) 123510
Friedl et al., Meas. Sci. Technol. 34 (2023) 055501

Quantitative analysis by collisional radiative (CR) modelling

Population density of excited state p

Hydrogen atom & molecule

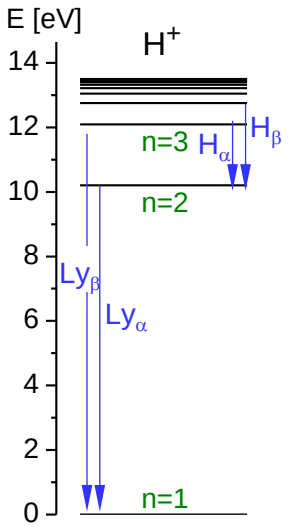

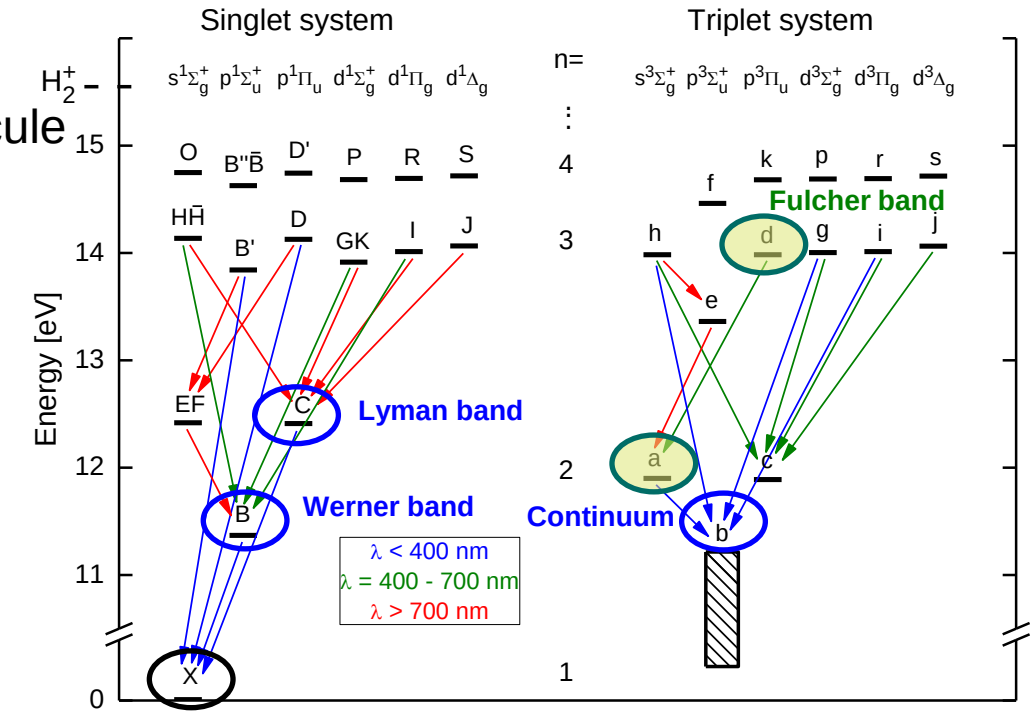

Set of ordinary differential equations
→ flexible solver Yacora

Quality of results correlates with accuracy of reaction probabilities

CR models for atomic hydrogen & molecular hydrogen
→ electronically resolved
→ X^1 vibrationally resolved
→ vibrationally resolved
→ ro-vibrationally resolved for selected transitions

Wünderlich et al. JQSRT 240 (2020) 106695

populating processes — de-populating processes

$$\frac{dn_p}{dt} = n_e[n_X X_{Xp}(T_e) + \sum_{q<p} n_q X_{qp}(T_e) + \sum_{q>p} n_q X_{qp}(T_e)] + \sum_{q>p} n_q A_{qp} - n_e[\sum_{q<p} n_p X_{pq}(T_e) + \sum_{q>p} n_p X_{pq}(T_e)] - \sum_{p>q} n_p A_{pq} - \sum_i n_i n_p X_{i,loss}(T_e)$$

direct excitation | stepwise exc. | coll. cascades | rad. cascades | down coll. | up coll. | radiation | further losses

CR model for atomic hydrogen – Coupling to other species

Ionising and recombining plasma regions & ion-ion plasma

Requires coupling to all hydrogen species in a CR model

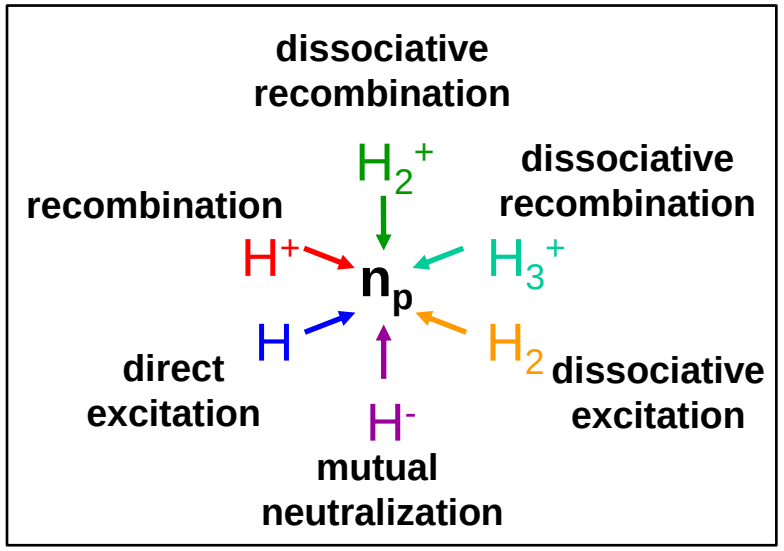

Ionizing plasma

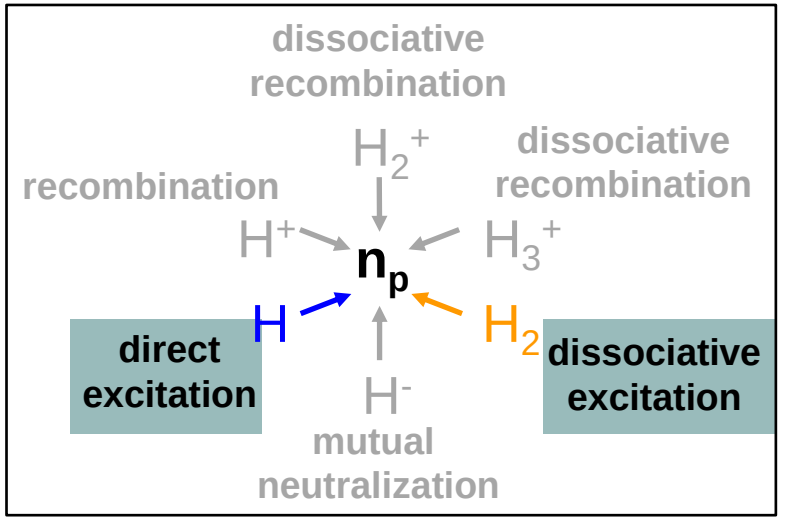

Recombining plasma

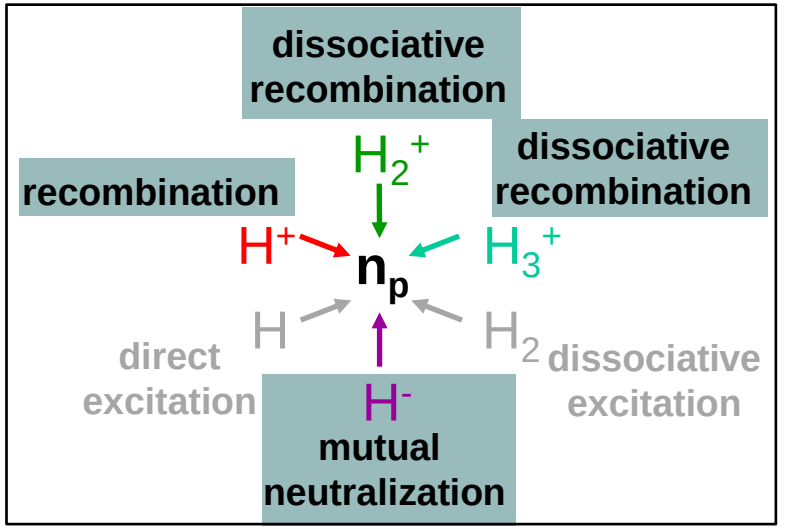

CR model: Yacora H

Wünderlich et al. Atoms. 4 (2016)26

Yacora on the Web: www.yacora.de

CR model for atomic hydrogen
Quantitative analysis

Negative hydrogen ion source

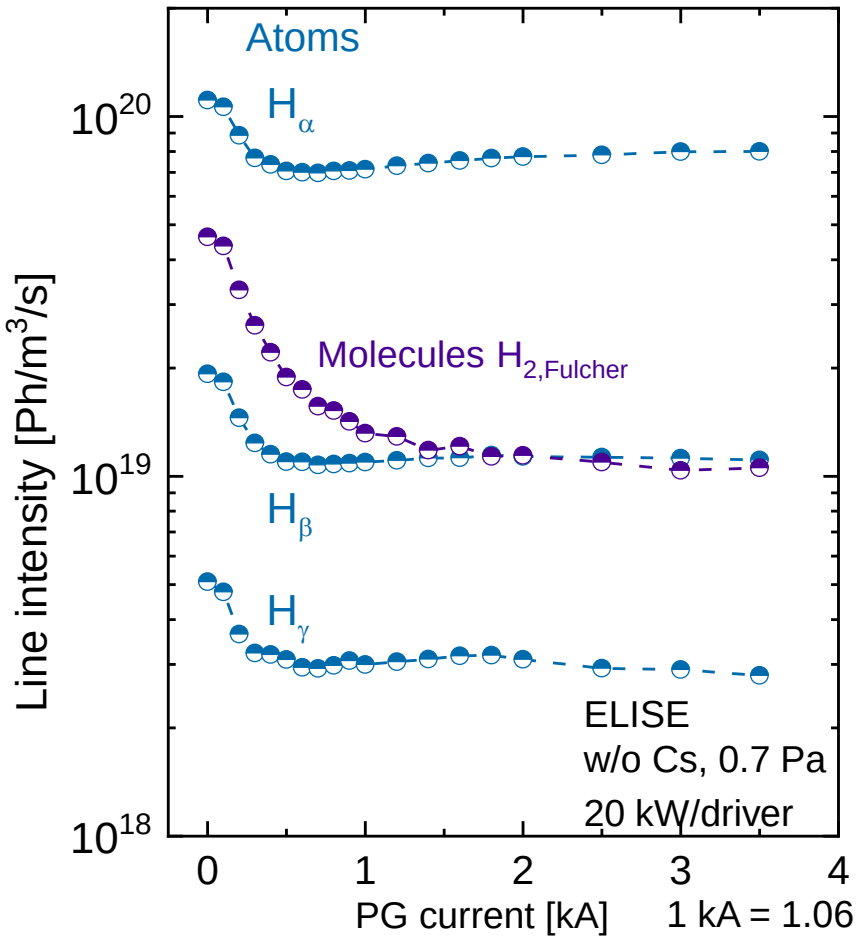

H^- source for NBI

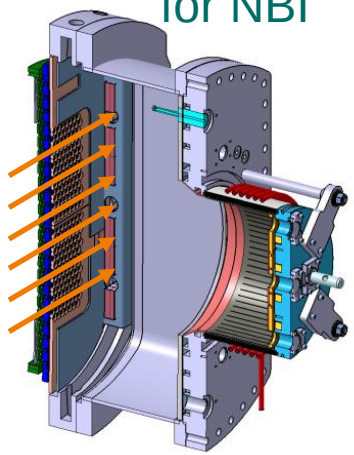

Magnetic filter field

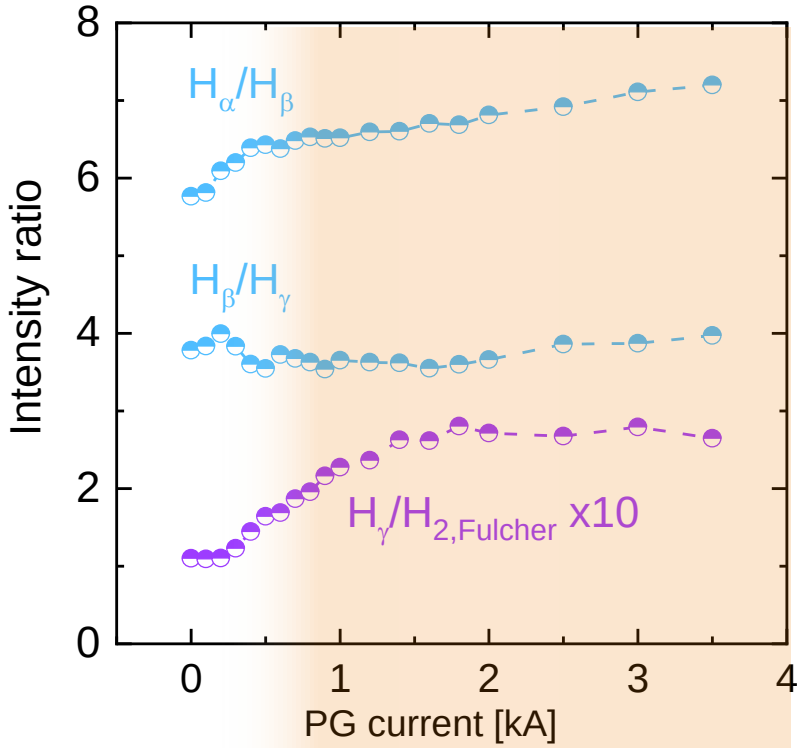

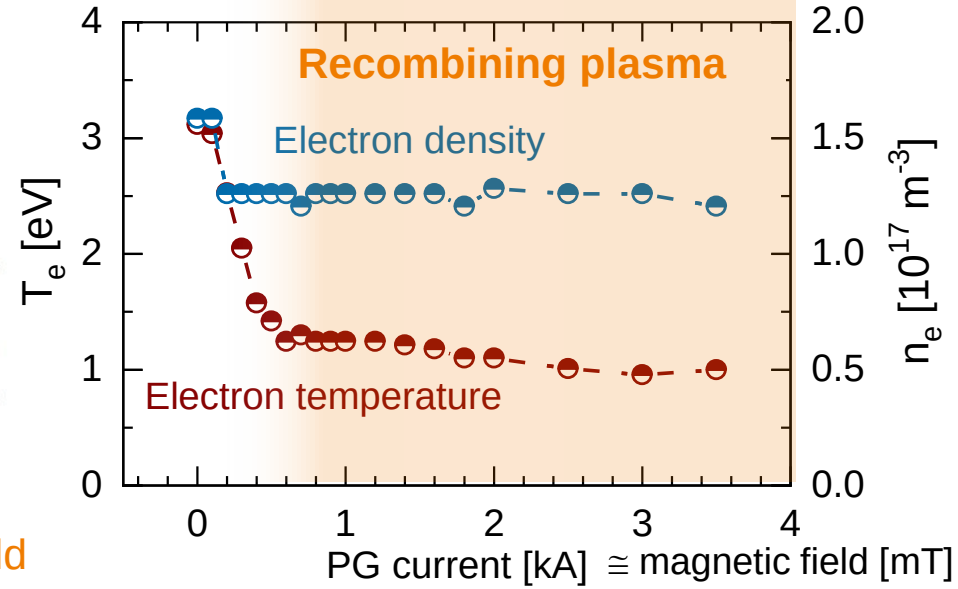

CR model for atomic hydrogen
Opacity of Lyman lines, self-absorption

Influences VUV radiation (photo-induced ionization) and Balmer emission

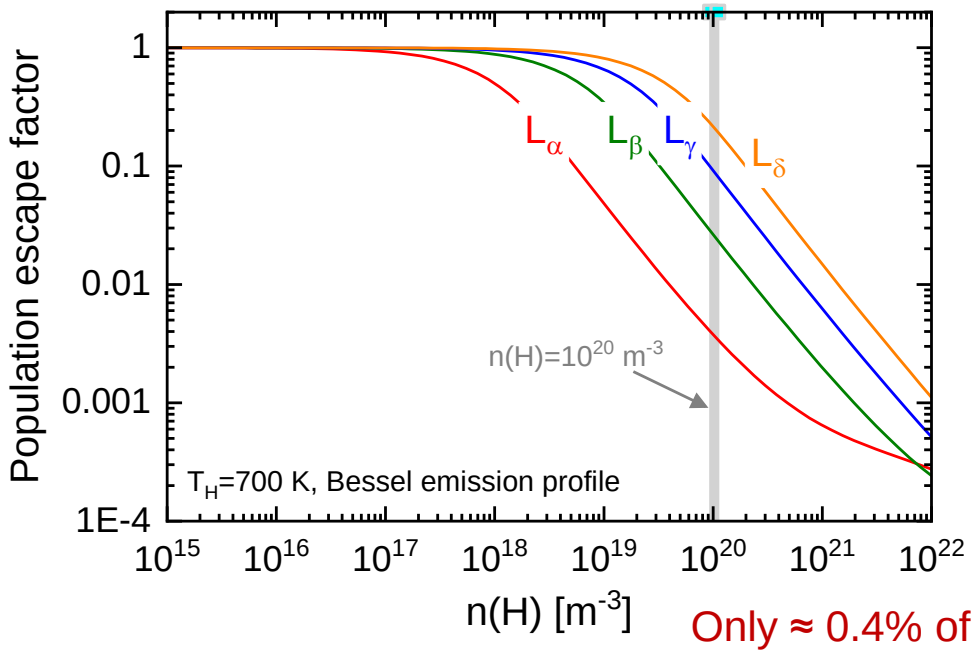

Only ≈ 0.4% of L_α radiation escapes!

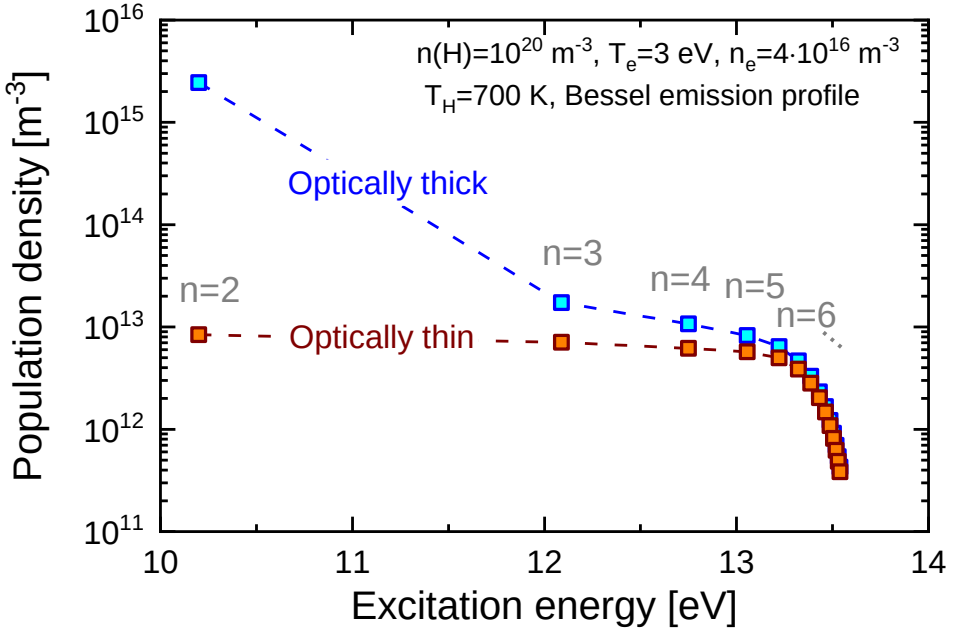

For divertor plasmas implemented in EIRENE photon module

Reiter et al, PPCF 44 (2002) 1723

CR models for molecular hydrogen
The Yacora family

Richard Bergmayr, PhD thesis, Augsburg University 2025

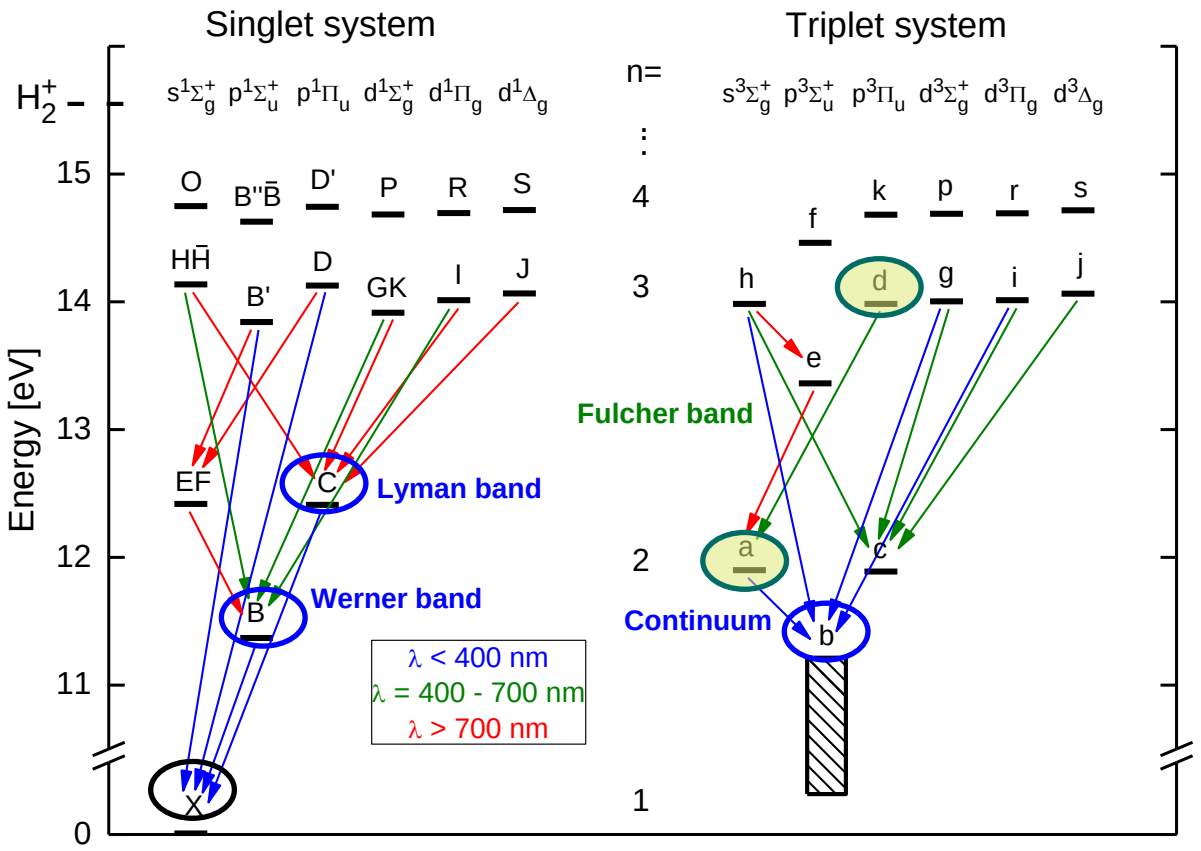

Electronic CR models

- Triplet system
- Singlet system
- Combined electronic model

Yacora-H2

Vibrationally resolved CR models

- Vibrationally resolved CR model for X^1

Yacora-H2(X1,v)

- Vibrationally resolved CR model for entire H_2 system

Yacora-H2(v)

Ro-vibrationally resolved models

- Corona model for Fulcher-α band

Yacora-H2(v,N)-Fulcher

- Extended corona model

Benchmarking

- Laboratory experiments
- Negative ion sources
- Linear devices
- Divertor plasmas
- EIRENE code, SOLPS-ITER code

Evaluation of the input data basis
Electronic CR models – Yacora-H2

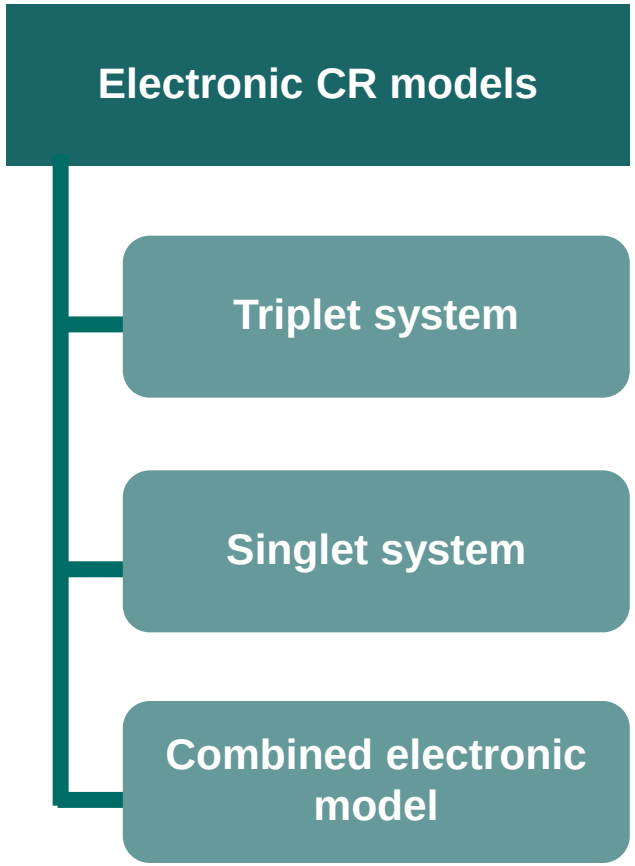

Electron impact excitation

$e + H_2(n) \rightarrow e + H_2(n')$

❶ Miles data set: semi empiric cross sections
Miles et al, J. Appl. Phys. 43 (1972) 678

❷ Janev: summary of measurements and calculations
Janev et al, Report JÜL-4105 (2003)

❷ Celiberto: calculations for a few transitions, 2001.
Celiberto et al. ADNDT 77, (2001)

} significant inconsistencies

❸ MCCC: molecular convergent close-coupling method in the adiabatic-nuclei formulation, fully quantum mechanical
Scarlett et al, ADNDT 137 (2021) 101361

→ close collaboration with Fursa group, Curtin University, Australia

Evaluation of the input data basis
Electronic CR models – Yacora-H2

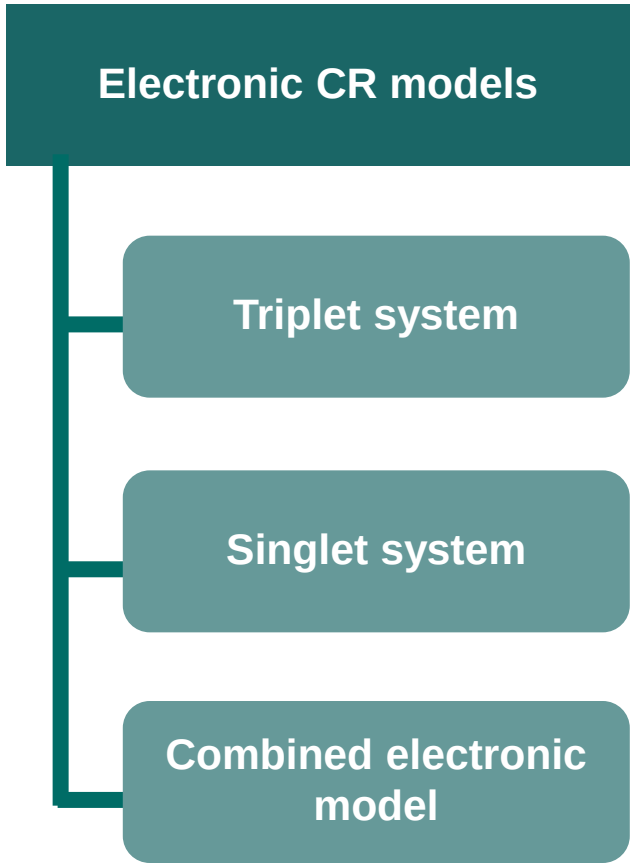

Electron impact excitation

$e + H_2(n) \rightarrow e + H_2(n')$

❶ Miles data set:

Miles et al, J. Appl. Phys. 43 (1972) 678

❷ Janev:

Janev et al, Report JÜL-4105 (2003)

❷ Celiberto:

Celiberto et al. ADNDT 77, (2001)

❸ MCCC:

Scarlett et al, ADNDT 137 (2021) 101361

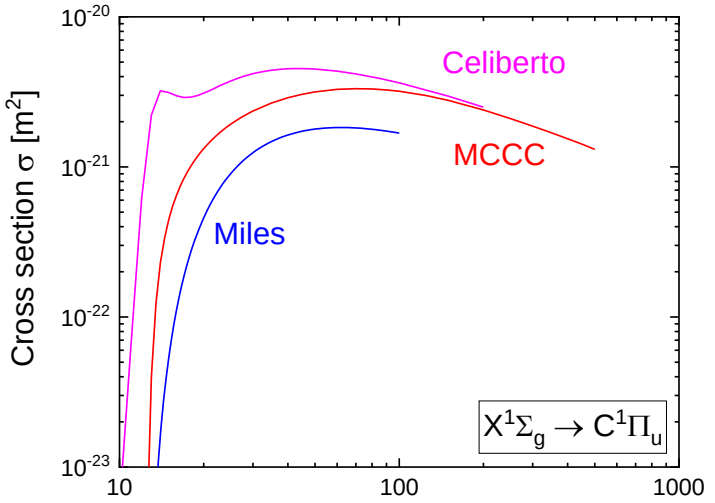

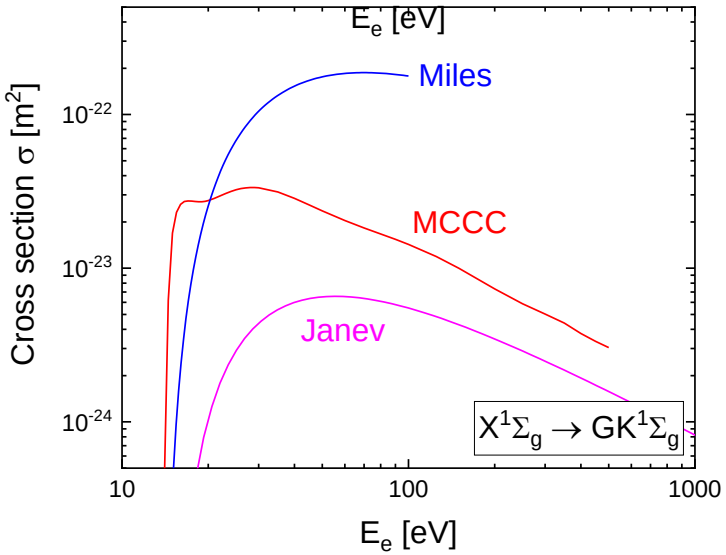

Improvement in the input data basis
Electronic CR models – Benchmark

ICP plasma, lab experiment

- T_e and n_e from Langmuir probe
- Electron densities < 10^{17} m^{-3}

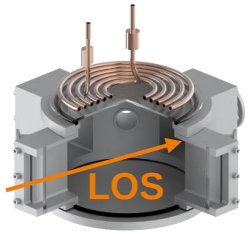

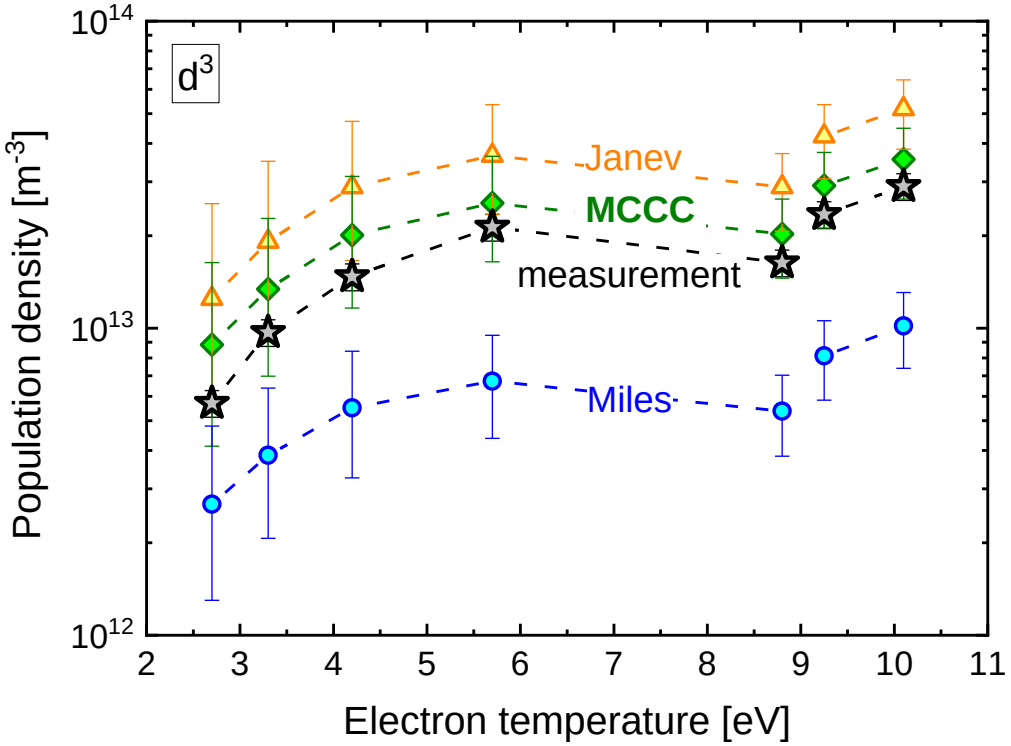

Wünderlich et al. 2021 J. Phys. D 54

Impact of data used in the analysis on density ratio

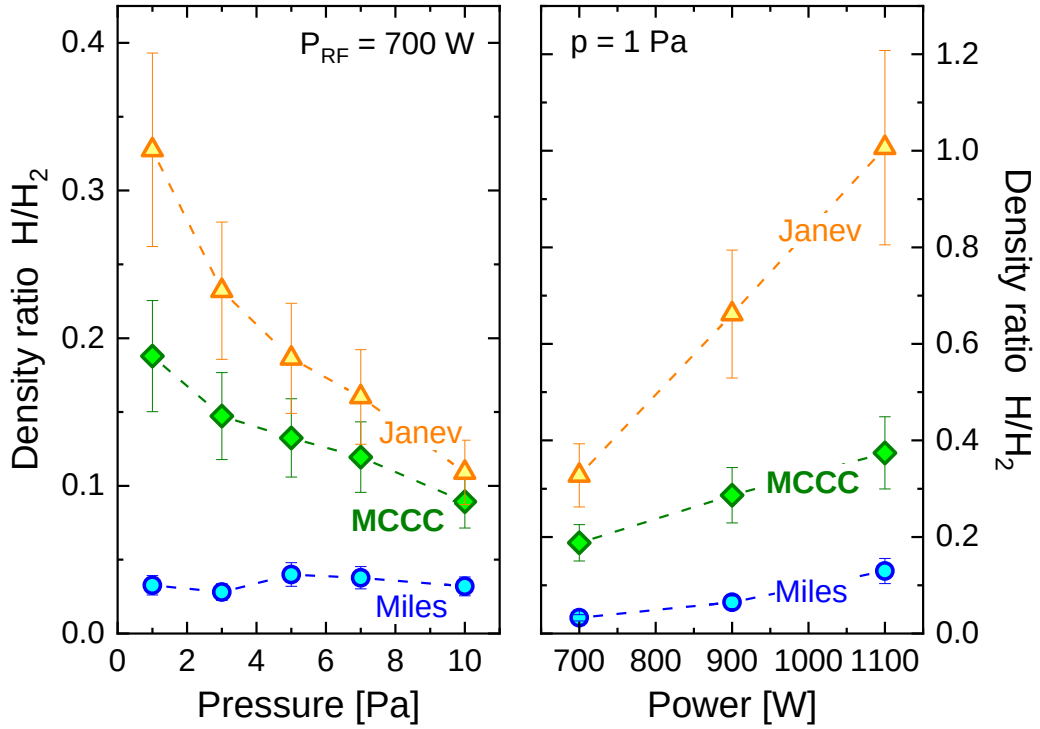

Improvement in the input data basis
Electronic CR models – Spin mixing

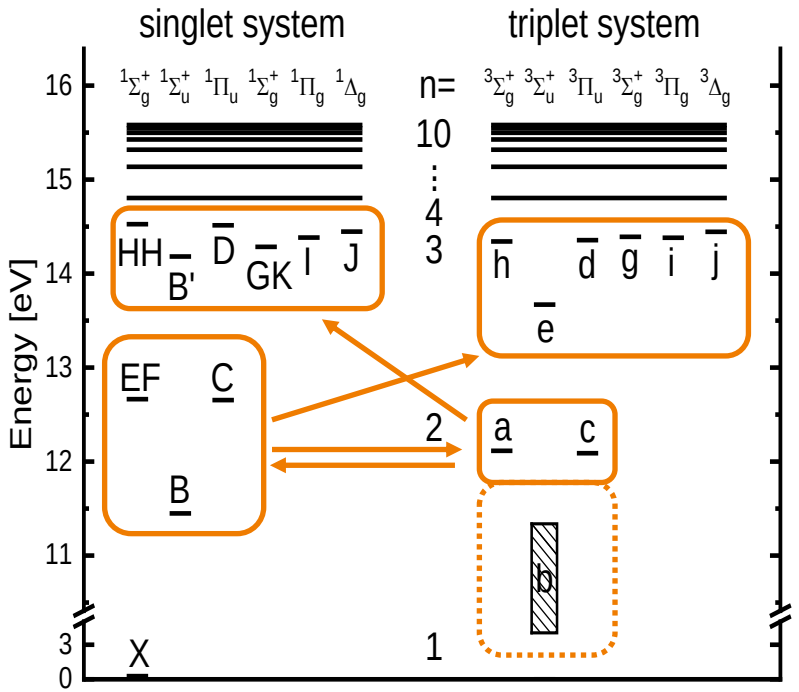

$e + H_2(n=2)_{singlet} \rightarrow e + H_2(n=2,3)_{triplet}$

$e + H_2(n=2)_{triplet} \rightarrow e + H_2(n=2,3)_{singlet}$

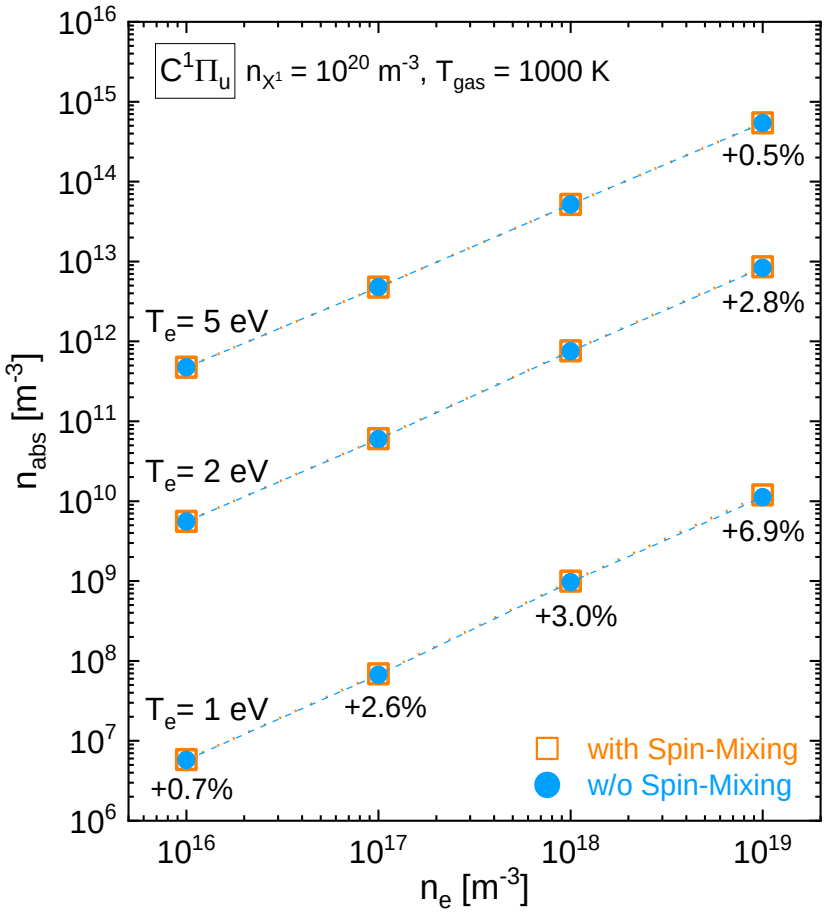

$$\frac{(n_{with} - n_{without})}{n_{without}}$$

Influence rather small but most pronounced for low T_e and high n_e.

Use of separate electronic models (singlet and triplet) sufficient

Vibrationally resolved CR model for X^1
Yacora-H2(X1,v)

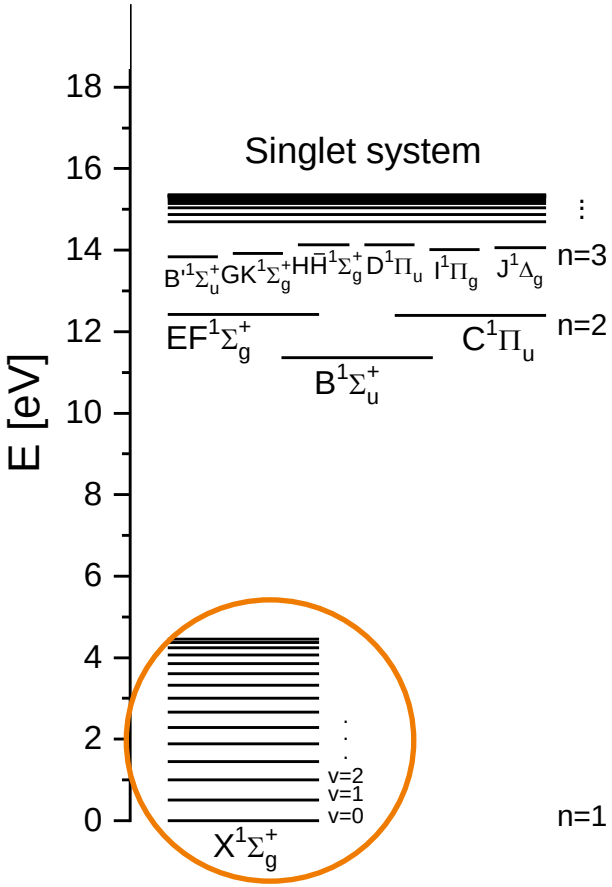

Measurement via
Fulcher band emission

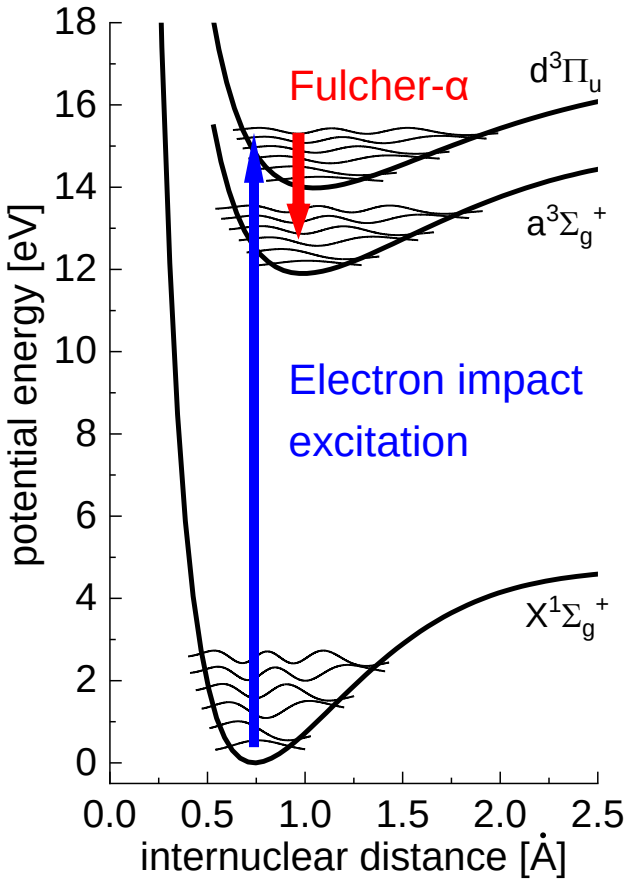

Ro-vibrational population
in the ground state

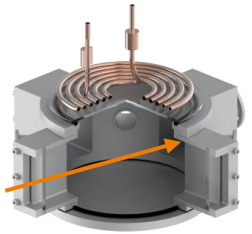

Briefi et al. 2020 Plasma Sources Sci. Technol. 29

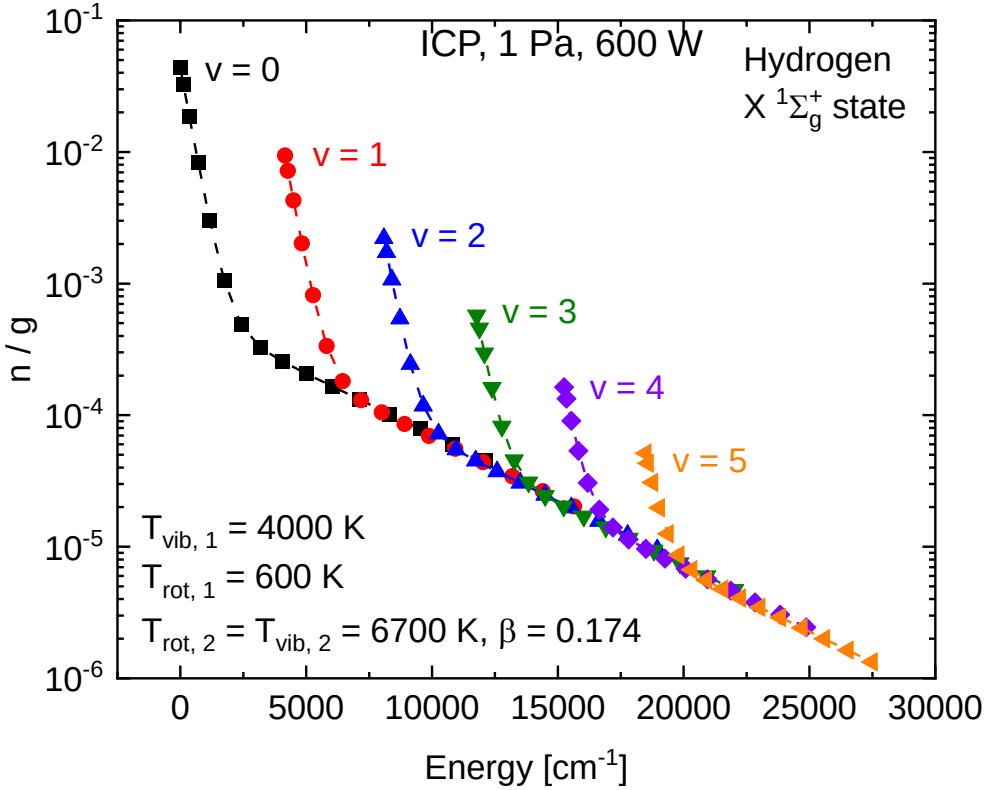

Vibrationally resolved CR model for X^1
Yacora-H2(X1,v)

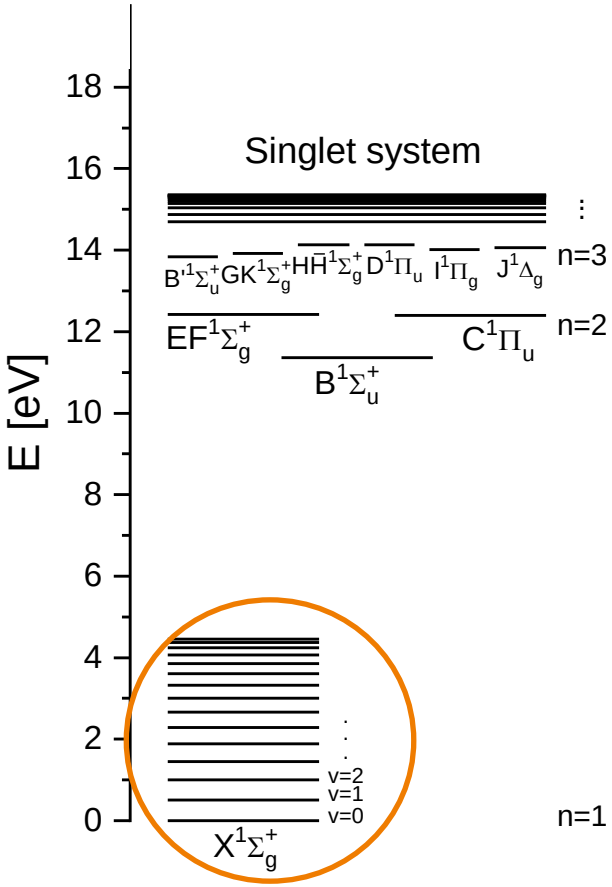

Measurement via
Fulcher band emission

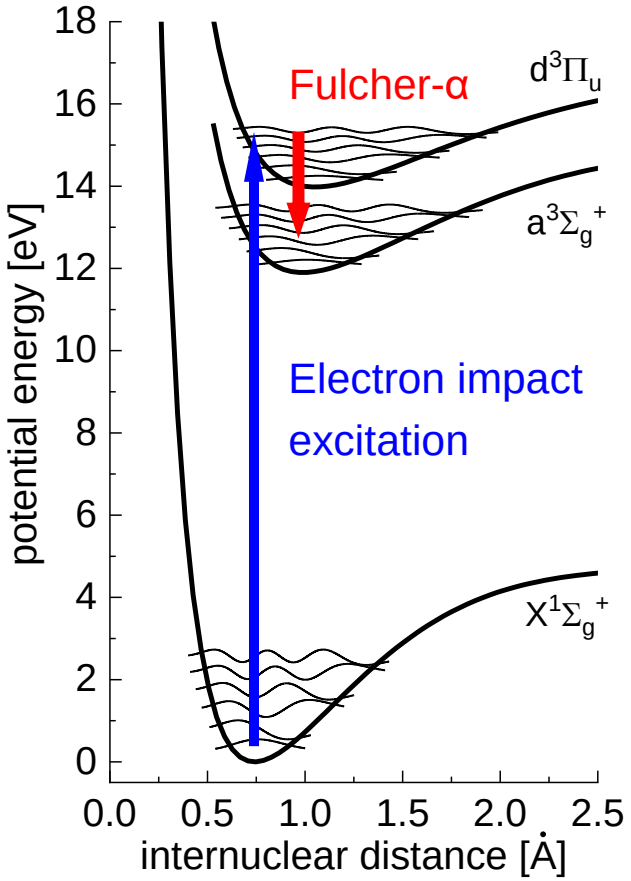

Low pressure plasma, H^- source
T_e = 2.5 eV, $n_e = 6 \cdot 10^{16}$ m^{-3}

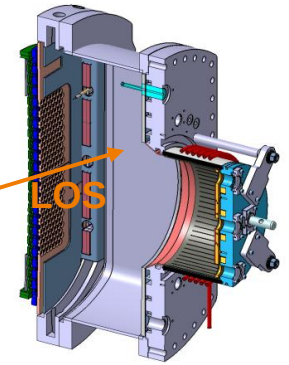

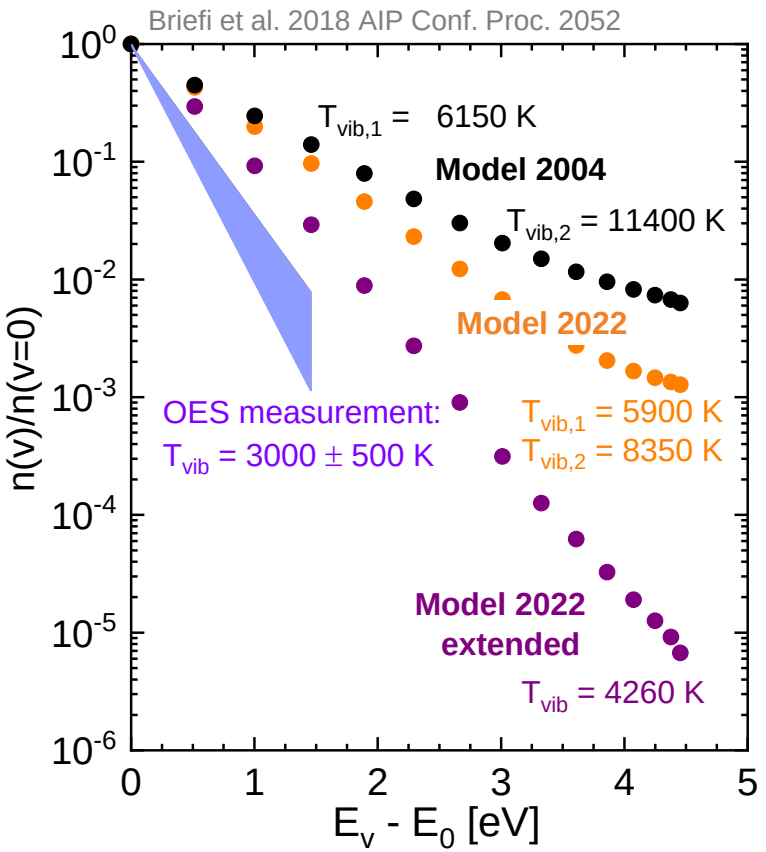

Vibrationally resolved CR model for X^1
Yacora-H2(X1,v)

Relevance of transport
$H_2(v)$ are metastable states

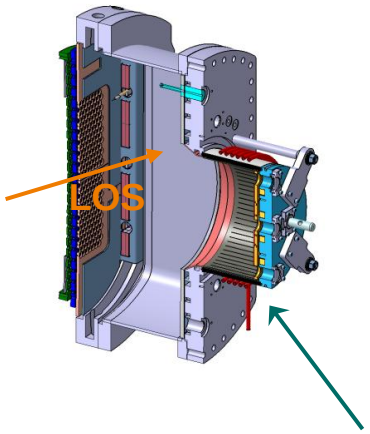

$H_2(v)$ are created in the driver

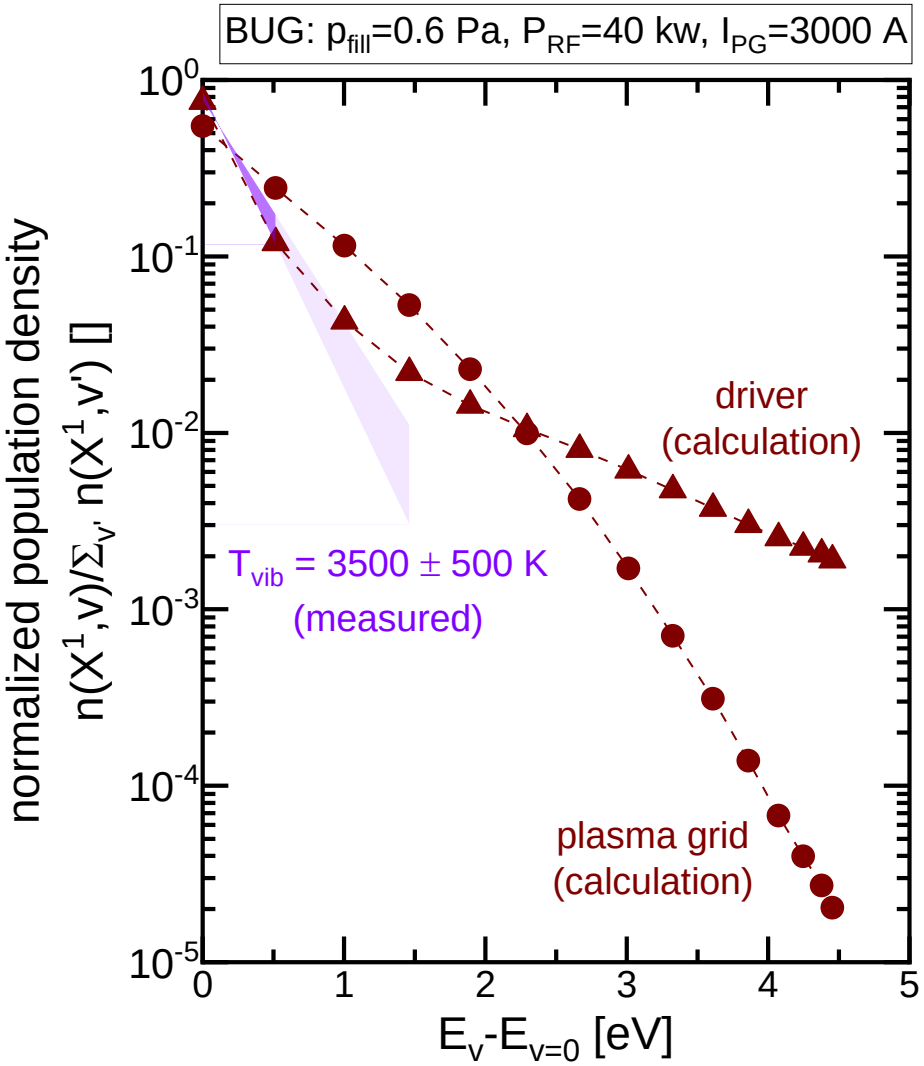

Fulcher	PG	driver
T_{vib}	3500 K	3500 K
T_{gas}	820 K	800 K
$T_{vib/rot\ 2}$	6410 K	4720 K
β	0.51	0.41

Yacora H	PG	driver
T_e	2.1 eV	8 eV
n_e	7 10^{16} m^{-3}	10^{18} m^{-3}
n_{H2}	4.8 10^{19} m^{-3}	8 10^{19} m^{-3}
n_H	1 10^{19} m^{-3}	1.5 10^{19} m^{-3}
n_{H+}	3 10^{16} m^{-3}	5 10^{17} m^{-3}
n_{H2+}	3 10^{16} m^{-3}	5 10^{17} m^{-3}
n_{H-}	1 10^{15} m^{-3}	0 m^{-3}
T_H	5600 K	5900 K

Ro-vibrationally resolved Corona model
Yacora-H2(v,N)-Fulcher

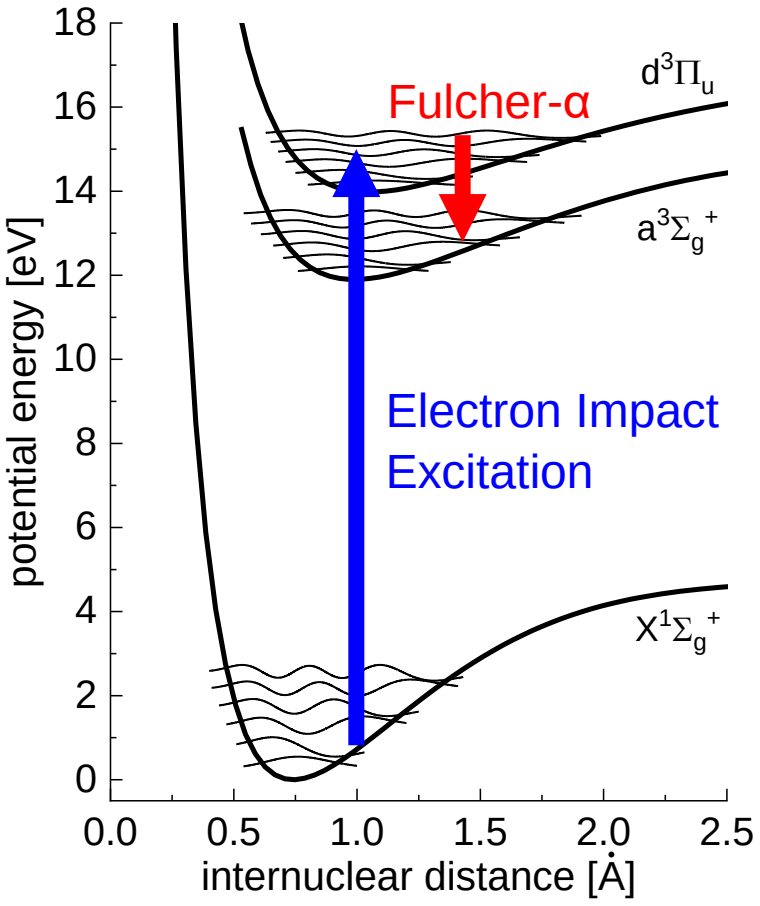

- Ground state n(X^1, v, N) according to two-temperature distribution

$$n(X^1, v', N') = n_{H2}\,[(1-\beta)\,\tilde{n}_{rot}(v', N', T_{gas})\,\tilde{n}_{vib}(v', T_{vib1}) + \beta\,\tilde{n}_{rot}(v', N', T_{rot2})\,\tilde{n}_{vib}(v', T_{rot2})]$$

- Rate equation: $\frac{dn_p}{dt} = \sum_{q<p} X_{qp} n_q n_e - \sum_{q<p} A_{pq} n_p$

Electron Impact Excitation (EIE)
e + $H_2(X^1,v,N)$ → e + $H_2(d^3,v',N')$
Spontaneous Emission
$H_2(d^3,v',N')$ → $H_2(a^3,v'',N'')$ + hf

- Separate treatment of d^3(v,N)+ and d^3(v,N)- (selection rules)
- 45 259 fully ro-vibrationally resolved MCCC cross sections applied

Scarlett et al. 2023 Phys. Rev. A 107

Improvement in the input data basis
Ro-vibrationally resolved Corona model – Yacora-H2(v,N)-Fulcher

Benchmark with spectra from lab experiment (ICP, p = 1.1 Pa, P_{RF} = 700 W)

T_e = 8.8 eV, n_e=1.84 10^{16} m^{-3} from Langmuir probe

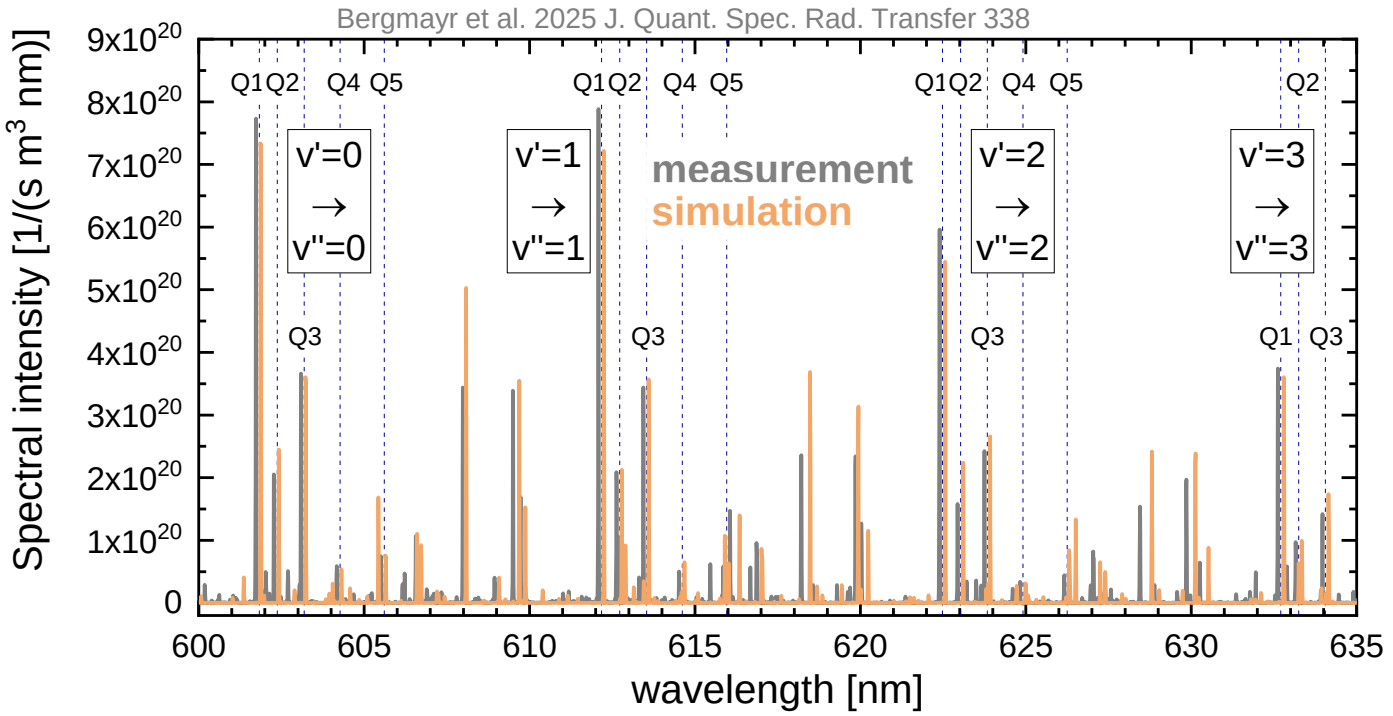

- Excellent agreement in absolute values
- Previous model → factor 3 higher emissivity
- Q-lines show general agreement

Ro-vibrationally resolved Corona models

Yacora-H2(v,N)-Fulcher, -Werner, -Lyman

Applicability of Corona model

→ check with **electronic CR model**

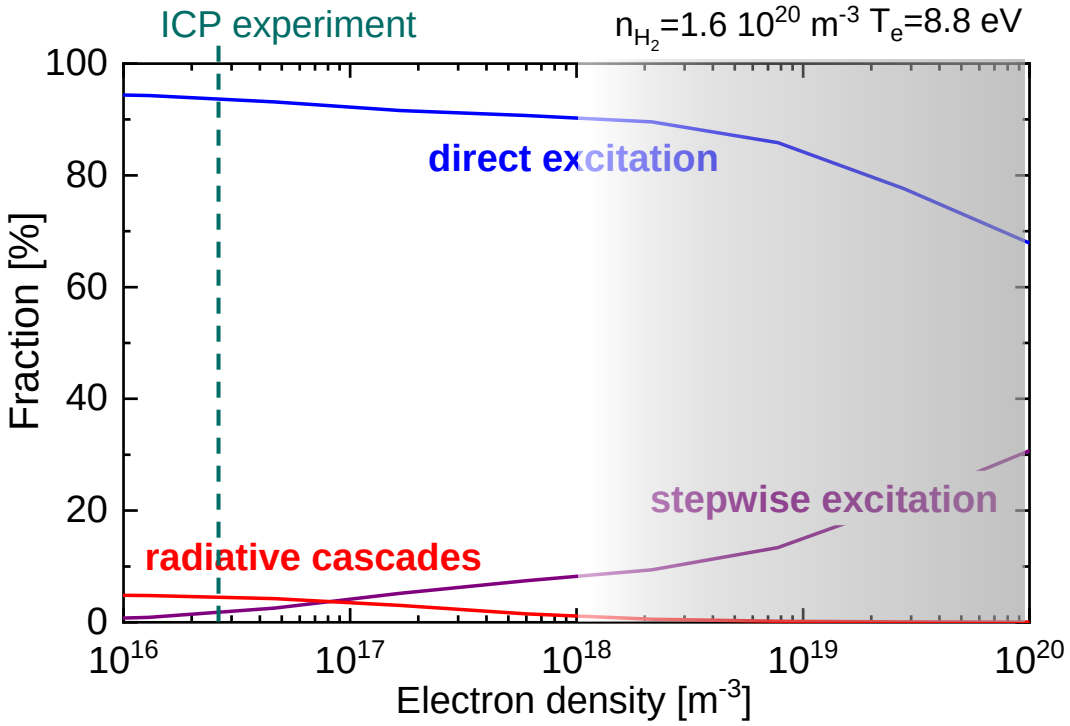

Fantz et al. 2016 Plasma Sources Sci. Technol. **25**

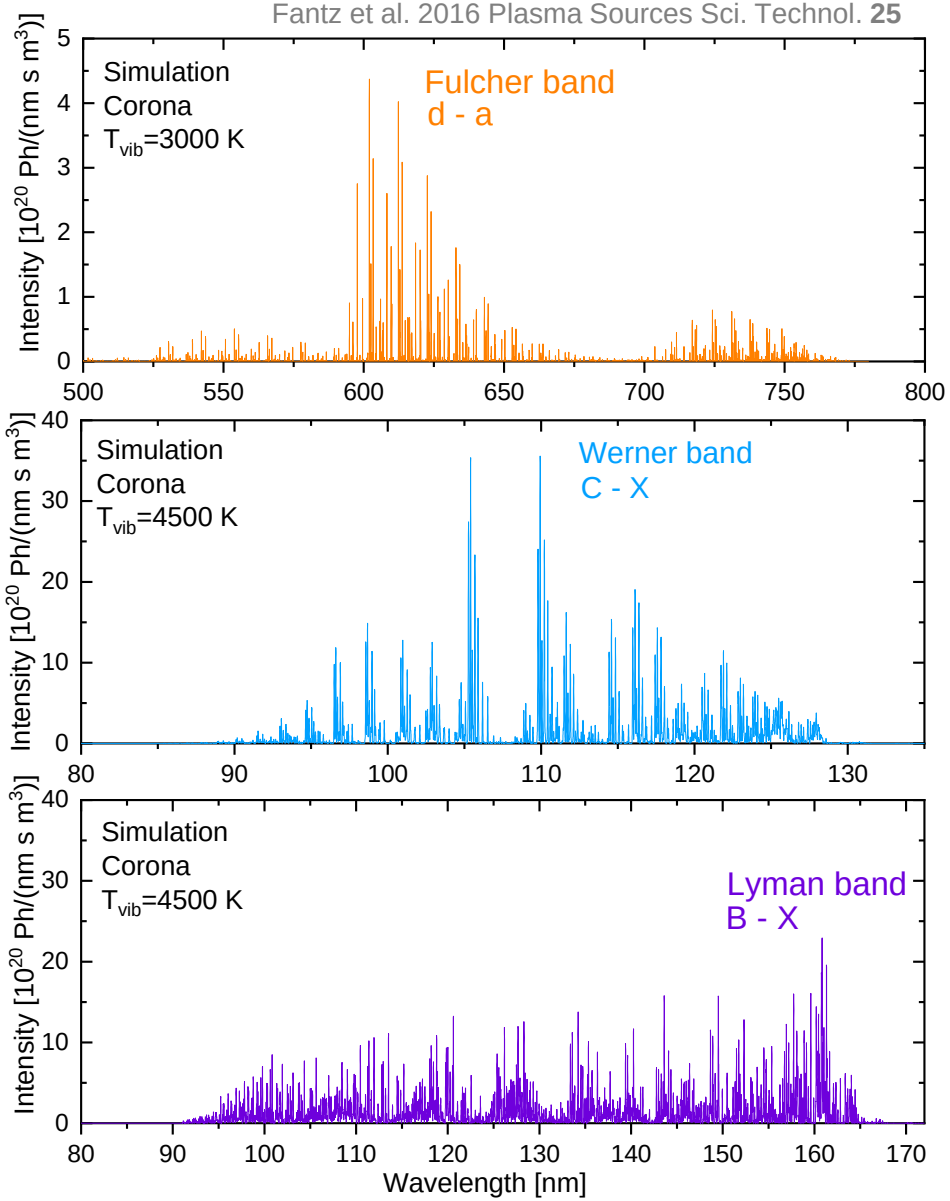

Low temperature hydrogen plasmas in fusion devices

Low temperature plasmas in fusion devices

View into the JET tokamak

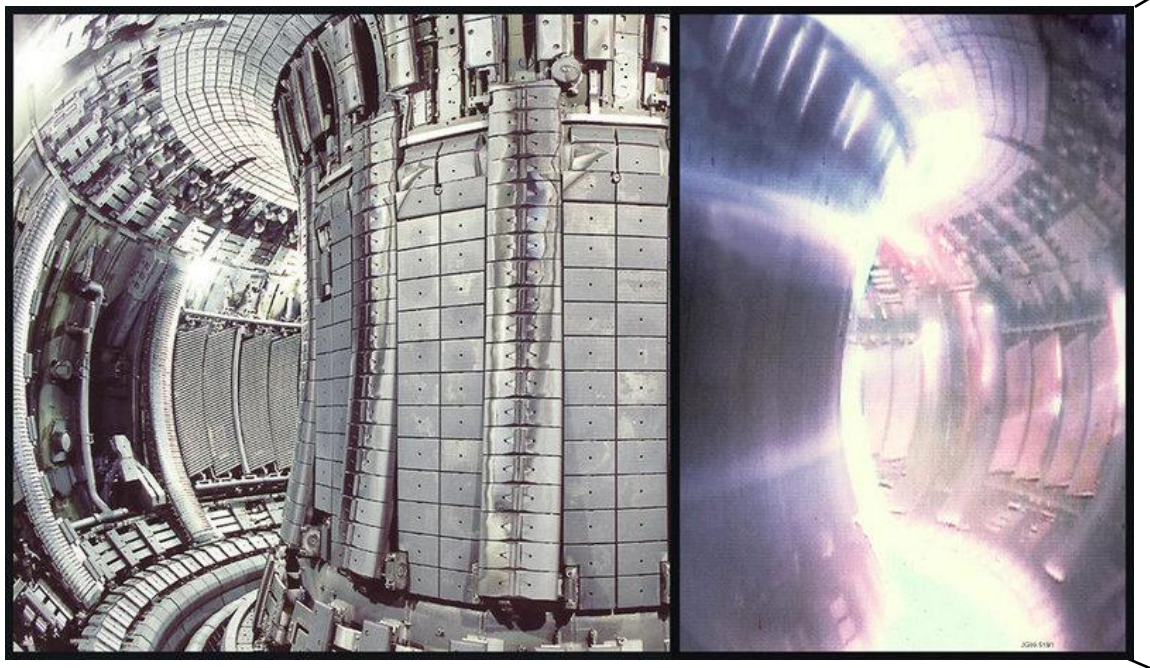

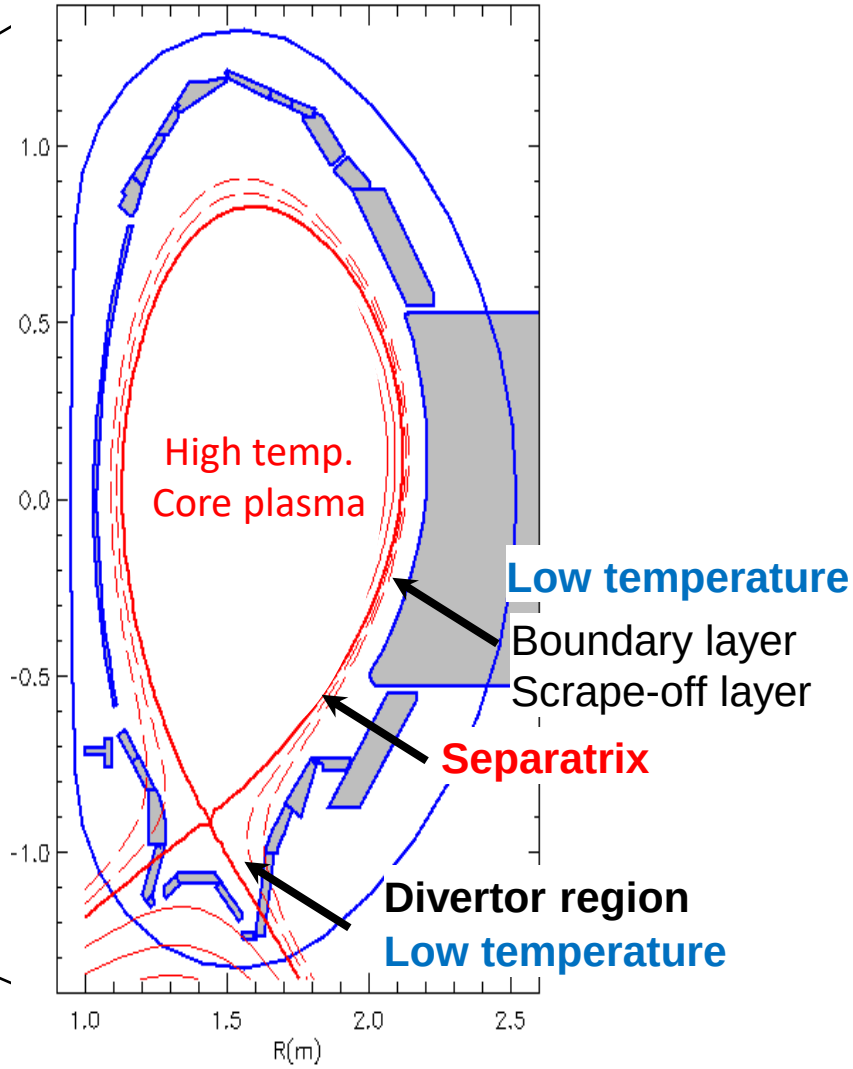

Wide parameter range

$T_e \approx 50$ eV ⟶ few eV ⟶ below 1 eV

$n_e \approx 10^{18} – 10^{21}$ m^{-3}

Ionising plasma ⟶ Recombining plasma

Cold plasma edge: SOL and divertor region

Linear plasma devices
Regimes of divertor plasmas

MAGNUM-PSI

DIFFER

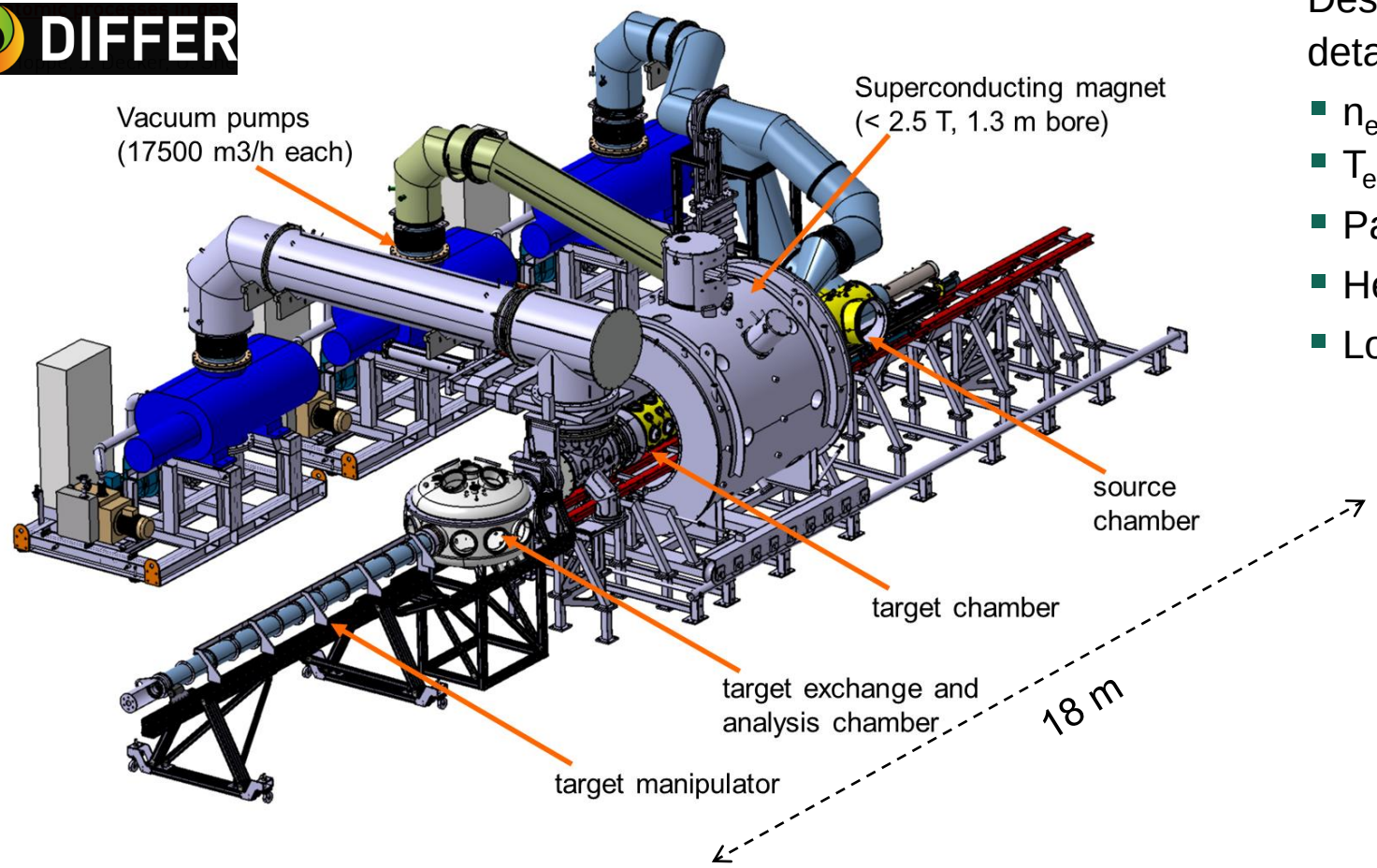

Van de pol et al. Fusion Engineering and Design 136 (2018)

Design values for high performance detached divertor operation in ITER:

- n_e ~ 10^{19} – 10^{21} m^{-3}
- T_e ~ 0.1 – 10 eV
- Particle flux ~ 10^{23} - 10^{25} m^{-2} s^{-1}
- Heat fluxes > 10 MW m^{-2}
- Low neutral background density < 1 Pa

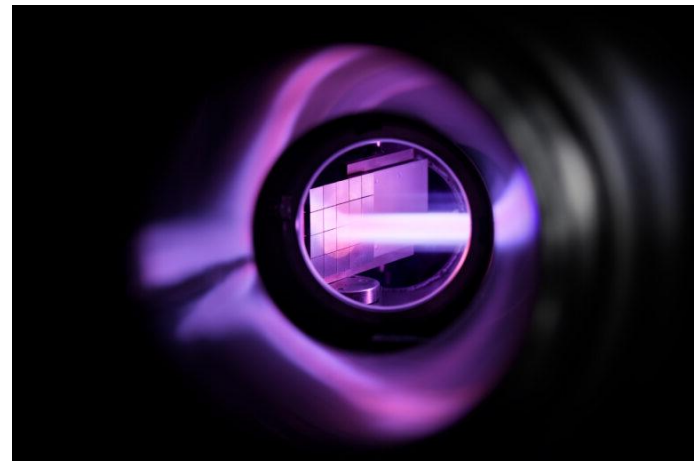

credit: DIFFER / Bart van Overbeeke

Exposure tungsten tile to plasma in Magnum-PSI

Linear plasma devices
Regimes of divertor plasmas

Kreter et al. 2015 Fusion Science and Technology 68

PSI-2

JÜLICH Forschungszentrum

- Arc current ~ 1000 A , Arc voltage ~ 150 V
- Diameter of plasma column ~ 6 cm
- Magnetic field in exposure chamber 0.1 T

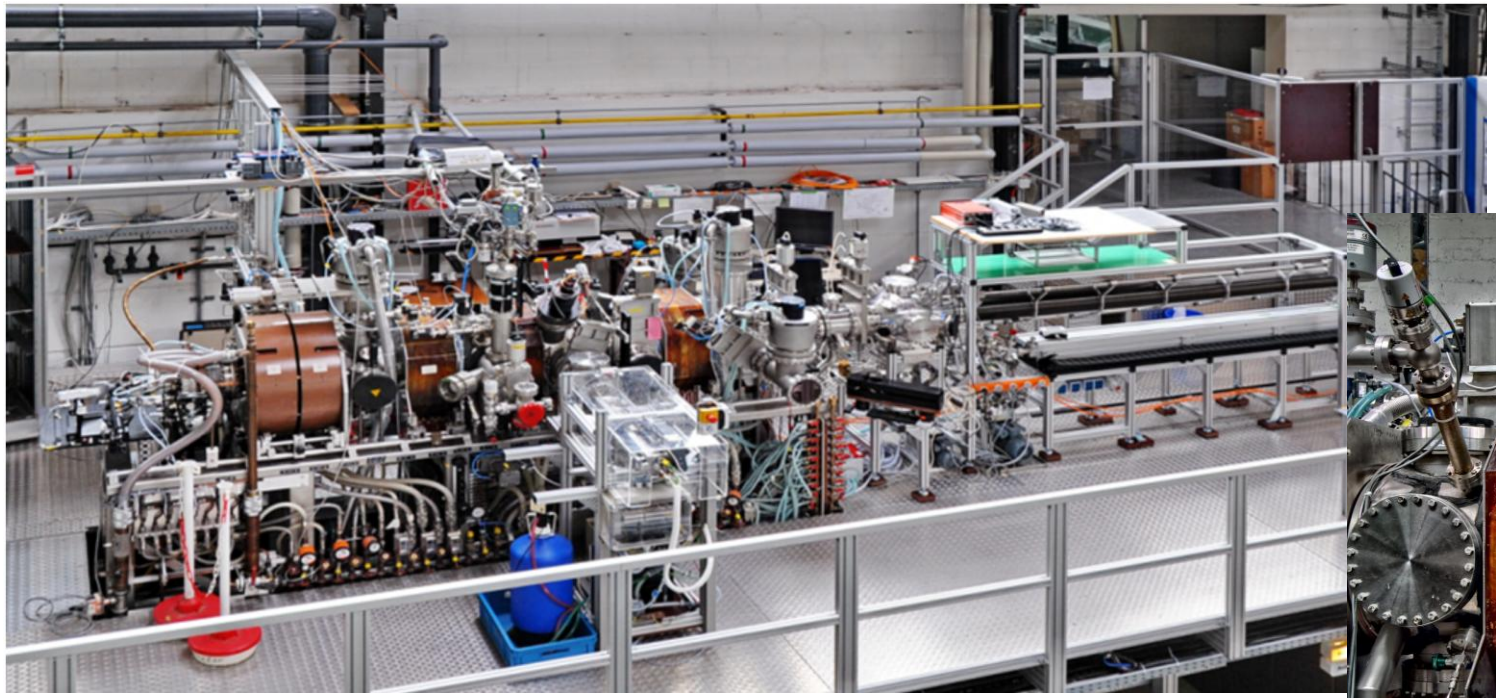

- T_e ~ 1 - 25 eV (in D), up to 40 eV (in He)
- T_{ion} ~ 0.5 - 5 eV
- n_e ~10^{17} - 10^{19} m^{-3}
- Ion flux ~10^{21} - 10^{23} m^{-2} s^{-1}
- Incident ion energy (bias) 10 - 300 V

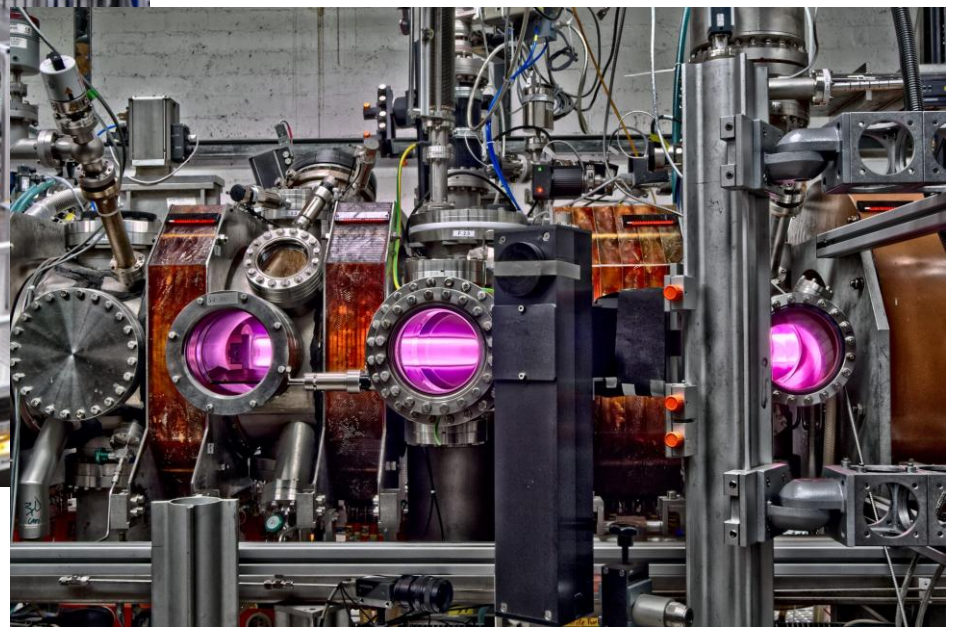

credit: Forschungszentrum Jülich

The role of molecules in recombination processes

Electron **I**on **R**ecombination **EIR**

$H^+ + e^- + e^- \rightarrow H^* + e^-$ 3-body rec. and/or

$H^+ + e^- \rightarrow H^* + h\nu$ radiative recombination

Plasma ionization

$H + e^- \rightarrow H^+ + 2e^-$ ionization of atoms and

$H_2(v) + e^- \rightarrow H_2^+ + 2e^-$ ionization of molecules

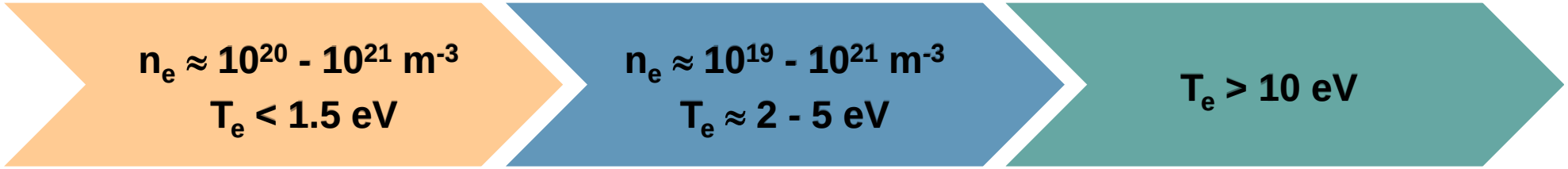

Molecular **A**ssisted **R**ecombination **MAR**

$\mathbf{H_2(v)} + H^+ \rightarrow H_2^+(v) + H$ charge exchange with

$H_2^+(v) + e^- \rightarrow H + H^*$ dissociative recombination

$\downarrow$

H

The role of molecules in recombination processes
Investigations at a linear device

Cascaded arc Pilot-PSI, UPP at DIFFER

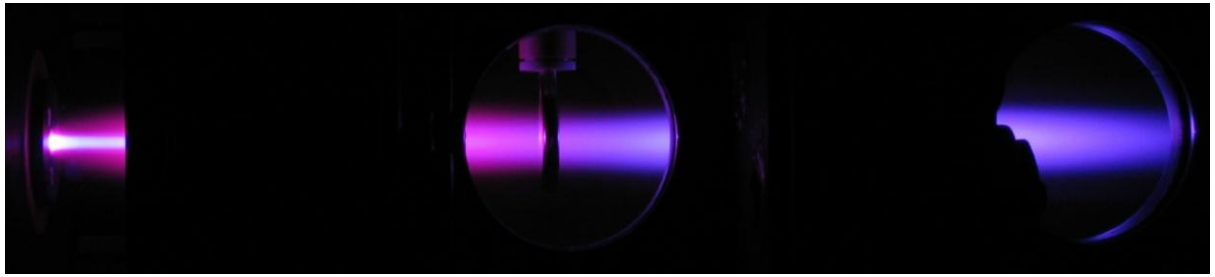

Electron **I**on **R**ecombination **EIR**

$H^+ + e + e \rightarrow H + e$ 3-body rec.

$H^+ + e \rightarrow H + h\nu$ radiative rec.

$n_e \approx 10^{20}$ - 10^{21} m^{-3}

$T_e < 1.5$ eV

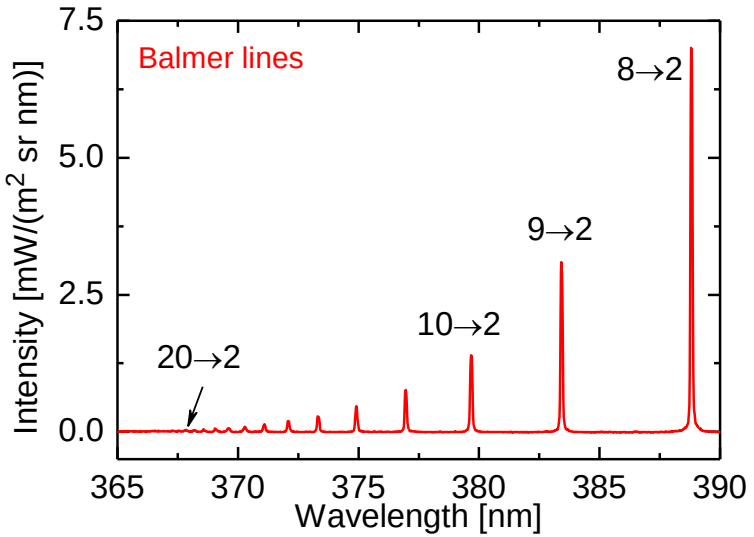

Molecular Assisted Recombination MAR

$H_2(v) + H^+ \rightarrow H + H_2^+$ charge exchange

$H_2^+ + e \rightarrow H + H^*$ dissociative rec.

$n_e \approx 10^{19}$ - 10^{21} m^{-3}

$T_e \approx 2$ - 10 eV

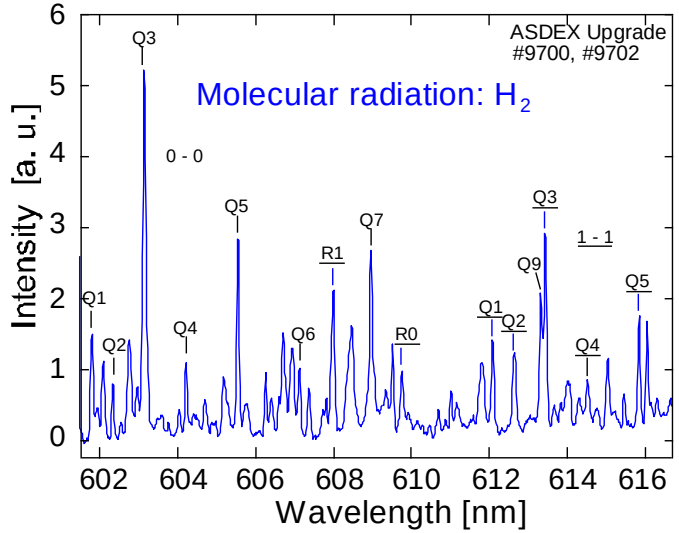

The role of molecules in recombination processes
Investigations at a linear device

Cascaded arc at TU/e

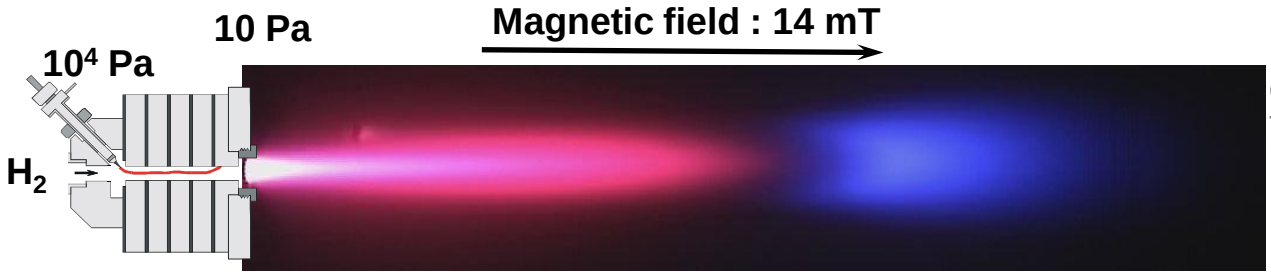

courtesy:
TU /e Eindhoven

0 cm **20 cm** **40 cm**

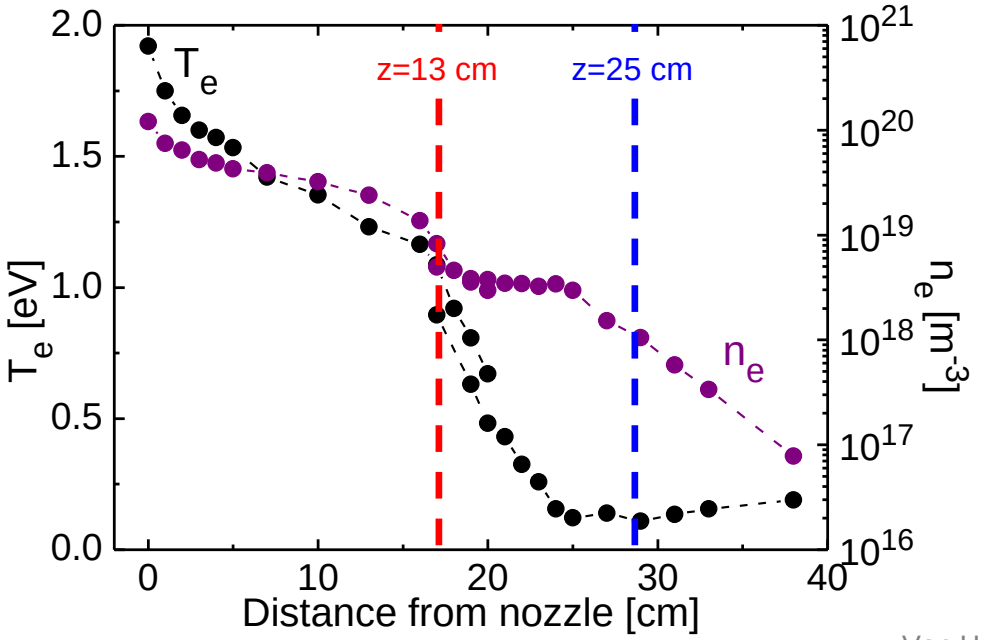

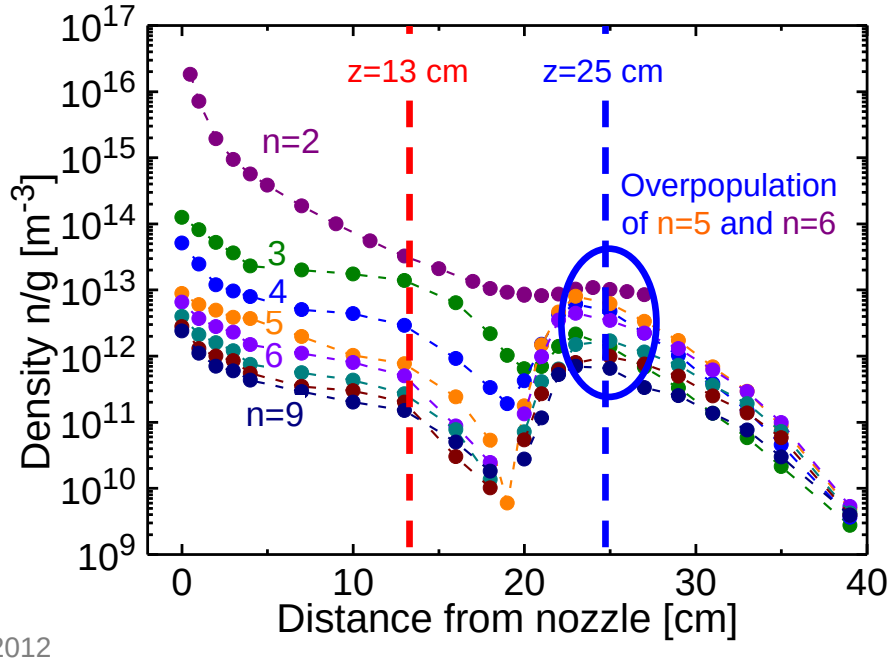

Van Harskamp, PhD Thesis, TU/e 2012

Plasma parameters from Thomson scattering, probes, OES, ...

The role of molecules in recombination processes
Investigations at a linear device

Cascaded arc at TU/e

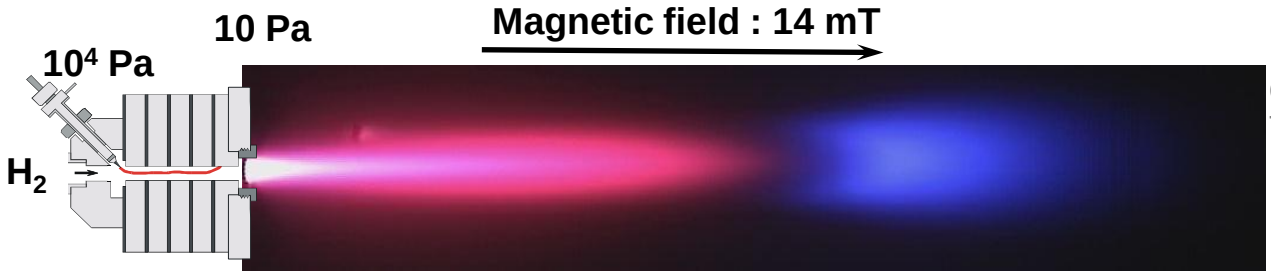

courtesy:
TU /e Eindhoven

0 cm **20 cm** **40 cm**

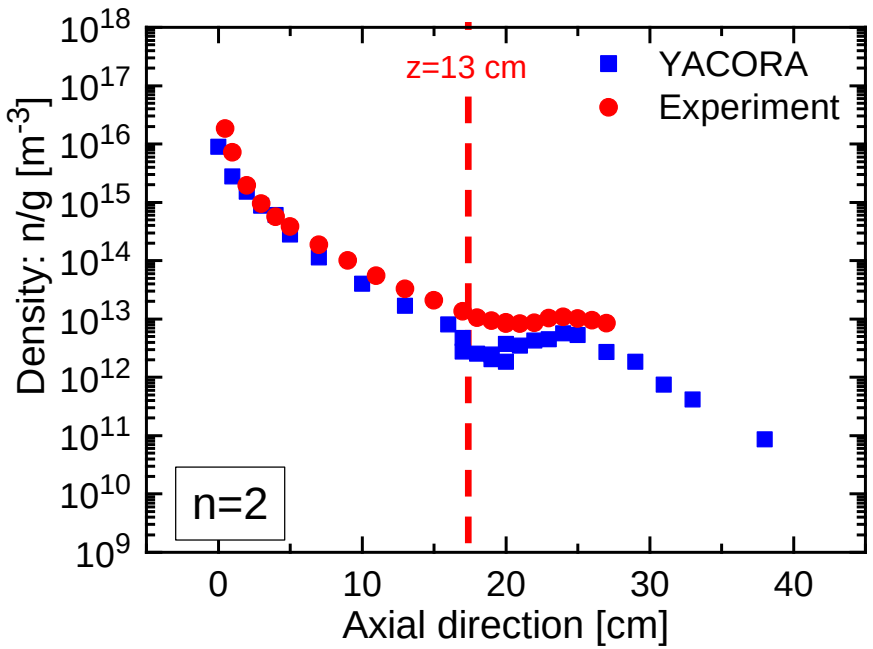

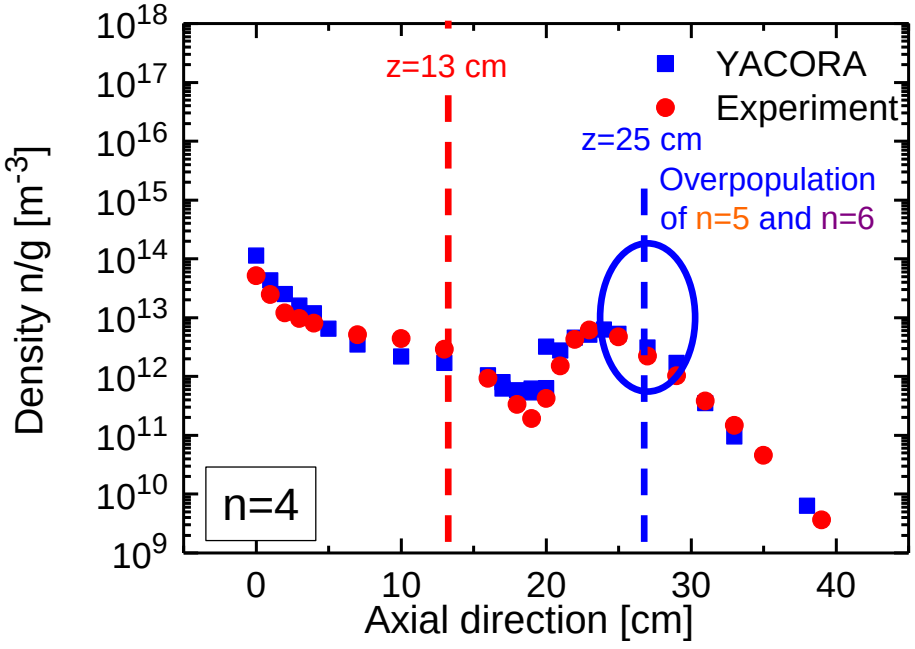

Plasma parameters from Thomson scattering, probes, OES, ...

The role of molecules in recombination processes
Investigations at a linear device

Cascaded arc at TU/e

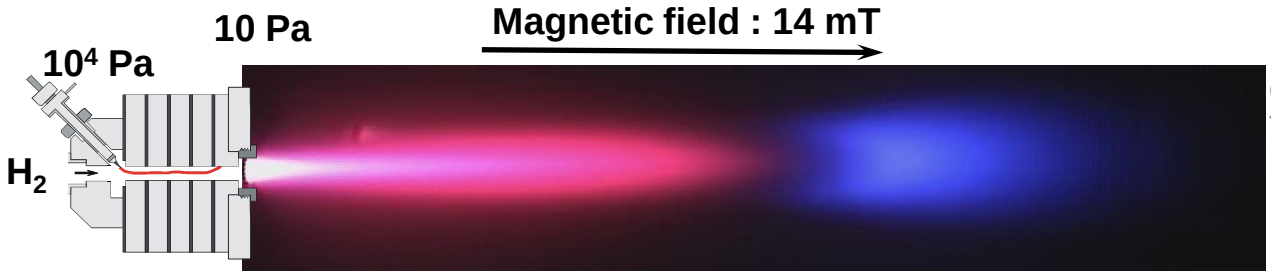

courtesy:
TU /e Eindhoven

0 cm **20 cm** **40 cm**

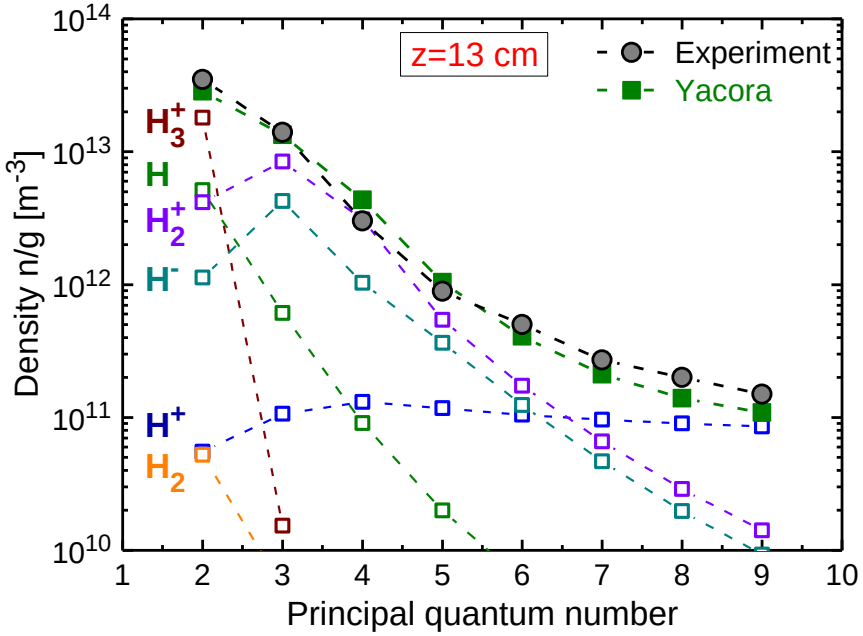

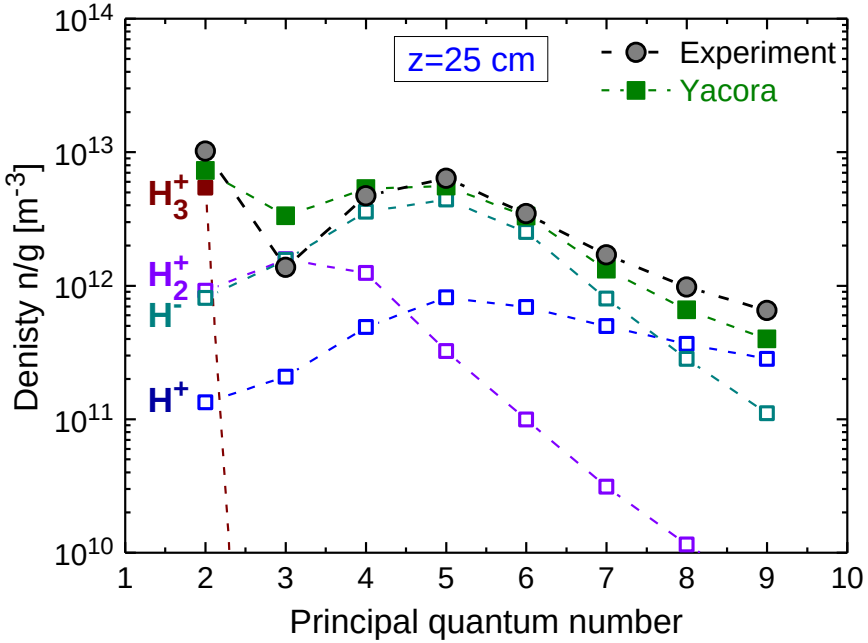

Contribution of individual channels by CR modelling

Application to divertor plasmas
Predictions by modelling using AMJUEL database

EDGE2D-EIRENE profiles

JET L-mode plasma

$n_e^{sep,omp}=1.3\ 10^{19}\ m^{-3}$

M. Groth et al. 2013 Nucl. Fusion 53

High-recycling plasma

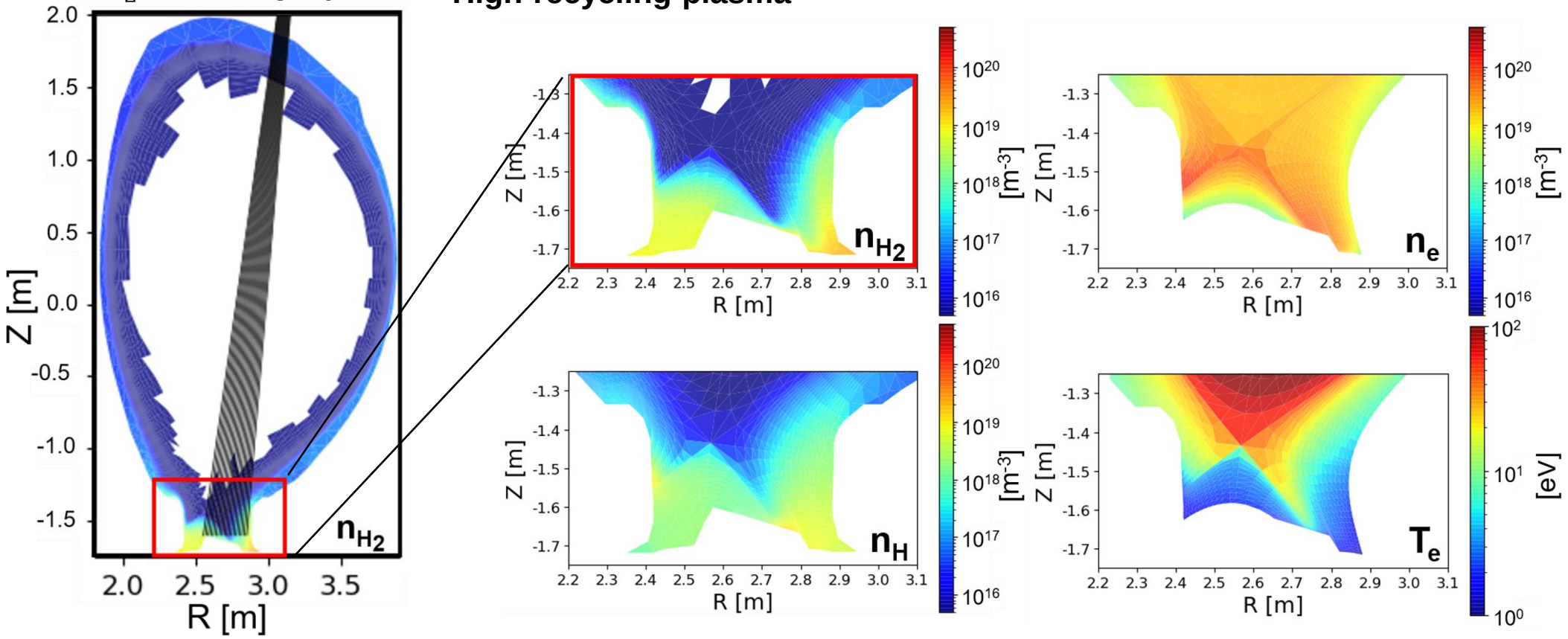

M. Groth et al. Nuclear Fusion, 53 (2023):093016

Application to divertor plasmas
Comparison of different data basis – Yacora-H2(v)

EDGE2D-EIRENE profiles

JET L-mode plasma

$n_e^{sep,omp}$=1.3 10^{19} m^{-3}

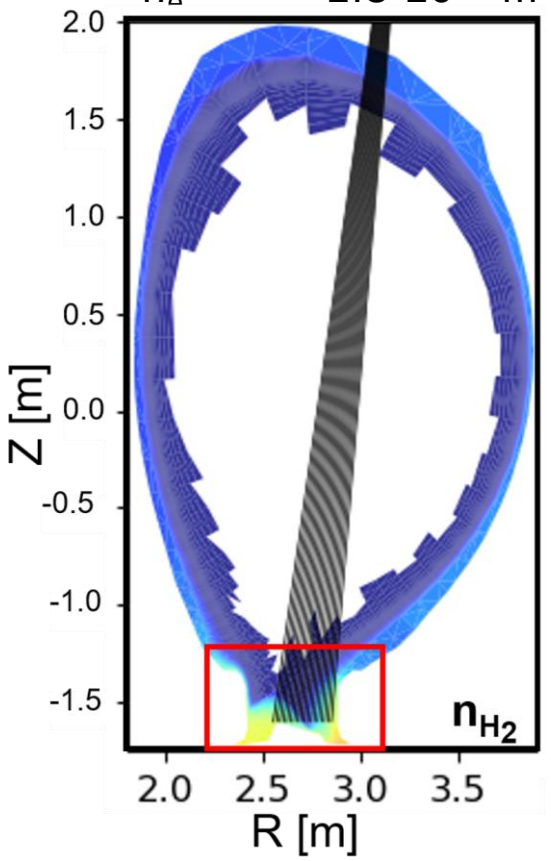

M. Groth et al. Nuclear Fusion, 53 (2023):093016

Begrmayr et al. 2025 Nucl. Mater. Energy 42

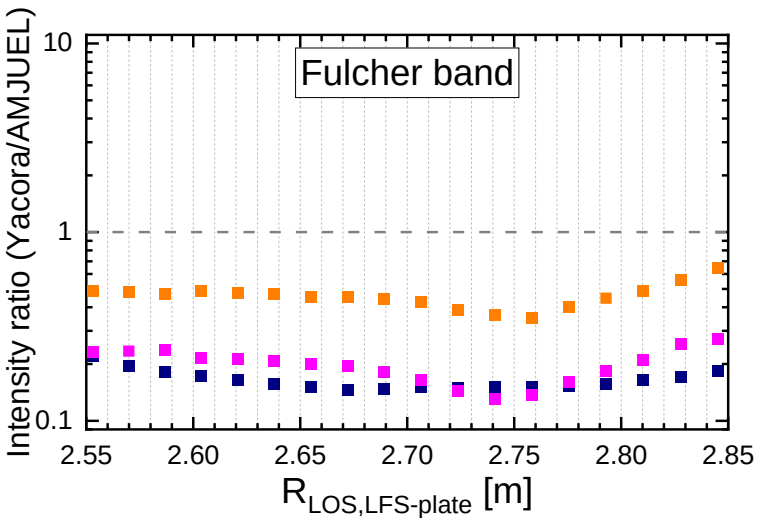

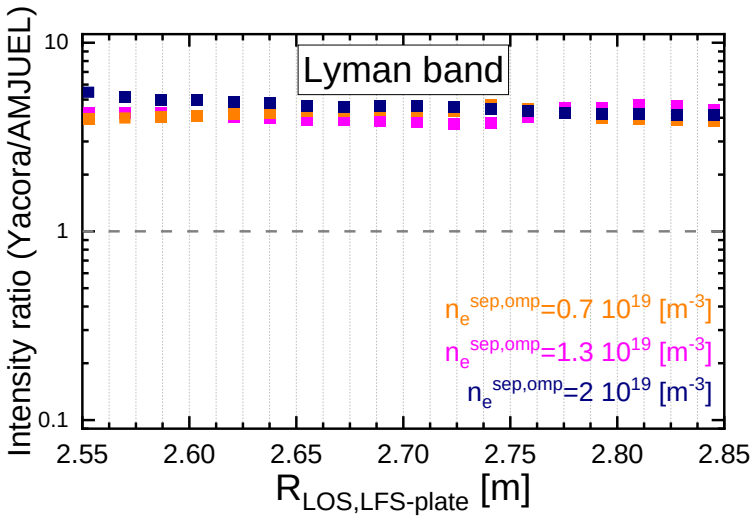

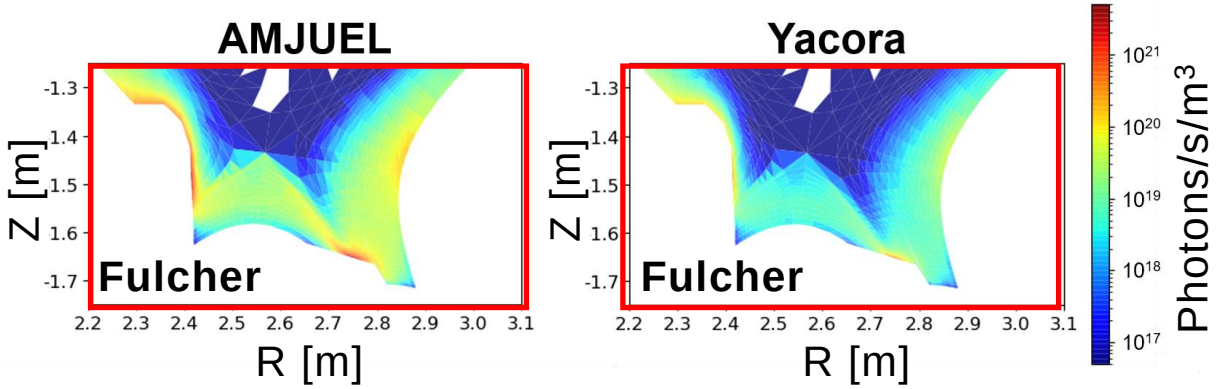

Discrepancies within an order of magnitude

Benchmarked required → Linear devices!

Low temperature hydrogen plasmas FOR fusion devices

Low temperature plasmas in fusion devices

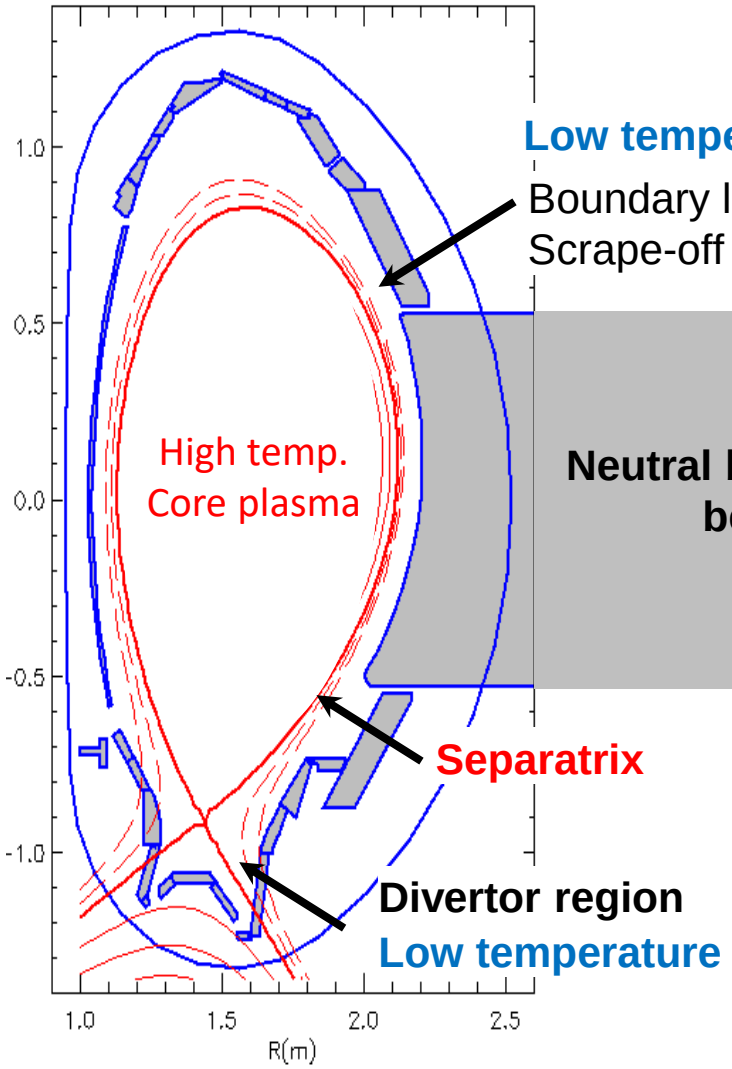

Low temperature

Boundary layer

Scrape-off layer

Neutral beam injection beamline

Separatrix

Divertor region

Low temperature

Ion source for

→ positive ions H^+, D^+

or

→ negative ions H^-, D^-

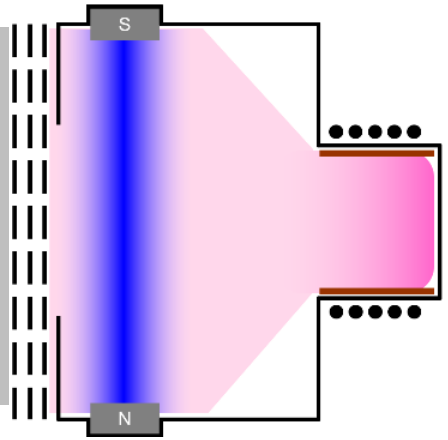

Wide parameter range

$T_e \approx 10$ eV → 1 eV

$n_e \approx 10^{18}$ → 10^{16} m^{-3}

Ionising plasma → Recombining plasma

Fusion experiments require powerful heating systems

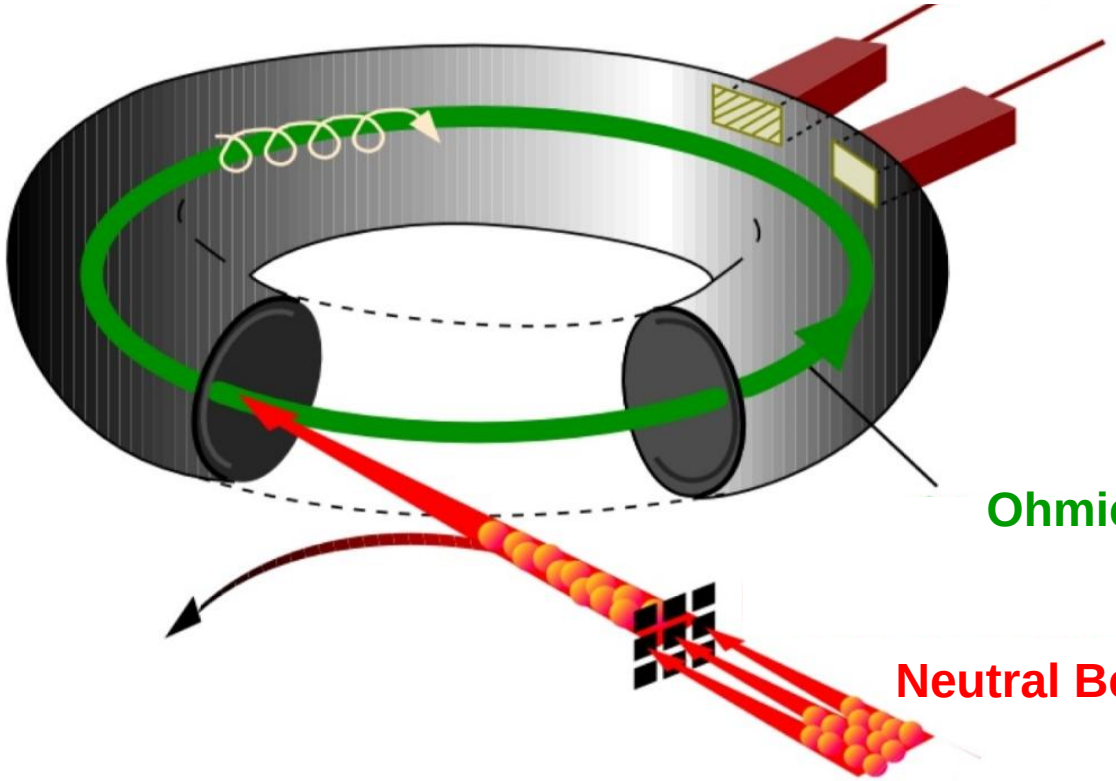

Radio Frequency Heating

Power installed at ITER

Electron cyclotron resonance heating, 170 GHz
ECRH: 40 MW → 67 MW

Ion cyclotron resonance heating, 40 - 55 MHz
ICRH: 10 → 20 MW

Ohmic Heating by the toroidal plasma current → 1 - 2 keV

Neutral Beam Injection Injection of energetic neutral atoms

NBI: 33 MW → 50 MW

Remark: α-particle heating sustains plasma temperature in a fusion reactor

How NBI heating works

Interaction of a fast neutral beam with the hot fusion plasma

H or D particles
intensity I_0

density n

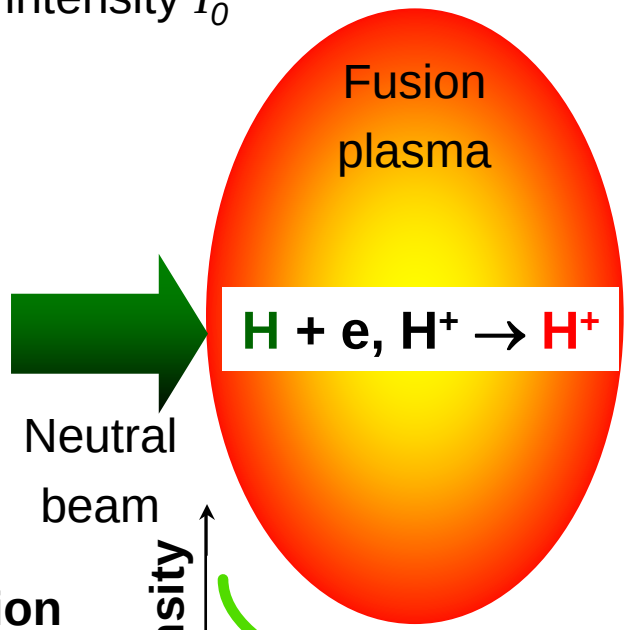

Beam attenuation

$$I = I_0 \exp\left(-\frac{x}{\lambda}\right)$$

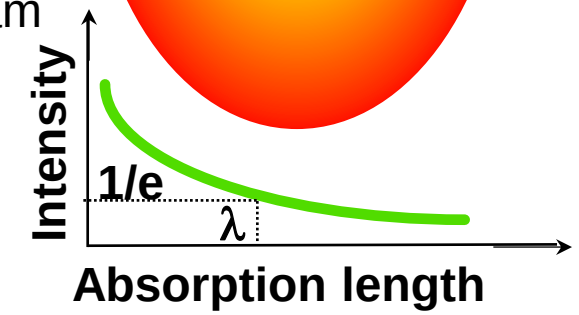

Generation of fast ions

Collisions with electrons and ions

- Ionization by electrons
- Ionization by ions
- Charge exchange with ions

$$\mathrm{H}_f^0 + e^- \rightarrow \mathrm{H}_f^+ + 2e^-$$
$$\mathrm{H}_f^0 + \mathrm{H}^+ \rightarrow \mathrm{H}_f^+ + \mathrm{H}^+ + e^-$$
$$\mathrm{H}_f^0 + \mathrm{H}^+ \rightarrow \mathrm{H}_f^+ + \mathrm{H}^0$$

&

Current drive for steady state operation requires beam energies of **1 MeV** for ITER

Positive and negative ion based systems

NBI systems based on **positive ions**
are routinely in use
JET, AUG, DIII-D,
JT-60U, …

negative ions
up to 300 kV
only at JT-60U,
JT-60SA, LHD

1 MeV D

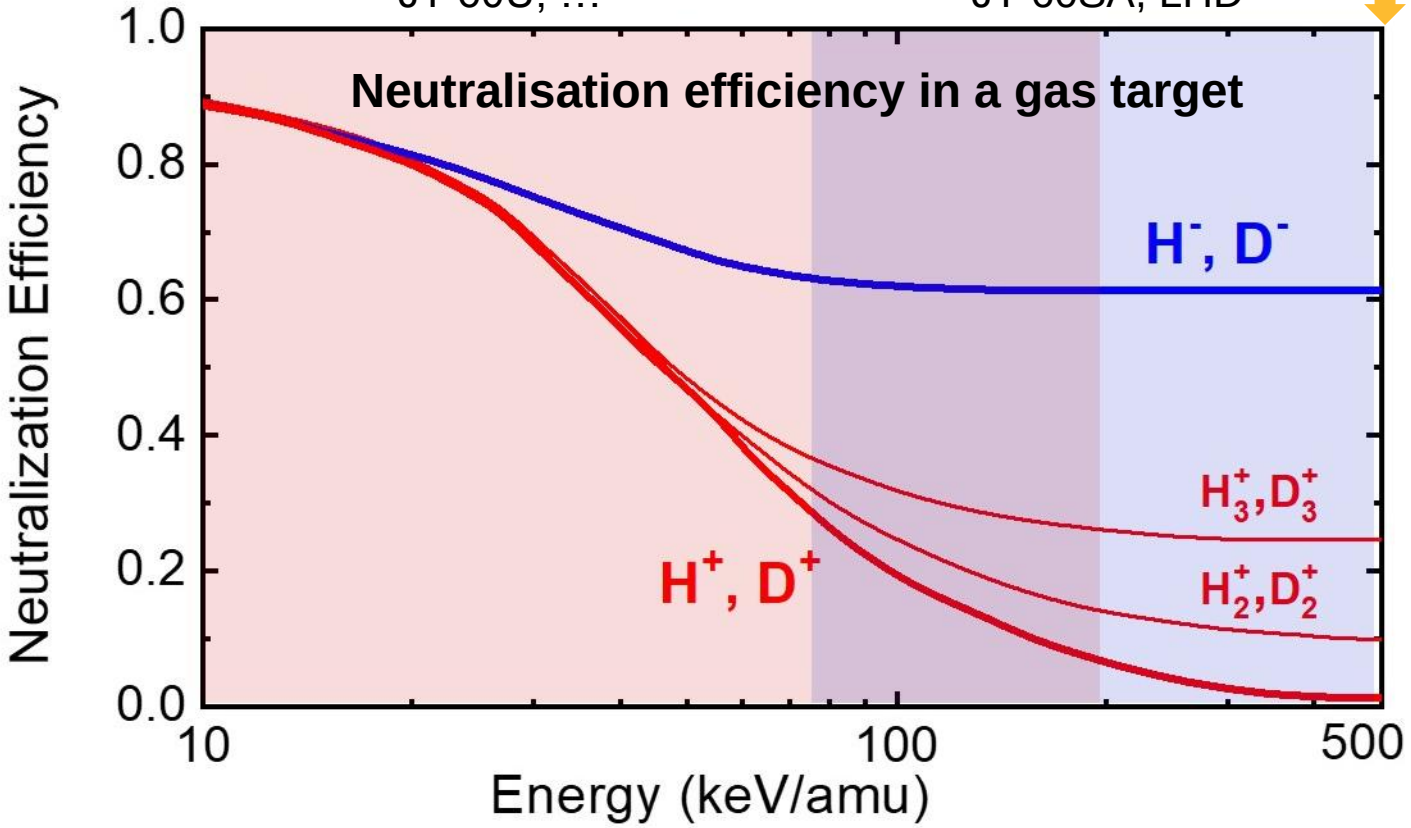

Neg. ions ~ 60 %
but j ≈ 200 A/m²

increase of
source size

Pos. ions < 10 %
with j ≈ 2000 A/m²

NBI systems at ITER and its functions

NBI functions

- Heating — HNB
- Current drive — HNB
- Plasma rotation — HNB
- Diagnostics — DNB

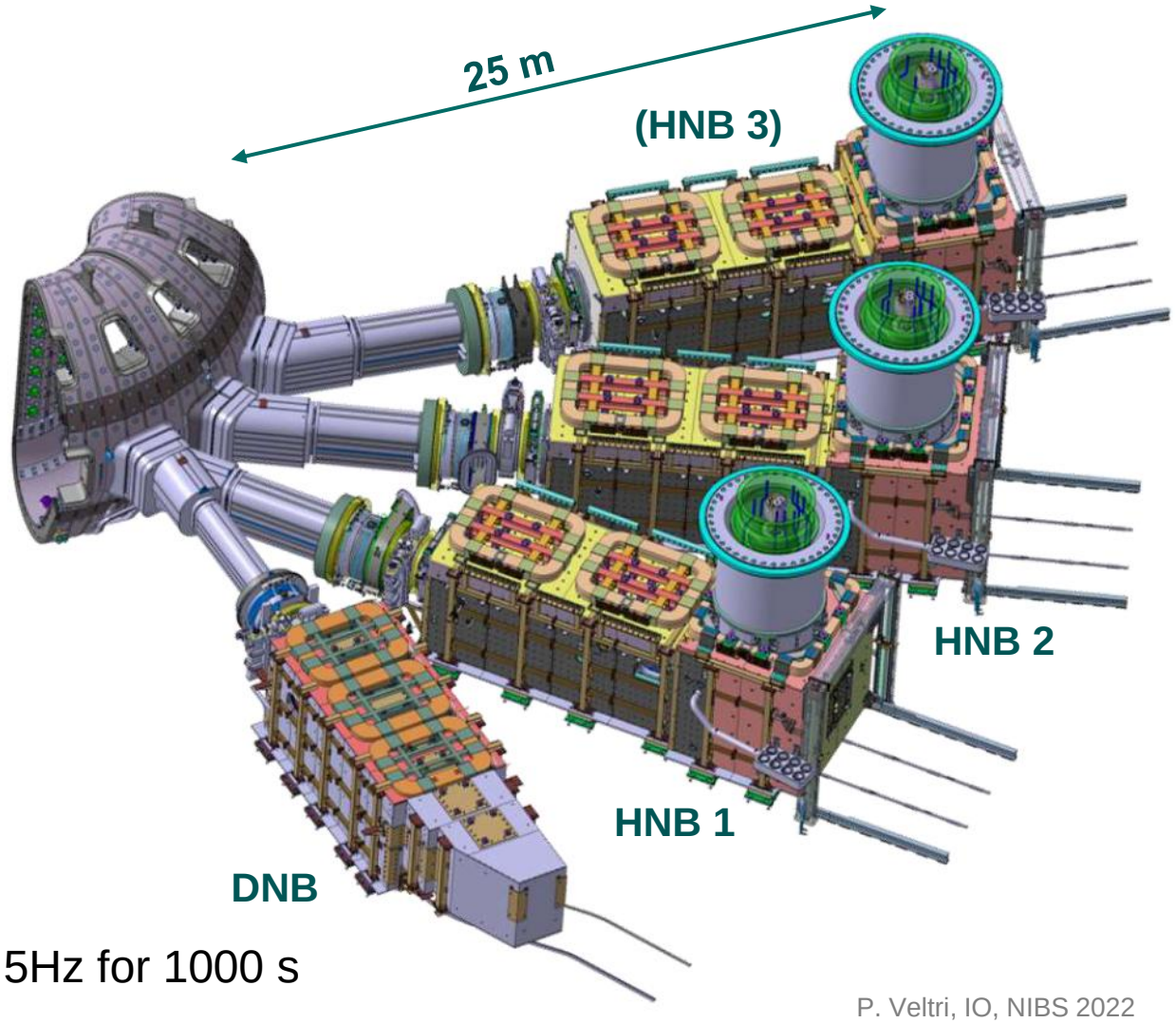

Hemsworth et al. 2017 *New J. Phys.* **19** 025005

HNB Heating beams (Europe, Japan)

33 MW (2 injectors) for 3600 s

1 MeV Deuterium, 870 keV Hydrogen

Singh et al. 2017 New J. Phys. **19** *055004*

DNB Diagnostic beam (India)

2.2 MW, 100 keV Hydrogen, 3s ON/20s OFF 5Hz for 1000 s

P. Veltri, IO, NIBS 2022

Beam line components

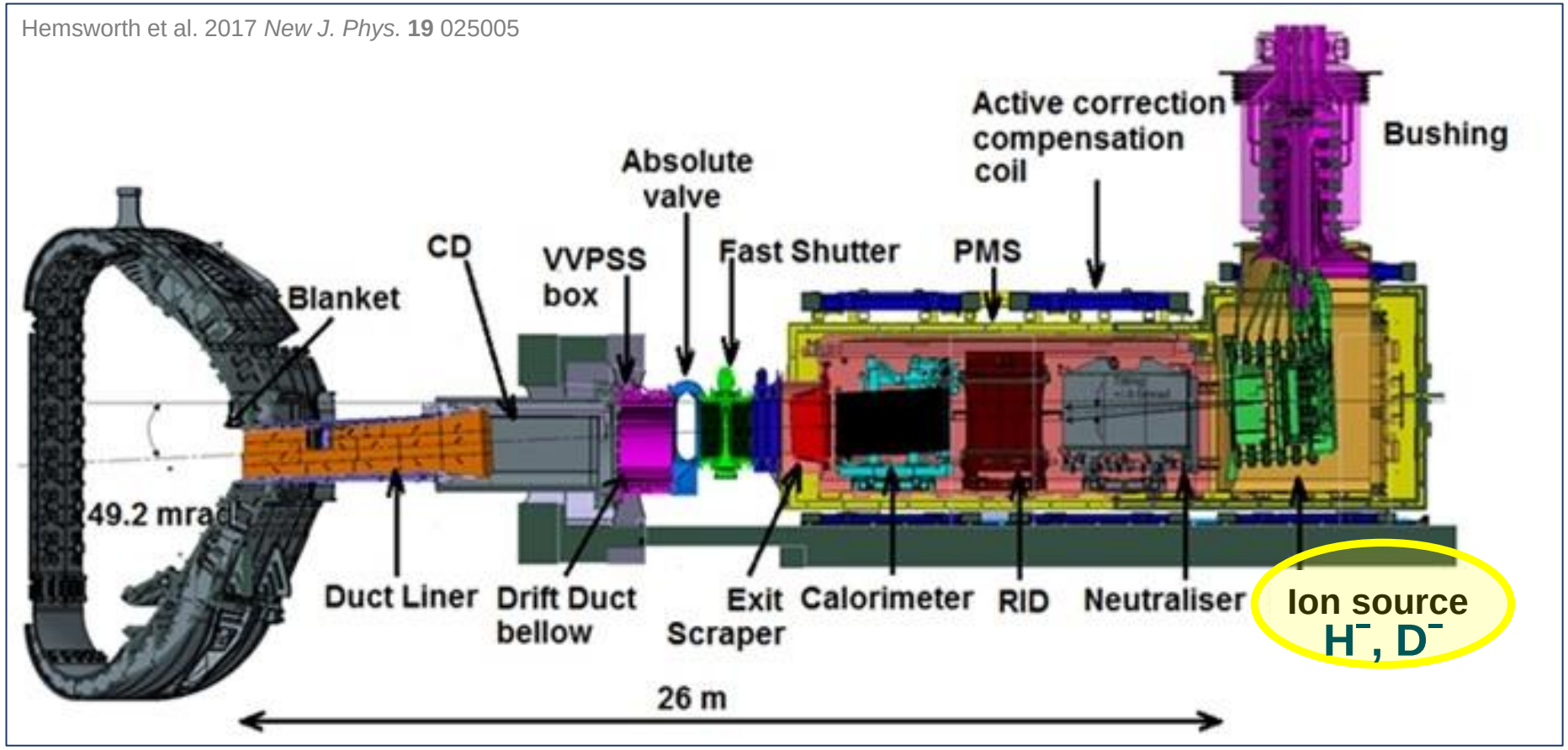

Injection | Transport with 7 mrad beam divergence | Neutralization | Acceleration | Generation

Concept of ion sources for NBI
Arc sources and RF-driven sources

Arc sources

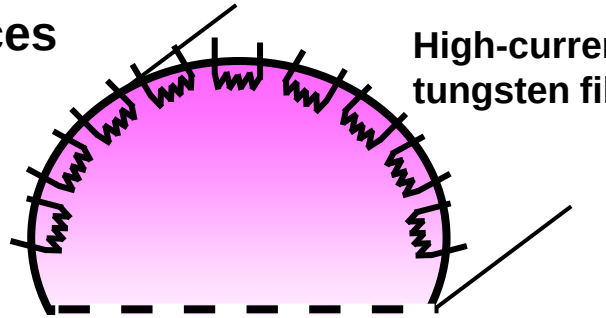

- Hot cathodes (2000 – 3000 K)
- DC voltage (≈ 100 V), Arc current (1000 A)

Filaments require regular maintenance

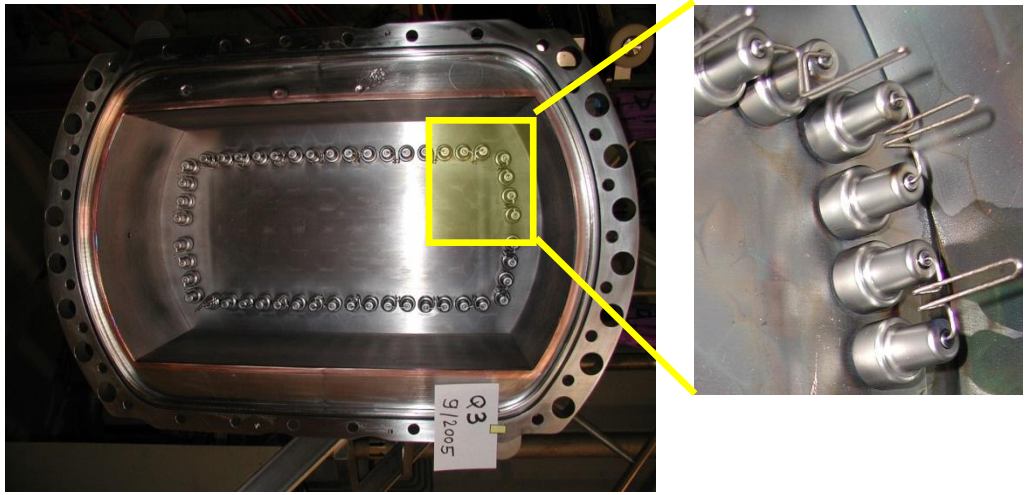

RF sources

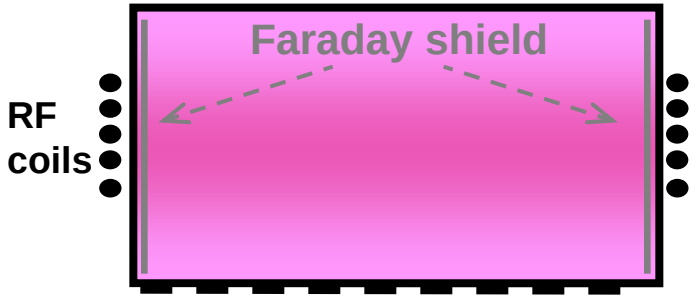

- Inductively driven source
- **RF power supply (≈ 100 kW), RF frequency 1 MHz**

Long lifetime

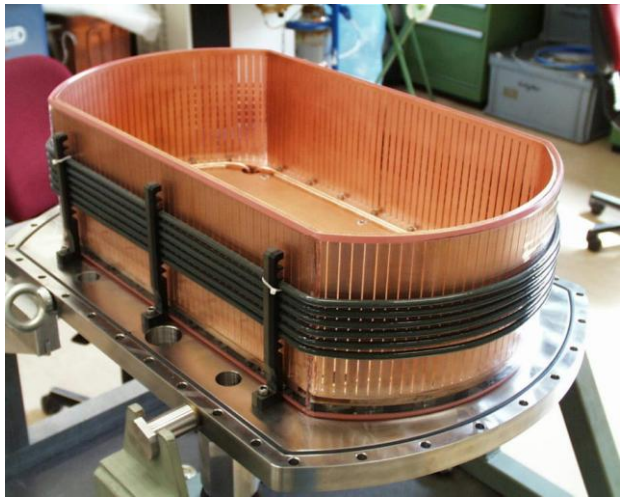

In routine operation for positive ions at AUG since more than 25 years

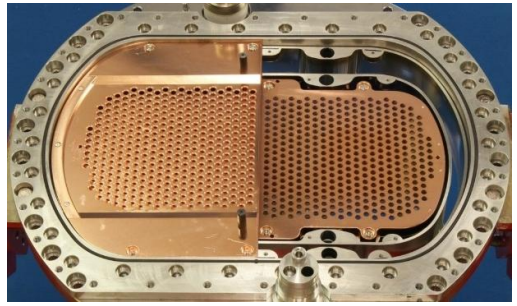

Requirements to the negative hydrogen (H^-, D^-) ion source

ITER requirements for D (H)

- Accelerated current **I = 40 A (46 A, 60 A DNB)**
- Extracted ion current density
  j_{ex} = 286 (329) A/m²
- Filling pressure ≤ 0.3 Pa (stripping < 30%)
- Co-extracted electrons: **$j_e/j_{ex} \leq 1$**
- Beam homogeneity > 90 %,
- Beam divergence < 7 mrad

Stable for 1 h (1000 s)

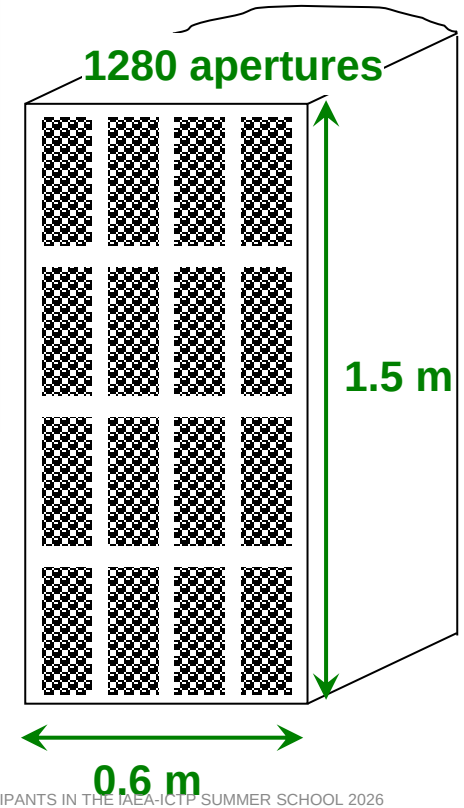

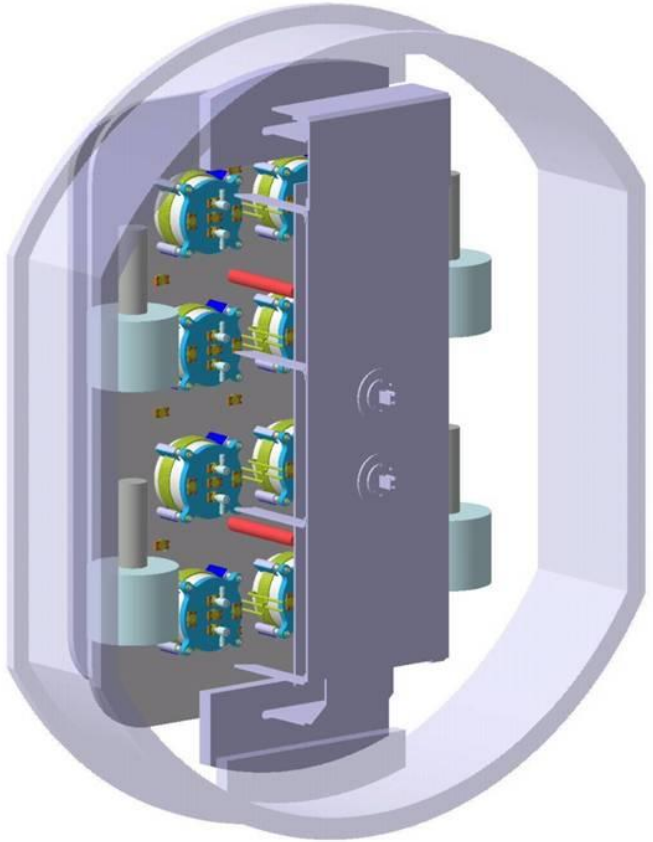

Large source area: 1 m × 2 m
Multi-aperture system: 1280

Formation of negative hydrogen ions in the plasma volume

$e^- + H_2 \rightarrow H_2(B,C) + e^- \rightarrow H_2(v) + e^- + h\nu$

hot electrons — **Vibrational excitation**

cold electrons

$e^- + H_2(v) \rightarrow H^- + H$

Dissociative attachment

Needs electrons and H_2 particles (pressure)

Concept of a tandem source

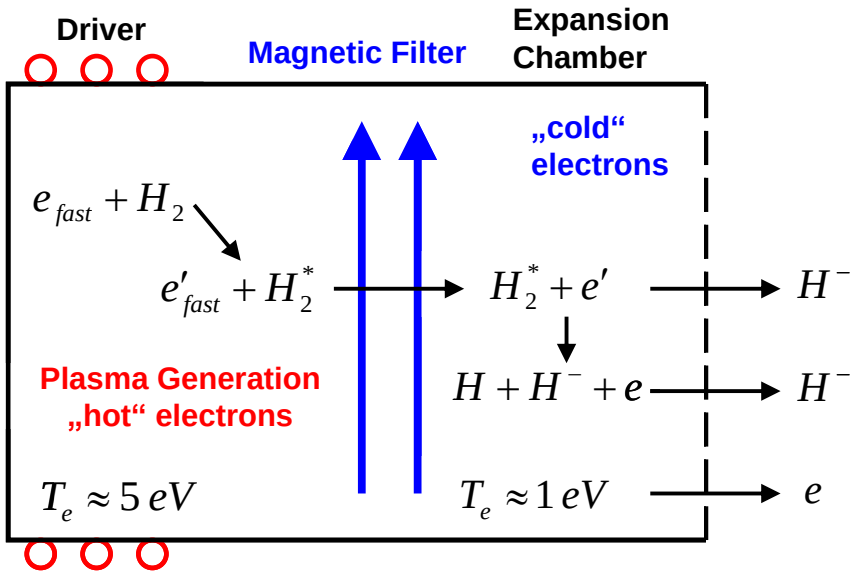

Issues for ion sources

- **High co-extracted electron current**
- Low ion current at low pressure (< 1 Pa)

Formation of negative hydrogen ions at the surface

Volume process dissociative attachment

$e^- + H_2(v) \rightarrow H^- + H$ $\quad j_{H^-} \approx 20\ A/m^2$, $j_e/j_{H^-} > 30$

effective at low work function

Surface conversion

$H, H_x^+ + \text{surface } e^- \rightarrow H^-$ **Cs evaporation**

Cs layer

low work function

≈ 10 × higher j_{H^-}

≈ 100 × lower j_e/j_{H^-}

at low pressure, 0.3 Pa

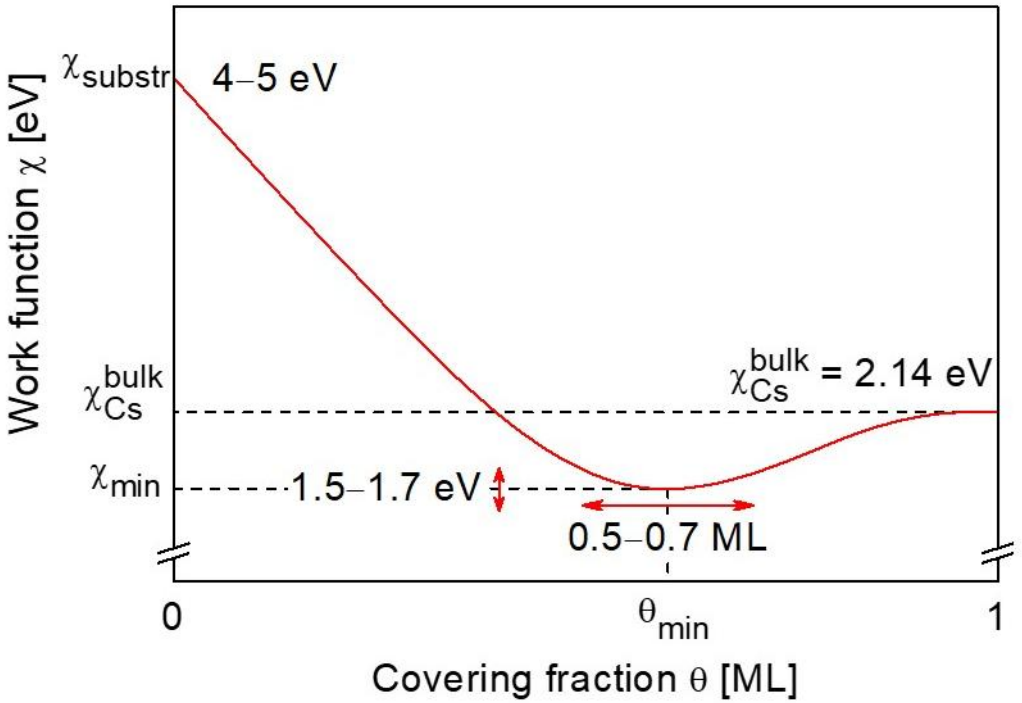

Destruction: volume processes

$H^- + e^- \rightarrow H + 2e^-$	Electron stripping
$H^- + H^+ \rightarrow H + H$	Mutual neutralisation
$H^- + H \rightarrow H_2 + e^-$ $\rightarrow H + H + e^-$	Associative detachment (non-associative)

The RF-driven ion source

ICP @
f = 1 MHz
P_{RF} ≤ 100 kW
p = 0.3 Pa

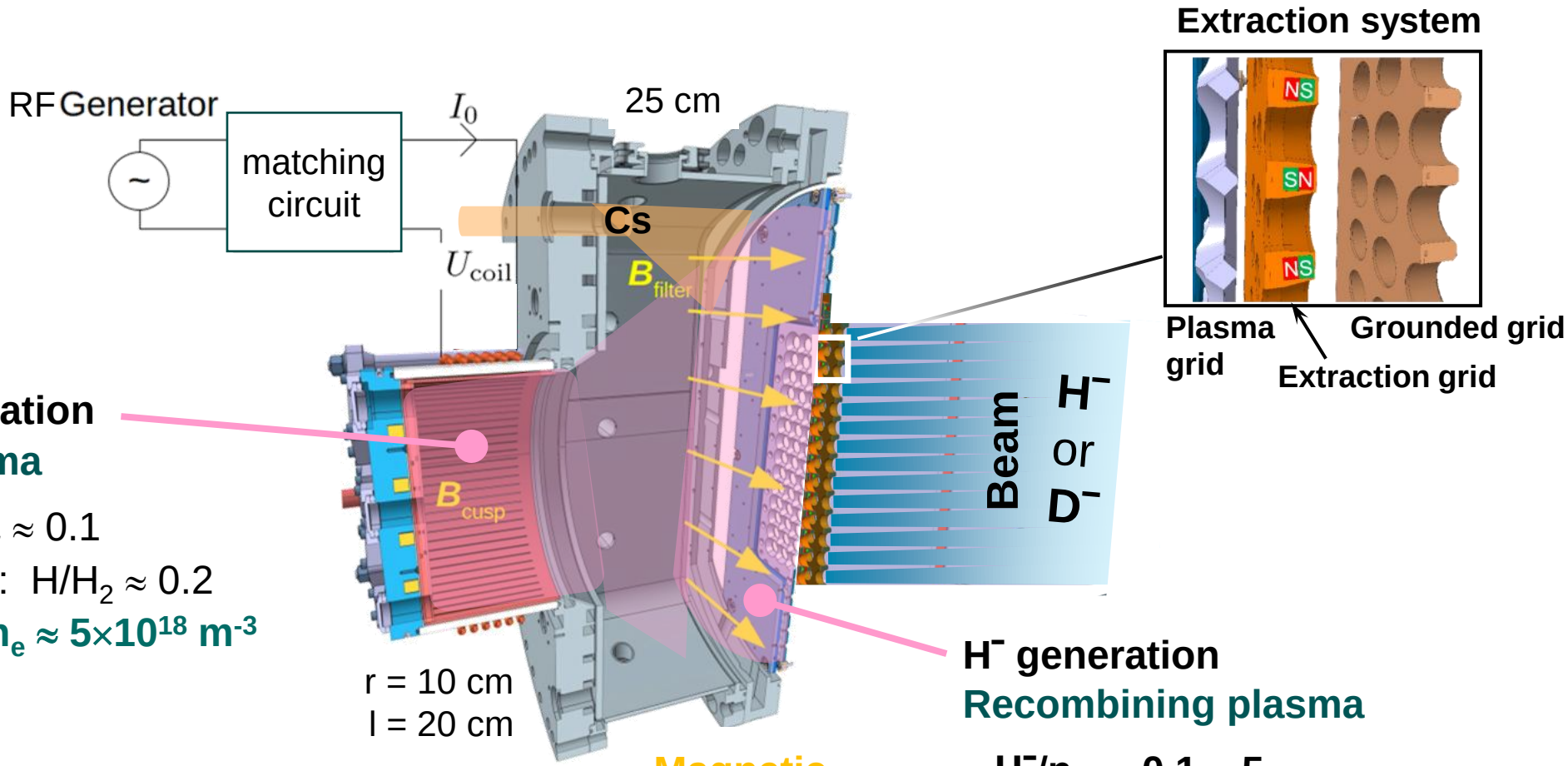

Plasma generation
Ionising plasma

- Ionisation: $\alpha \approx 0.1$
- Dissociation: $H/H_2 \approx 0.2$
- **$T_e \approx 10$ eV, $n_e \approx 5\times10^{18}$ m^{-3}**

Magnetic filter field
grad-B drifts

H^- generation
Recombining plasma

- **$H^-/n_e \approx$ 0.1 – 5**
- $Cs^+/n_e \approx 0.01 – 0.1$
- **$T_e \approx 2$ eV, $n_e \approx 6\times10^{16}$ m^{-3}**

Plasma parameters by OES, Langmuir probes, …

Ionising and recombining plasma regions & ion-ion plasma

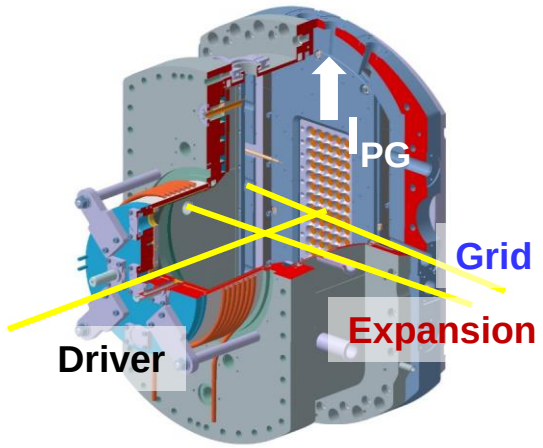

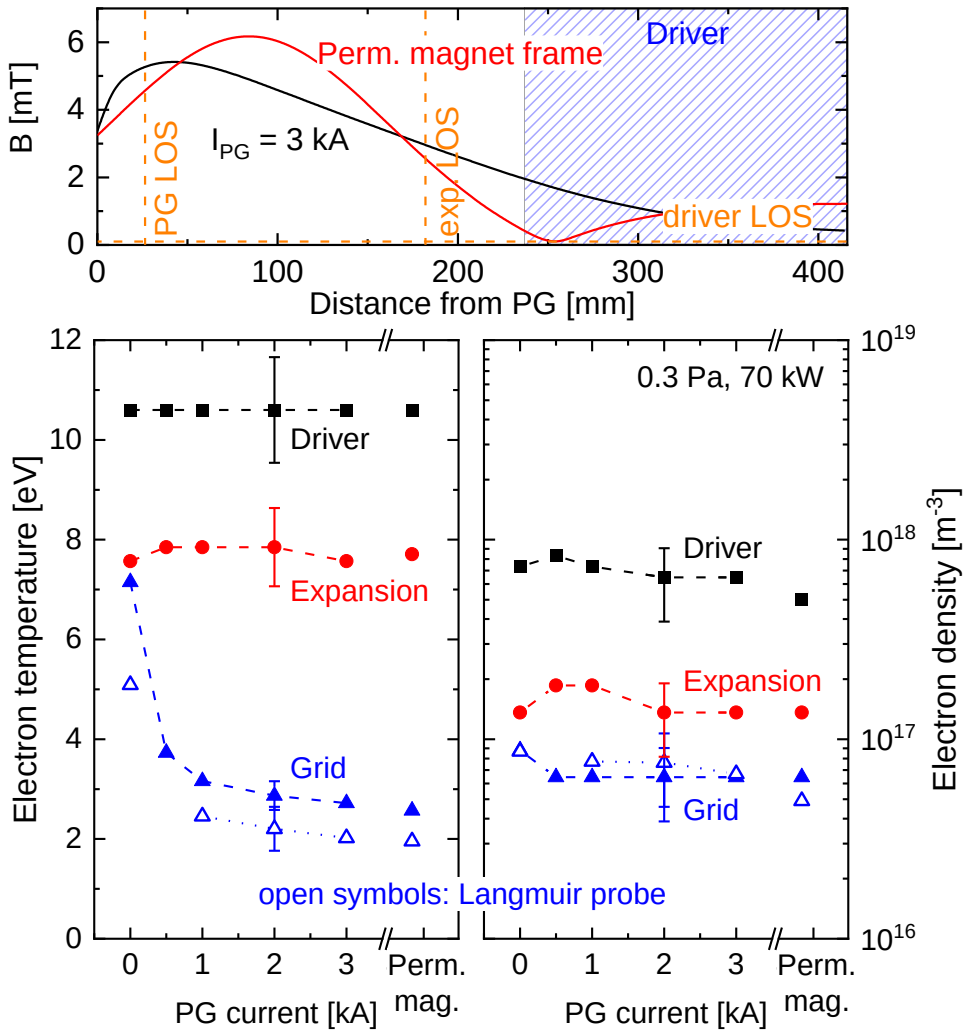

	OES Method	Results
T_{gas}	H_2 Fulcher	630 K
T_{vib}	H_2 Fulcher	3000 K
T_H	H_γ 2nd order	2200 K & 2.5 eV
n_H / n_{H_2}	H_γ /$H_{2,\ Fulcher}$	0.3 ± 0.1

	Method	Results
$n(H^-)$	CRDS	10^{17} m^{-3}
n(Cs)	TDLAS	10^{15} m^{-3}
$n(Cs^+)$ / n(Cs)	Simu.	~70%
n(Cs) vacuum	TDLAS	5×10^{14} m^{-3}

Briefi et al. 2018 AIP Conf. Proc. 2052

Transition to an H_x^+/H^- plasma during the Cs conditioning

Langmuir probe measurements

Heinemann et al. 2017 New J. Phys. 19

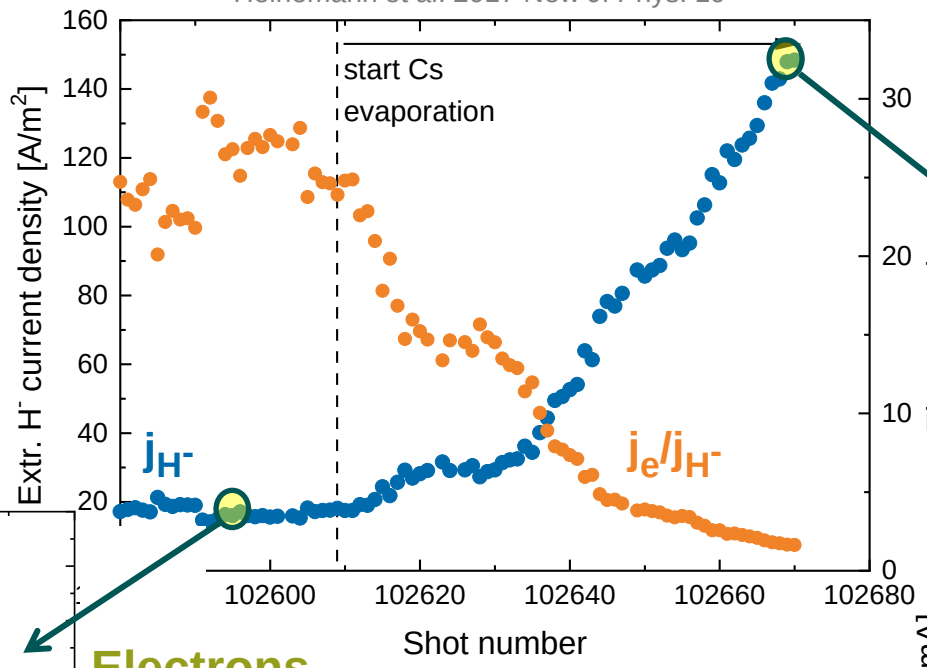

Negative ions
as dominant neg. species

Volume process

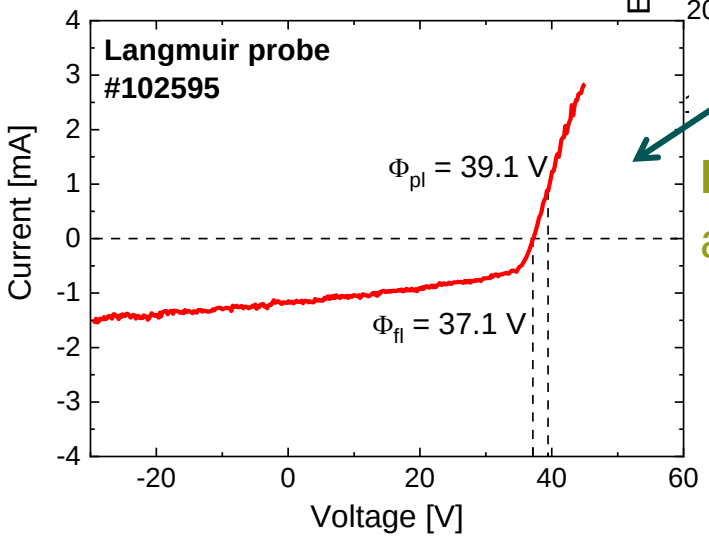

Electrons
as dominant negative species

Surface process

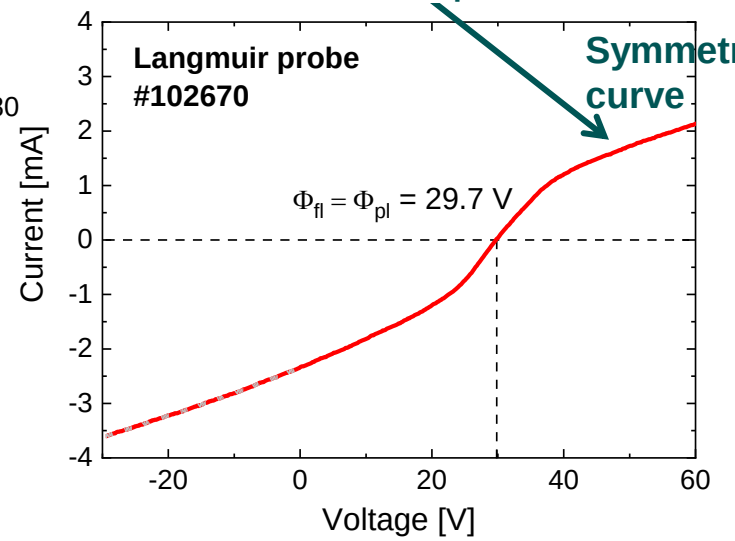

The European step ladder approach

Modular concept of the RF-driven H^-, D^- ion sources

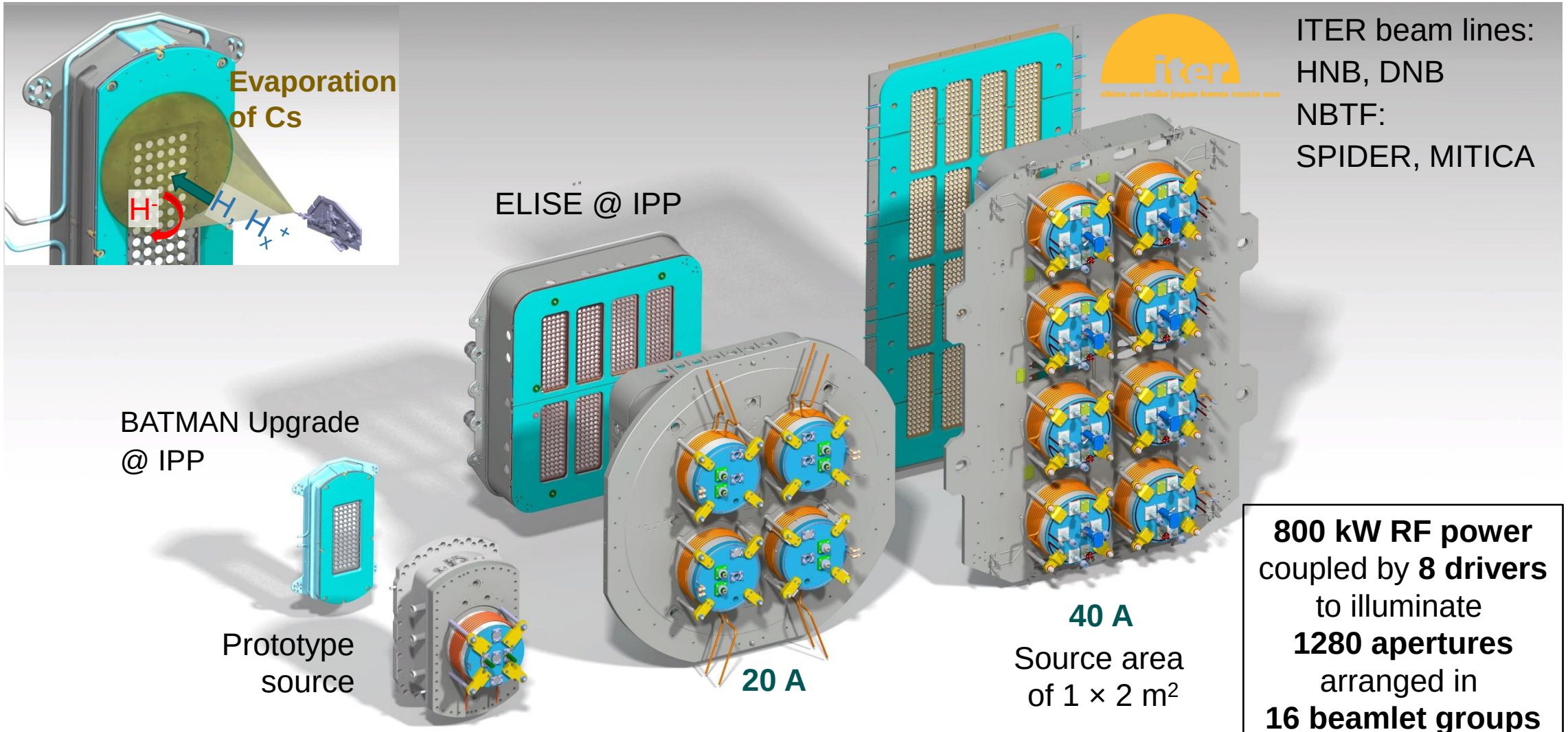

ELISE – A half size ITER source

Extraction from a **L**arge **I**on **S**ource **E**xperiment

Ion source with dome

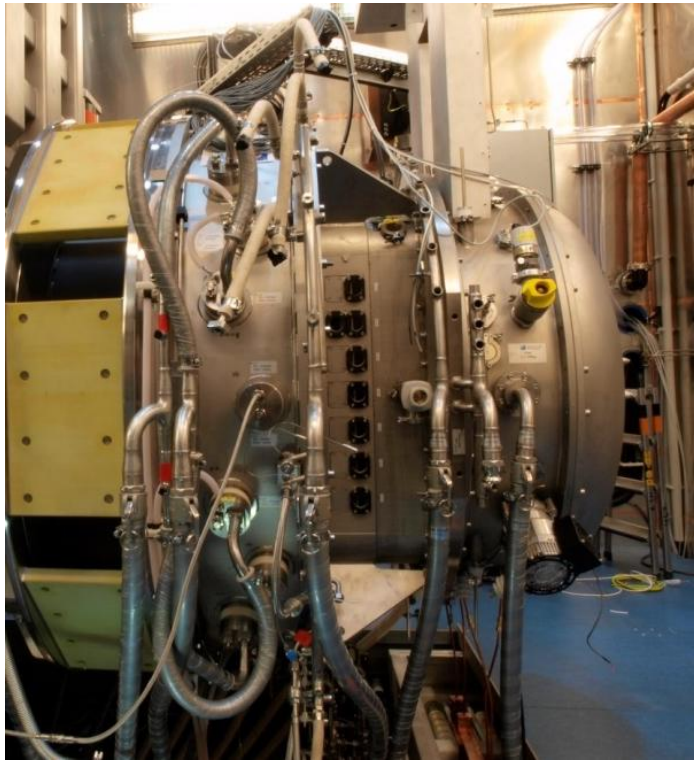

RF drivers in the dome

Source with grid system

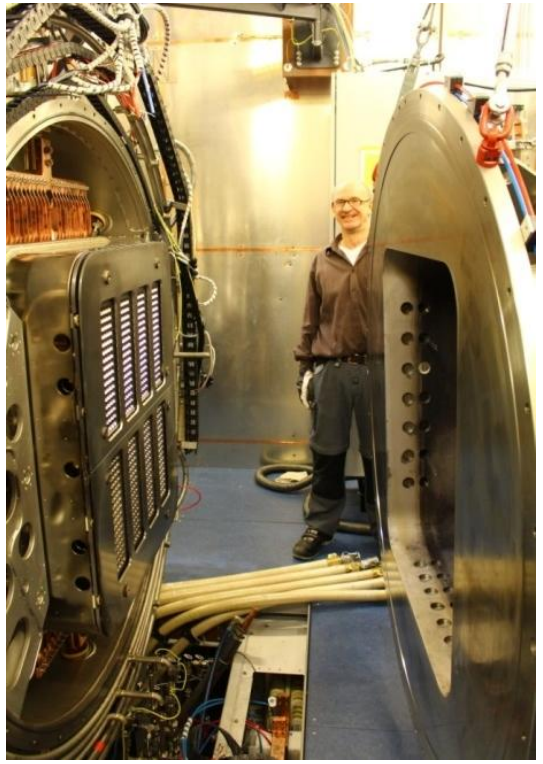

Negative hydrogen ion sources – utilizing low temperature plasmas in ITER's neutral beam systems

High power plasma sources
for negative hydrogen ions (H^-, D^-)

$T < 10$ eV

Source area: 1 m × 2 m

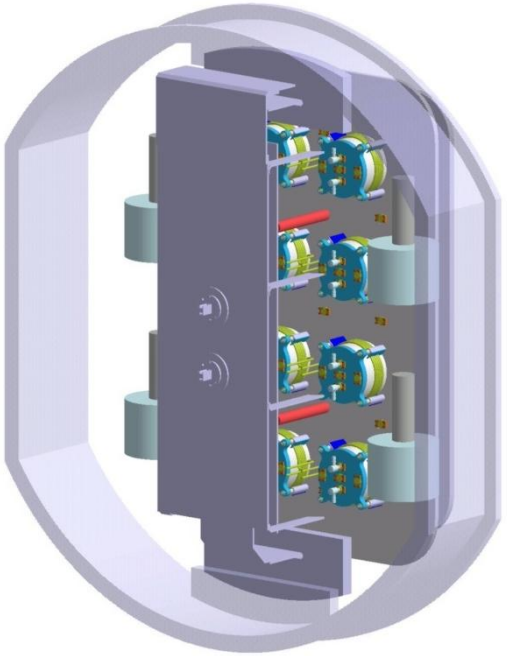

Acceleration to
1 MeV

40 A D^- for 1 hour

40 MW
generated

17 MW
to the torus

Fusion plasma

$D + T \rightarrow {}^4He + n + 17.6$ MeV

$T > 10$ keV

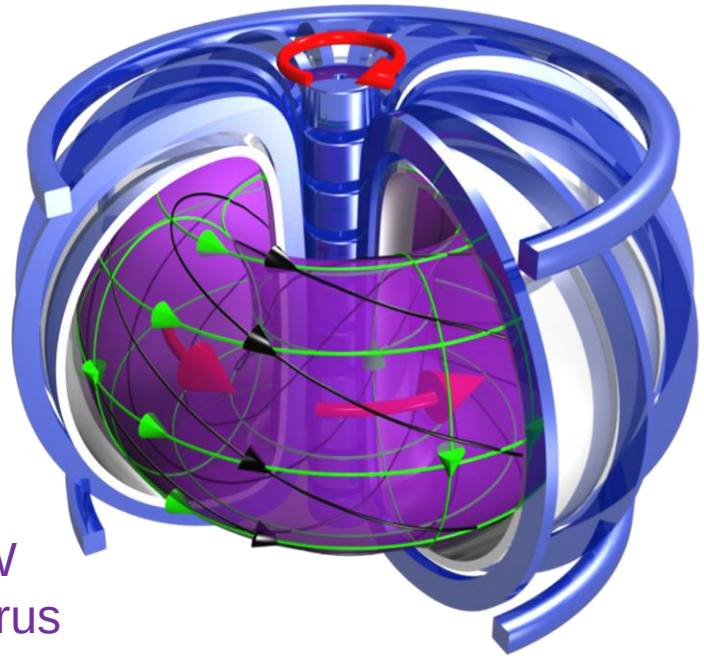

Hydrogen isotopes

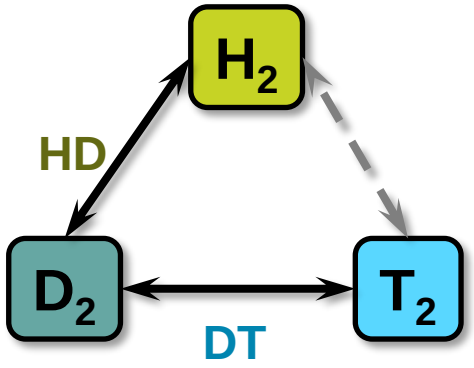

Towards deuterium

Atomic model

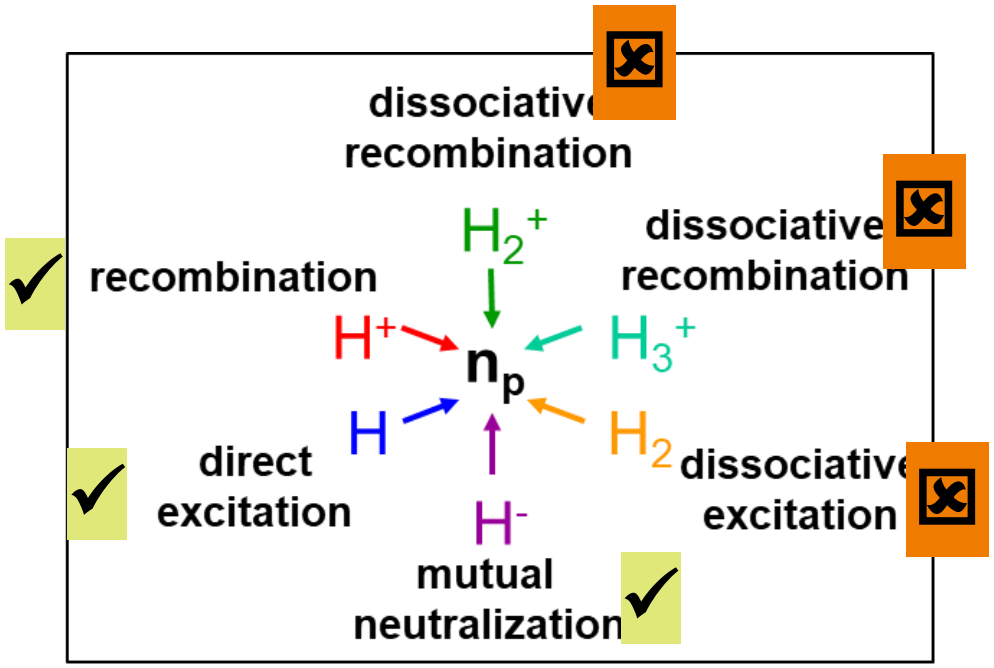

and opacity effects

Molecules

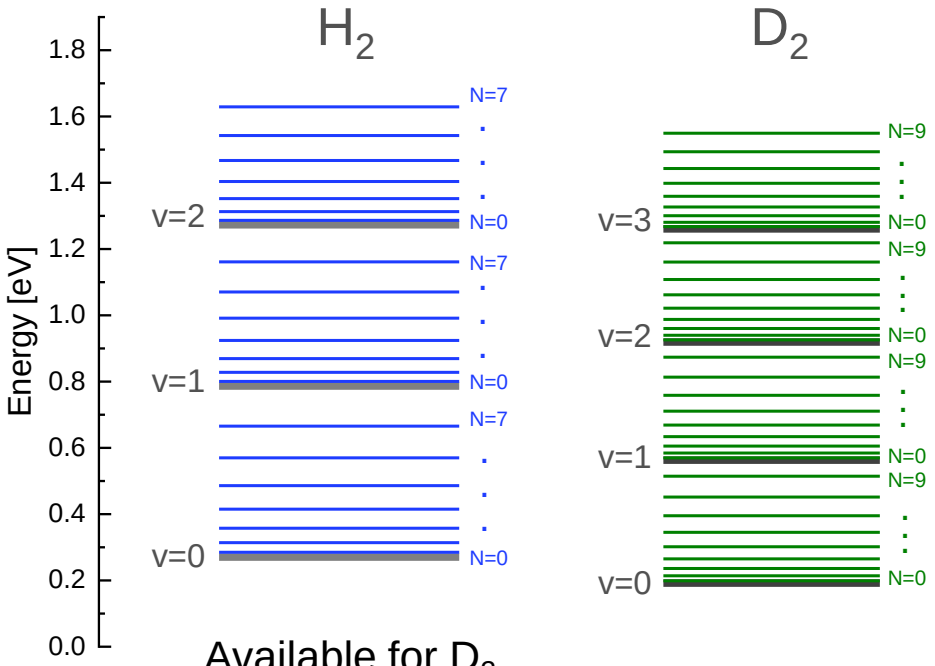

Available for D_2

- Transition probabilities A_{ik}
- Dissociative attachment (Laporta)
- Ionisation Gryzinski method and MCCC

In planning: Yacora-D2(v) with MCCC data

Benchmark at linear devices
is a necessity

Fulcher spectrum from MAGNUM-PSI

DIFFER

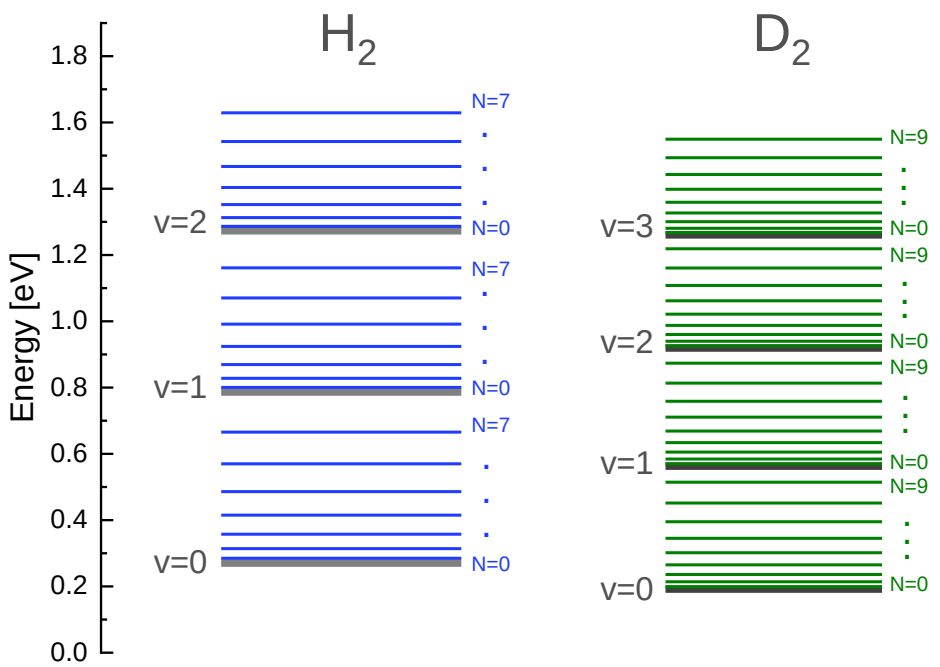

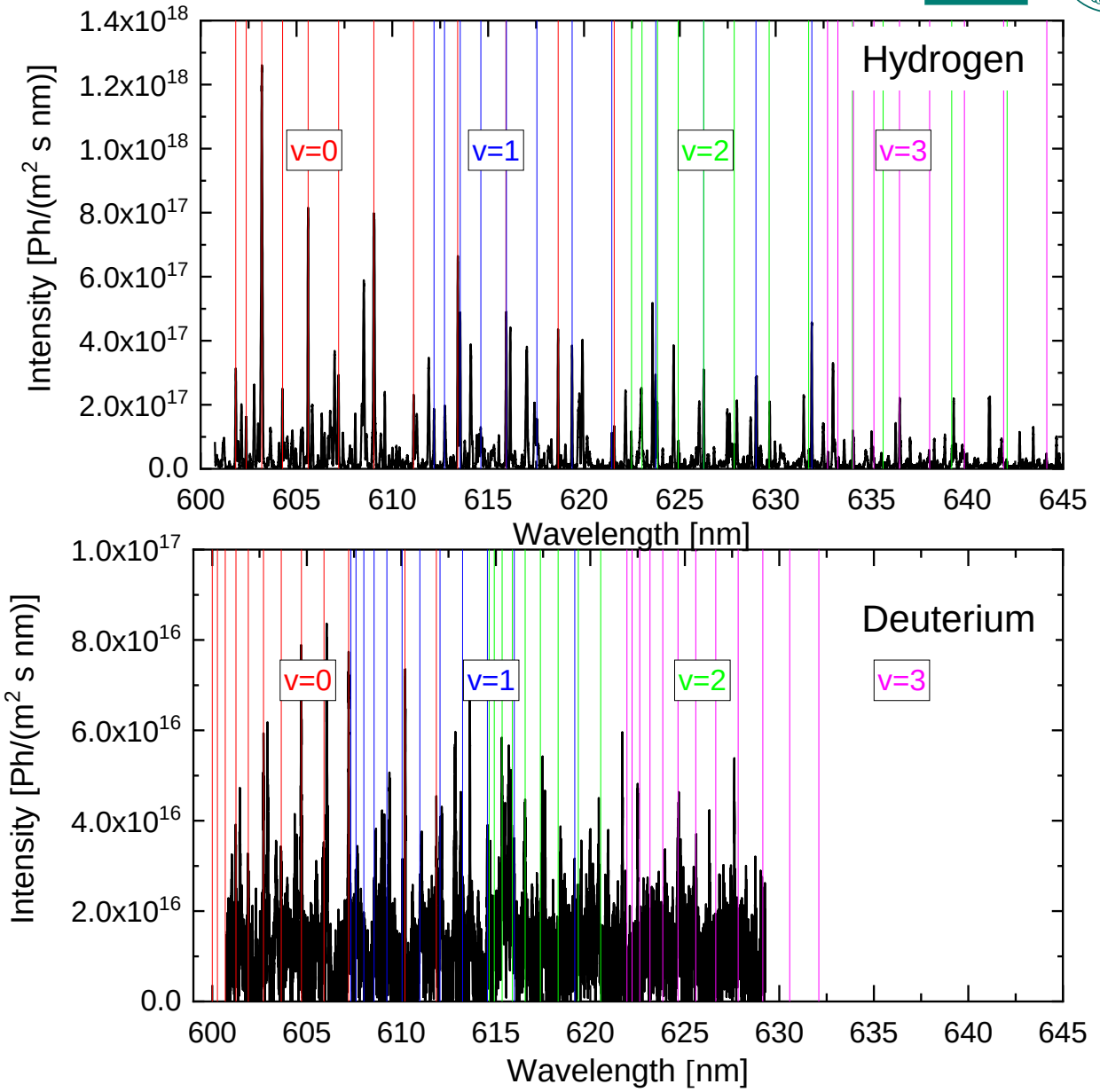

Summary

Low temperature plasmas
Properties, diagnostics & their relevance in fusion

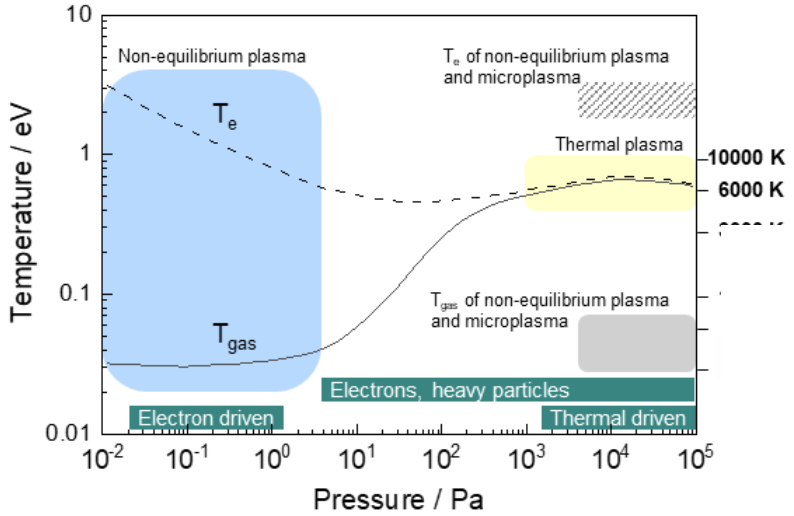

$T_e \approx 10$ eV ⟶ below 1 eV

$n_e \approx 10^{15}$ m^{-3} ⟶ 10^{22} m^{-3}

Ionising ⟶ **recombining**

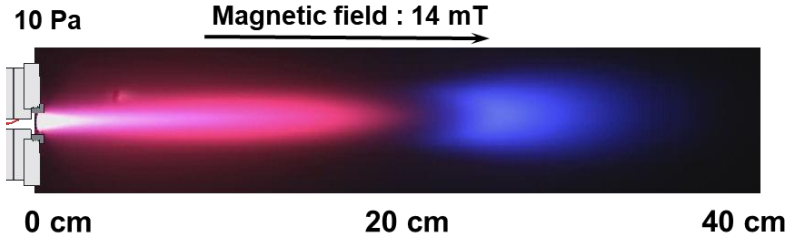

Linear plasma devices

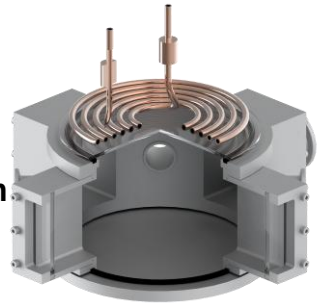

∅ = 15 cm
h = 10 cm

H^- source

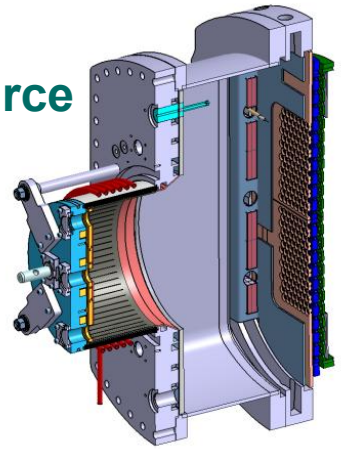

area:
0.52 x 0.26 m²

Divertor plasmas

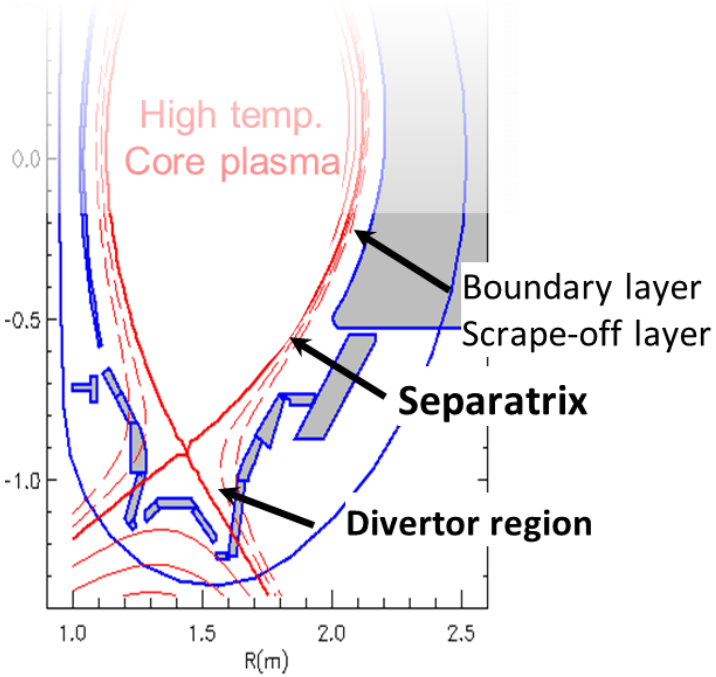

Plasmas for technology applications

ICP, ECR, DBD, MW torch, Surfaguide, …